UNIVERSIDADE ESTADUAL DE LONDRINA

JULIANA BONAMETTI OLIVATO

BLENDAS DE AMIDO TERMOPLÁSTICO E POLIÉSTER:

ESTUDO DA INFLUÊNCIA DE COMPATIBILIZANTES E AGENTES DE REFORÇO

Londrina
2013

JULIANA BONAMETTI OLIVATO

BLENDAS DE AMIDO TERMOPLÁSTICO E POLIÉSTER:
ESTUDO DA INFLUÊNCIA DE COMPATIBILIZANTES E AGENTES DE REFORÇO

Tese apresentada ao Curso de Doutorado em Ciência de Alimentos, do Departamento de Ciência e Tecnologia de Alimentos, como requisito para obtenção do título de Doutor.

Orientador: Profa. Dra. Maria Victoria Eiras Grossmann
Co-orientador: Prof. Dr. Fabio Yamashita

Londrina
2013

Catalogação elaborada pela Divisão de Processos Técnicos da Biblioteca Central da Universidade Estadual de Londrina

Dados Internacionais de Catalogação-na-Publicação (CIP)

O48b Olivato, Juliana Bonametti.
Blendas de amido termoplástico e poliéster : estudo da influência de compatibilizantes e agentes de reforço / Juliana Bonametti Olivato. - Londrina, 2013
158 f. : il.

Orientador: Maria Victoria Eiras Grossmann. Coorientador: Fábio Yamashita.
Tese (Doutorado em Ciência de Alimentos) - Universidade Estadual de Londrina, Centro de Ciências Agrárias, Programa de Pós-Graduação em Ciência de Alimentos, 2013.
Inclui bibliografia.

1. Alimentos - Embalagens - Teses. 2. Filmes biodegradáveis - Processo de extrusão - Teses. 3. Plásticos nas embalagens - Teses. 4. Termoplásticos - Teses. 5. Amido - Teses. 6. Ácidos orgânicos - Teses. I. Grossmann, Maria Victoria Eiras. II. Yamashita, Fábio. III. Universidade Estadual de Londrina. Centro de Ciências Agrárias. Programa de Pós-Graduação em Ciência de Alimentos. IV. Título.

CDU 664.004.3

JULIANA BONAMETTI OLIVATO

BLENDAS DE AMIDO TERMOPLÁSTICO E POLIÉSTER: ESTUDO DA INFLUÊNCIA DE COMPATIBILIZANTES E AGENTES DE REFORÇO

Tese apresentada ao Curso de Doutorado em Ciência de Alimentos, do Departamento de Ciência e Tecnologia de Alimentos, como requisito para obtenção do título de Doutor.

BANCA EXAMINADORA

_____

Orientadora. Prof. Dra. Maria Victoria Eiras Grossmann
UEL – Londrina – PR

_____

Prof. Dr. Alfredo Tibúrcio Nunes Pires (membro)
UFSC – Santa Catarina – PR

_____

Profa. Dra. Carmen Maria Oliveira Müller (membro)
UFSC – Santa Catarina – PR

_____

Profa. Dra. Suzana Mali (membro)
UEL – Londrina – PR

_____

Profa. Dra. Gizilene Maria de Carvalho (membro)
UEL – Londrina – PR

Londrina, 30 de setembro de 2013.

Dedico esse trabalho a minha familia e amigos pelo apoio incondicional e incessante e a todos aqueles que durante esses anos me apoiaram nos momentos difíceis e não me deixaram desistir.

AGRADECIMENTOS

Agradeço a minha orientadora, Maria Victoria, não só pela constante orientação neste trabalho, mas, sobretudo pela sua amizade e por apoiar e considerar, sempre com carinho, todas as minhas sugestões e pelas idéias tão valiosas que tornaram possível a realização deste trabalho.

Ao meu co-orientador, Fabio Yamashita, pela confiança, amizade e pelas diversas vezes em que provocou um *"brain storm',* me levando a novos caminhos.

Ao Professor Dr. Luc Avérous, da Université de Strasbourg, que tão gentilmente me recebeu em seu laboratório e compartilhou conhecimento e experiência durante os meses de doutorado sanduíche.

À Professora Dra. Suzana Mali, do Departamento de Bioquímica da Universidade Estadual de Londrina, que me "apresentou" ao grupo de tecnologia em polímeros biodegradáveis e despertou meu interesse pela área que até agora tem sido minha paixão e foco do meu estudo.

Com muito carinho à Dra. Carmen Müller por ceder seu tempo na realização de muitas análises, além de paciência para ensinar e explicar como ninguém os resultados. Até mesmo os mais inexplicáveis.

À Professora Dra. Gizilene Maria de Carvalho do Departamento de Química da Universidade Estadual de Londrina, pelas análises de RMN e pela inestimável contribuição nas interpretações e conclusões dos resultados.

Ao Professor Dr. Alexandre Urbano do Departamento de Física da Universidade Estadual de Londrina, pela contribuição com a realização e interpretação dos espectros de difração de raios-X.

Ao Nelson Fuzinato, técnico do laboratório de Tecnologia em Alimentos da Universidade Estadual de Londrina, por toda a inestimável ajuda, toda a preocupação com o experimento e todo o carinho comigo durante muitos anos. Nada seria concreto neste experimento sem sua contribuição.

Aos amigos que fiz, ainda no mestrado, Marcelo Medre e Juliane

Alves, que permaneceram como pessoas muito especiais, que me deram forças sempre. Ainda ao Marcelo, agradeço por toda a experiência compartilhada, pelas constantes aulas sobre qualquer coisa e sobretudo, por muitas risadas.

Aos amigos "importados", Juliano Marini, Bruno Bernardes e Heveline Follmann, que conheci no finzinho do doutorado e que fizeram toda a diferença, seja pela alegria da Heveline, pelas risadas com o Bruno ou por todo o conhecimento compartilhado, a amizade sem limites, toda a ajuda na realização das análises e por horas de conversa do Juliano. Vocês estarão sempre em meu coração.

Aos amigos e parceiros de grupo, Ana Paula Bilck, Marianne Shirai, Monica Reis, Juliano Zanela, Adriana Passos Dias, Jaqueline Camisa, por ótimos momentos no laboratório e por compartilhar conhecimento e todas as idéias que tornaram possível esse trabalho.

A minha mãe, por toda a força e apoio, pelo amor incondicional e por correr com os braços abertos em todos os momentos em que precisei. Também aos meus irmãos, Tatiane e Claudio, sempre importantes em minha vida.

A alguém realmente muito paciente e compreensivo, que suportou como ninguém meu estresse, minha ausência e esteve sempre ao meu lado. Não seria real sem você, Hugo Machado.

Ao CNPq pela concessão da bolsa de doutorado no país e à CAPES pela bolsa de doutorado sanduíche no exterior.

Agradeço ainda a todas as pessoas que de alguma forma contribuíram para a realização deste projeto.

"A mente que se abre a uma nova idéia jamais voltará ao seu tamanho original"

Albert Einstein

OLIVATO, Juliana Bonametti. **Blendas de amido termoplástico e poliéster**: estudo da influência de compatibilizantes e agentes de reforço. 2013. 158f. Tese (Doutorado em Ciência de Alimentos) – Universidade Estadual de Londrina, Londrina, 2013.

RESUMO

A produção de materiais biodegradáveis tem sido o foco de inúmeras pesquisas atualmente. Como forma de superar as limitações do amido termoplástico, propõe-se a produção de blendas deste com polímeros de melhor desempenho. Nesse sentido, blendas de amido/poli (adipato co-tereftalato de butileno) (PBAT) adicionadas dos ácidos cítrico, málico ou tartárico em concentrações de 0,375; 0,75 e 1,5 g.100g^{-1}, foram produzidas por extrusão reativa em uma única etapa. A inclusão dos ácidos orgânicos aumentou a resistência à tração e reduziu a permeabilidade ao vapor de água dos filmes, em função de sua atuação como compatibilizantes. O ácido tartárico (TA) mostrou resultados promissores e representa uma alternativa ainda não abordada por outros autores. Com isso, sua influência nas blendas foi investigada por meio de um planejamento de misturas. Diferentes e concomitantes papéis foram observados para o TA, desde a compatibilização das blendas, com a redução da tensão interfacial e obtenção de materiais mais homogêneos, até a hidrólise parcial das cadeias de amido, causando enfraquecimento dos materiais quando utilizado em elevadas proporções (> 1.5 g.100g^{-1}). Análises de infravermelho (FT-IR) e ressonância magnética nuclear (13C CPMAS NMR) apontaram para a ocorrência de reações de esterificação / transesterificação promovidas pelo ácido tartárico, sendo esse seu principal mecanismo de ação como compatibilizante, o que é refletido nas demais propriedades dos materiais. De acordo com a técnica da Desejabilidade, a formulação mais desejada, isto é, a que produziu filmes mais resistentes, continha proporção intermediária de ácido tartárico (0.8 g.100g^{-1}). Sacolas plásticas biodegradáveis produzidas utilizando-se a proporção otimizada entre os componentes (amido, PBAT, glicerol e TA) foram aprovadas em todos os ensaios constantes na norma ABNT NBR 14937:2010, o que indica que este material é adequado para o uso comercial. Em uma segunda etapa, com o objetivo de avaliar o efeito reforçador da nanoargila sepiolita, blendas de amido/PBAT, contendo 1, 3 e 5 g.100g^{-1} deste nanosilicato, foram produzidas utilizando-se duas proporções entre as fases poliméricas (50:50 e 80:20 amido termoplástico (TPS)/PBAT, respectivamente). A análise das imagens de microscopia eletrônica de varredura e dos espectros de difração de raios-x evidenciaram que a sepiolita apresentou-se bem dispersa e não alterou a morfologia e o perfil cristalino das blendas, mas aumentou significativamente o torque registrado durante o processamento dos materiais, como consequência da redução da mobilidade molecular. Ainda, foi observado um efeito reforçador significativo (aumento do módulo de Young e resistência à tração), principalmente para as formulações contendo 80:20 TPS/PBAT, uma vez que a sepiolita parece estar concentrada na fase de TPS, devido a sua maior compatibilidade molecular. Por fim, a inclusão de 5 g.100g^{-1} de sepiolita na matriz com proporção 50:50 TPS/PBAT levou a um aumento de 25°C na temperatura de transição vítrea (Tg) relativa à fase de amido, sem alteração na Tg do PBAT, reforçando a ideia da provável localização da nanoargila na blenda. Ainda, a análise dos dados referentes ao registro do ganho de água dos nano-biocompósitos com o tempo, em geral, mostraram menor velocidade de

absorção de água e menor quantidade de água absorvida com a inclusão de sepiolita nas blendas. Dessa forma, a sepiolita mostrou-se uma alternativa interessante e promissora como agente de reforço em materiais a base de amido.

Palavras-chave: Amido termoplástico. Poli (adipato co-terefetalato de butileno) (PBAT). Compatibilizantes. Sepiolita. Blendas biodegradáveis.

OLIVATO, Juliana Bonametti. **Blends of thermoplastic starch and polyester**: study of the influence of compatibilizers and reinforcing agents. 2013. 158p. Thesis (Doctor Degree in Food Science) – Universidade Estadual de Londrina, Londrina, 2013.

ABSTRACT

The production of biodegradable materials has been the focus of numerous studies currently. With the aim to overcome the thermoplastic starch drawbacks, blends with better performance materials has been proposed. In this direction, starch/poly (butylene adipate co-terephthalate) (PBAT) blends added of citric, malic or tartaric acids (in concentrations of 0.375; 0.75 e 1.5 g.100g~^{1}) were produced by one-step reactive extrusion. The inclusion of organic acids increased the tensile strength and reduced the water vapour permeability of the films, as a consequence of their role as compatibilisers. Tartaric acid (TA) presented promisor results and represents an alternative not covered by other authors. Therefore, their influence in the blends was investigated by means of a mixture design. Different and concomitant roles of TA were observed, as the blends compatibilisation, reducing the interfacial tension and obtaining more homogeneous materials and, also the partial hydrolysis of the starch chains, weakening the materials when used in elevated proportions (> 1.5 g.100g~^{1}). Infrared analysis (FT-IR) and nuclear magnetic resonance (13C CPMAS NMR) pointed to the occurrence of esterification / transesterification reactions promoted by tartaric acid, related with their compatibilising action, which is reflected in the other materials properties. According to the Desirability method, the most desirable formulation, i. e., which produced more resistant films, had intermediate proportions of tartaric acid (0.8 g.100g~^{1}). Biodegradable bags produced using the optimised proportion between the components (starch, PBAT, glycerol and TA) were approved in all the requirements contained in the ABNT NBR 14937:2010 standard, indicating that they are appropriate for commercial use. In a second step, with the aim to evaluate the reinforcing effect of sepiolite, starch/PBAT blends, containing 1, 3 and 5 g.100g^{-1} of the nanoclay, were produced using two proportions between the polymeric phases (50:50 and 80:20 thermoplastic starch (TPS)/PBAT, respectively). Scanning electron microscopy analysis and x-ray diffraction spectra demonstrated that sepiolite was well dispersed and did not change the morphology and the crystalline profile of the samples, but increased the registered torque during the materials processing, as a consequence of the reduced molecular mobility. Moreover, a positive reinforcing effect was observed (higher Young's module and tensile strength), mostly for the 80:20 TPS/PBAT formulations, since sepiolite seems to be concentrated at TPS phase, due their greater molecular compatibility. Lastly, the inclusion of 5 g.100g^{-1} of sepiolite in the matrix with 50:50 TPS/PBAT proportion, increased the glass transition temperature (Tg) of starch phase in 25°C, without change the Tg of PBAT, which consolidate the probable localisation of the nanoclay in the blends. At least, data analysis referent to the water gain registered against time for the nano-biocomposites, showed, in general, that sepiolite decreased the water adsorption rate even as the water adsorption capacity of the materials. Thus, sepiolite clays represents an interesting and promisor alternative to reinforce starch-based materials.

Keywords: Thermoplastic starch. Poly (butylene adipate co-terephthalate) (PBAT). Compatibilisers. Sepiolite. Biodegradable blends.

LISTA DE FIGURAS

CAPÍTULO 1 – Revisão Bibliográfica

CAPÍTULO 2 – Effect of organic acids as additives on the performance of thermoplastic starch/polyester blown films

CAPÍTULO 7 – Starch/polyester nano-biocomposites based on sepiolite clays: Thermo-mechanical and water sorption properties

APÊNDICE

ÍNDICE DE TABELAS

LISTA DE ABREVIATURAS E SIGLAS

õ	Deslocamento químico
ABNT	Associação Brasileira de Normas Técnicas
ANOVA	Análise de variância
ASTM	*American Society for Testing and Material*
CA	Ácido cítrico
CEC	Capacidade de troca iônica
CETEA	Centro de Pesquisa e Desenvolvimento de Embalagens
DMA	Análise dinâmico-mecânica
DMTA	Análise termo-dinâmico mecânica
DSC	Calorimetria diferencial de varredura
FT-IR	Espectroscopia de infravermelho com transformada de Fourier
GLY	Glicerol
INMETRO	Instituto Nacional de Metrologia, Qualidade e Tecnologia
MA	Ácido málico
NBR	Norma brasileira
PBAT	Poli (adipato co-tereftalato de butileno)
PHA	Poli (hidroxialcanoato)
PLA	Poli (ácido lático)
PVA	Poli (álcool vinílico)
RH	Umidade relativa
SEM	Microscopia eletrônica de varredura
TA	Ácido tartárico
TPS	Amido termoplástico
Tc	Temperatura de cristalização
Tg	Temperatura de transição vítrea
TGA	Análise termogravimétrica
Tm	Temperatura de fusão
WAXD	Difração de raios-x de alto ângulo
WVPR	Taxa de permeabilidade ao vapor de água
WVP	Permeabilidade ao vapor de água
XRD	Difração de raios-x

13C CPMAS NMR	Espectroscopia de ressonância magnética nuclear de polarização cruzada com rotação em torno do ângulo mágico de 13C em estado sólido.

SUMÁRIO

INTRODUÇÃO

A necessidade de se reduzir a quantidade de materiais plásticos depositados no ambiente tem sido motivo de preocupação mundial, impulsionando as pesquisas voltadas para materiais biodegradáveis e oriundos de fontes renováveis, com ênfase naqueles de origem vegetal, como potenciais substitutos das embalagens plásticas não biodegradáveis e provenientes de recursos fósseis (AVÉROUS; FRINGANT, 2001).

Os agro-polímeros, como o amido, possuem a vantagem de possuir custo reduzido, associada à sua abundância e biodegradabilidade, o que é atrativo do ponto de vista comercial e de sustentabilidade. Na presença de um plastificante e em elevadas temperaturas e cisalhamento, o amido nativo tem sua estrutura granular destruída, dando origem a uma matriz polimérica essencialmente amorfa, chamada amido termoplástico (TPS), que se funde e flui com comportamento semelhante aos polímeros sintéticos, o que permite seu processamento pelas técnicas comumente empregadas para a produção de embalagens plásticas, como a extrusão, moldagem por injeção e sopro. Entretanto, sua fragilidade e sensibilidade à umidade tornam limitada a aplicação do TPS puro em materiais de embalagem (AVÉROUS; FRINGANT; MORO, 2001).

Tendo isso em consideração, uma das formas mais eficientes de melhorar as propriedades do amido termoplástico é a obtenção de blendas com polímeros de melhor desempenho. Nesse contexto insere-se o poli (adipato co-tereftalato de butileno) (PBAT), um copoliéster alifático-aromático com propriedades mecânicas e de barreira adequadas a contornar as deficiências do TPS, com a vantagem de manter a biodegradabilidade do produto final (REN et al., 2009).

Blendas imiscíveis, como as obtidas de amido termoplástico (hidrofílico) e PBAT (hidrofóbico), necessitam de adição de substâncias capazes de atuar reduzindo a tensão interfacial e aumentando a adesão entre as diferentes fases, os chamados compatibilizantes, para que um material homogêneo seja obtido e a transmissão da tensão aplicada a ele possa ocorrer efetivamente entre os componentes das blendas (MALIGER et al., 2006).

Ácidos orgânicos, em especial os policarboxílicos, permitem a modificação da natureza hidrofílica do amido, uma vez que promovem reações de esterificação com um ou mais de seus grupos hidroxílicos, introduzindo novos

grupamentos éster nas cadeias, os quais fornecem, ainda, potenciais pontos para a realização de ligações cruzadas (transesterificação). Esse fato é associado às vantagens evidentes de segurança e compatibilidade com os alimentos quando o objetivo da produção de tais materiais é a embalagem alimentar (Da RÓZ et al, 2011; SHI et al., 2007).

A produção de nano-biocompósitos, isto é, incorporação de ao menos um componente em escala nanométrica em uma matriz biodegradável, tem despertado o interesse também como alternativa para melhorar as propriedades de materiais a base de amido. A sepiolita, um silicato de magnésio de morfologia fibrosa, com formato semelhante a agulhas, representa uma opção interessante a ser aplicado em materiais contendo amido termoplástico, devido a seu caráter hidrofílico resultante da presença de grupos silanol em sua superfície. Além disso, resultados prévios de outros autores apontam para a obtenção de materiais com melhores propriedades térmicas e mecânicas com sepiolita quando comparados às mesmas matrizes incorporadas com montmorillonita, por exemplo (CHIVRAC et al., 2010).

Dessa forma, blendas de amido termoplástico e PBAT, contendo ácidos orgânicos como compatibilizantes ou incluídas da nanoargila sepiolita, apontam para uma possível tentativa de obtenção de materiais biodegradáveis que apresentam bom desempenho e atendem aos requisitos necessários para a sua aplicação industrial, como uma alternativa ecologicamente favorável às embalagens sintéticas disponíveis atualmente.

Para isso, o presente trabalho teve como objetivo produzir blendas de amido termoplástico com um poliéster biodegradável com melhores propriedades mecânicas e de barreira, como o poli (adipato co-tereftalato de butileno) (PBAT) e ainda avaliar a utilização de ácidos orgânicos e sepiolita como possíveis formas de melhorar as propriedades das blendas.

Este trabalho está dividido em sete capítulos, organizados da seguinte forma:

- Capítulo 1 - Revisão bibliográfica
- Capítulo 2 - Estudo da influência de diferentes ácidos orgânicos nas propriedades das blendas de amido/PBAT e seleção do ácido tartárico como melhor compatibilizante. Este capítulo foi publicado como:

OLIVATO, J. B; GROSSMANN, M. V. E; BILCK, A. P; YAMASHITA, F. Effect of organic acids as additives on the performance of thermoplastic starch/polyester blown films. **Carbohydrate Polymers,** v. 90, p. 159-164, 2012.

- Capítulo 3 - Avaliação de comportamento do ácido tartárico, de acordo com um planejamento de misturas, nas propriedades mecânicas, térmicas e de barreira de filmes. Este capítulo foi publicado como:

OLIVATO, J. B; NÓBREGA, M. M; MÜLLER, C. M. O; SHIRAI, M. A; YAMASHITA, F; GROSSMANN, M. V. E. Mixture design applied for the study of the tartaric acid effect on starch/polyester films. **Carbohydrate Polymers,** v. 92, p. 1705-1710, 2013.

- Capítulo 4 - Caracterização morfológica e estrutural do material obtido, investigando a ação compatibilizante do ácido tartárico nas blendas amido/PBAT.

- Capítulo 5 - Emprego da técnica de Desejabilidade para a escolha da melhor formulação contendo ácido tartárico e estudo da viabilidade de produção de sacolas plásticas a partir da formulação otimizada. Este capítulo foi publicado como:

OLIVATO, J. B; GROSSMANN, M. V. E; BILCK, A. P; YAMASHITA, F; OLIVEIRA, L. M. Starch/polyester films: Simultaneous optimisation of the properties for the production of biodegradable plastic bags. **Polímeros: Ciência e Tecnologia,** v. 23, n. 2, p. 1-5, 2013.

- Capítulo 6 - Estudo do efeito da incorporação de sepiolita nas propriedades mecânicas, morfológicas e estruturais de blendas de amido/PBAT.

- Capítulo 7 - Propriedades termo-mecânicas, de barreira e ópticas de blendas de amido/PBAT adicionadas de sepiolita.

- Apêndice - Imagens complementares das amostras obtidas nas diferentes etapas do trabalho e outras relacionadas à metodologia de análise dos materiais.

OBJETIVOS

Objetivo geral

Avaliar as propriedades mecânicas e a morfologia de blendas biodegradáveis de amido/PBAT empregando ácidos orgânicos como compatibilizantes ou nanoargila sepiolita como reforço.

Objetivos específicos por capítulo

Capítulo 1 - Revisão bibliográfica

Realizar o levantamento bibliográfico necessário a reunir informações na literatura já publicada sobre o tema as quais são necessárias para a inserção do problema da pesquisa dentro de um contexto global.

Capítulo 2 - Influência de diferentes ácidos orgânicos nas propriedades das blendas

Produzir blendas de amido/PBAT incorporadas com três concentrações diferentes dos ácidos cítrico, málico ou tartárico;

Avaliar as propriedades mecânicas, a permeabilidade ao vapor de água, e empregar espectroscopia de infravermelho na análise de alterações estruturais e microscopia eletrônica de varredura para análise morfológica dos materiais;

Capítulo 3 - Atuação do ácido tartárico como compatibilizante

Determinar a influência da formulação (teores de ácido tartárico, glicerol e amido+PBAT) nas propriedades mecânicas e de barreira do material, por meio de um planejamento de misturas.

Obter informações acerca da estrutura cristalina das blendas com análises de difração de raios-x e de seu comportamento termo-mecânico por meio de análise dinâmico-mecânica (DMA).

Capítulo 4 - Investigação das alterações estruturais nas blendas

Investigar a possível ocorrência de reações de esterificação / transesterificação com a adição de ácido tartárico, utilizando técnicas de caracterização estrutural (FT-IR e 13C CPMAS NMR);

Analisar a ação compatibilizante do ácido tartárico por meio da morfologia das blendas amido/PBAT, assim como sua influência nas propriedades ópticas.

Capítulo 5 - Otimização da formulação e aplicação na produção de sacolas biodegradáveis

Empregar a técnica de Desejabilidade como ferramenta estatística para a obtenção de uma formulação com concentrações ótimas de ácido tartárico, glicerol, amido e PBAT;

Produzir, por extrusão-sopro, sacolas plásticas biodegradáveis a partir da formulação mais desejável;

Analisar as propriedades das sacolas por meio de norma brasileira que assegura a qualidade desses produtos no país.

Capítulo 6 - Inclusão de sepiolita como agente reforçador

Produzir nano-biocompósitos com adição de diferentes concentrações de sepiolita às blendas de amido/PBAT;

Investigar o comportamento da sepiolita quando incorporada em blendas com duas proporções entre as fases poliméricas;

Avaliar a morfologia das blendas com diferentes proporções entre TPS e PBAT e o papel da sepiolita nas alterações morfológicas;

Estudar os efeitos do nanosilicato nas propriedades mecânicas, estruturais e na degradação térmica dos nano-biocompósitos.

Capítulo 7 - Papel da sepiolita nas propriedades termo-mecânicas dos materiais e de sorção de umidade

Investigar o efeito da sepiolita na cristalização, transição vítrea e fusão das fases poliméricas;

Estudar o comportamento dos materiais em relação ao ganho de água com a inclusão da sepiolita;

Analisar a alteração das características ópticas (cor e opacidade) devido à inclusão da nanoargila.

CAPÍTULO 1 – REVISÃO BIBLIOGRÁFICA

1 Polímeros Biodegradáveis

A capacidade do planeta de absorver e transformar resíduos resultantes da vida moderna parecia ser inesgotável. No entanto, o aumento da população mundial e o crescente acúmulo de resíduos tem atraído grande interesse para a utilização de recursos renováveis e biodegradáveis pela indústria, uma consequência natural deste panorama mundial (LAROTONDA et al., 2004).

Existem muitas fontes de plásticos biodegradáveis, desde polímeros sintéticos a polímeros naturais. Polímeros sintéticos são em sua maioria derivados de monômeros provenientes do petróleo, enquanto os agro-polímeros, como os polissacarídeos, estão amplamente distribuídos na natureza como recursos renováveis (ZULLO; IANACE, 2009).

A biodegradabilidade é o fim de vida útil desejável para as embalagens de uso doméstico, que podem retornar ao ciclo de vida natural, se abandonadas no ambiente externo ou descartadas com a fração orgânica dos resíduos domésticos destinada à compostagem. Polímeros biodegradáveis estão em constante crescimento e desenvolvimento visando numerosas aplicações (FUKUSHIMA et al., 2010).

Os polímeros biodegradáveis têm sido classificados em quatro grupos principais, segundo Avérous (2004):

a. Polímeros originados da biomassa, como os agro-polímeros derivados de recursos agrícolas (exemplo: amido, celulose);

b. Polímeros obtidos por produção microbiana (exemplo: poli (hidroxialcanoato) (PHA));

c. Polímeros sintetizados a partir de monômeros obtidos de agro-recursos (exemplo: poli (ácido lático) (PLA));

d. Polímeros obtidos por síntese a partir de monômeros sintéticos (exemplo: poli (adipato co-tereftalato de butileno) (PBAT)).

Dentre as quatro diferentes categorias, somente três (a, b e c) são obtidas a partir de recursos renováveis.

Recentemente, os polímeros biodegradáveis tem atraído um crescente interesse pela redução da utilização dos recursos fósseis e pelo aumento

da conscientização ambiental. Esses fatos motivaram pesquisas acadêmicas com o objetivo de desenvolver novos materiais ambientalmente favoráveis, isto é, materiais produzidos de recursos alternativos, biodegradáveis e não tóxicos ao meio ambiente (BORDES; POLLET; AVÉROUS, 2009).

2 Amido

O amido é um carboidrato abundante, amplamente distribuído na forma de grânulos, sendo a principal substância de reserva dos vegetais superiores. Cereais, como milho e trigo, e tubérculos, como mandioca e batata, representam as principais fontes comerciais de amido para fins alimentícios e industriais (THARANATHAN, 2005; LEONEL; CEREDA, 2002). O Brasil se destaca na produção de amido, sendo o segundo maior produtor de amido de mandioca (LEONEL; CEREDA, 2002; MIRANDA; CARVALHO, 2011).

O amido é um complexo macromolecular contendo dois principais componentes. Um deles é a amilose, com estrutura essencialmente linear e constituída por resíduos de a-D-glicopiranose ligados em a-(1,4), com poucas ligações a-(1,6), geralmente entre 0,3 a 0,5% do total das ligações. O outro é a amilopectina, que é o componente ramificado do amido, formado por resíduos de a-D-glicopiranose unidos em a-(1,4), sendo fortemente ramificada, com 4% a 6% das ligações em a-(1,6) (Figura 1) (LIU et al., 2009; THARANATHAN, 2005). A forma, o tamanho dos grânulos e a proporção entre amilose e amilopectina são características da fonte botânica.

Os grânulos de amido nativo são parcialmente cristalinos, com as cadeias da amilose e os pontos de ramificação da amilopectina dando origem às regiões amorfas, e a amilopectina, organizada em dupla hélice, representando o principal componente cristalino. Vários tipos de estruturas cristalinas podem ser encontradas nos grânulos de amido, tipos -A, -B, -C, que diferem entre si na densidade das estruturas em dupla hélice, principalmente. A cristalinidade do tipo A ocorre na maioria dos cereais como milho, trigo e aveia e a cristalinidade do tipo B é típica de tubérculos (batata, mandioca). A estrutura do tipo C é um intermediário, raro de ser encontrado (VAN SOEST et al., 1996; VAN SOEST; VLIEGENTHART, 1997; SOUZA; ANDRADE, 2000).

Figura 1 – Estruturas químicas e esquemas representando as organizações da amilose (a) e amilopectina (b).

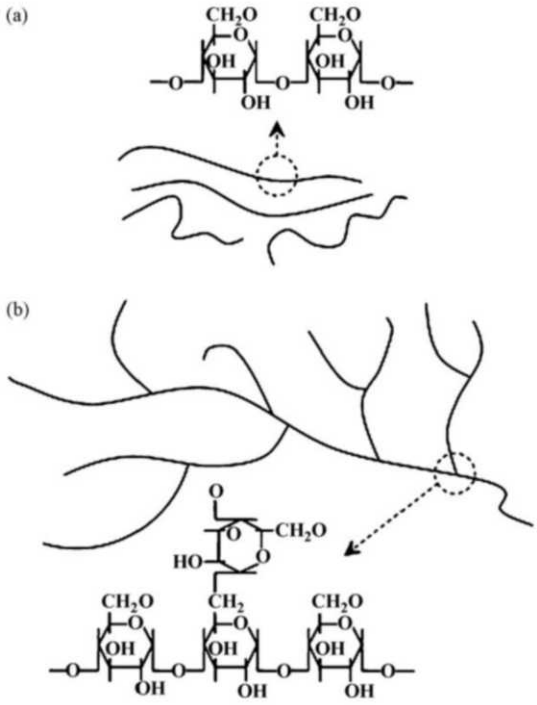

Fonte: Liu et al., 2009.

Quando visto em luz polarizada, o grânulo de amido é birrefringente, devido às propriedades de refração de suas regiões cristalinas, resultando no modelo físico típico de "Cruz de Malta", que caracteriza a orientação das moléculas. Quando observados em microscópio óptico, os grânulos de amido consistem em anéis semi-cristalinos e amorfos, alternadamente, e cujo centro, ou hilum, é o ponto inicial de crescimento do grânulo (Figura 2) (VANDEPUTTE; DELCOUR, 2004).

Figura 2 – Representação esquemática do grânulo de amido mostrando os anéis de crescimento amorfos e semi-cristalinos.

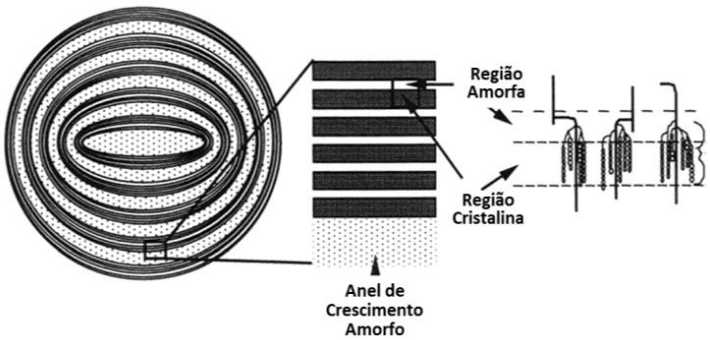

Fonte: Vandeputte; Delcour, 2004

Como material polimérico, o interesse sobre o amido tem crescido ultimamente devido a sua abundância, baixo custo, biodegradabilidade e por permitir o processamento através das técnicas convencionais aplicadas aos polímeros sintéticos (RODRIGUEZ-GONZALEZ; RAMSAY; FAVIS, 2004).

3 Amido Termoplástico (TPS)

O amido é um material abundante, renovável, de baixo custo e biodegradável que representa uma alternativa aos plásticos sintéticos (VAN SOEST; VLIEGENTHART, 1997). Para a obtenção de um material termoplástico a base de amido, sua estrutura granular precisa ser destruída para dar origem a uma matriz polimérica homogênea e essencialmente amorfa (SOUZA; ANDRADE, 2000).

Durante o tratamento térmico, em umidade reduzida, a obtenção de uma fase amorfa de amido requer a fusão das estruturas cristalinas, que se inicia com a desorganização interna dos grânulos de amido. Durante o processamento mecânico, o grânulo tem sua estrutura desestruturada, isto é, o cisalhamento induz a fragmentação das estruturas granulares, que resultam apenas em perda parcial da cristalinidade. Mesmo com elevado cisalhamento, este processo isoladamente não é capaz de levar ao completo rompimento dos cristais. Assim, durante o processamento, as ações concomitantes da temperatura e cisalhamento são necessárias para a obtenção de amido essencialmente amorfo e homogêneo, a nível macroscópico (Figura 3) (LIU et al., 2009; AVÉROUS, 2004; BARRON et al., 2001).

O material obtido após o processamento térmico e mecânico tem uma composição complexa, sendo formado por grânulos de amido parcialmente fundidos, deformados ou completamente rompidos, ou ainda intactos, mostrando al guma cristalinidade residual, dependendo das condições de processo adotadas. Entretanto, uma rede contínua de amido termoplástico amorfo é obtida em elevadas temperaturas e sob cisalhamento. Esse material é denominado amido termoplástico (TPS) e pode ser processado via extrusão, moldagem por injeção, moldagem por compressão e prensagem a quente (LIU et al., 2009; VAN SOEST; VLIEGENTHART, 1997; VAN SOEST et al., 1996).

Figura 3 – Representação esquemática da desestruturação do amido sob cisalhamento e temperatura.

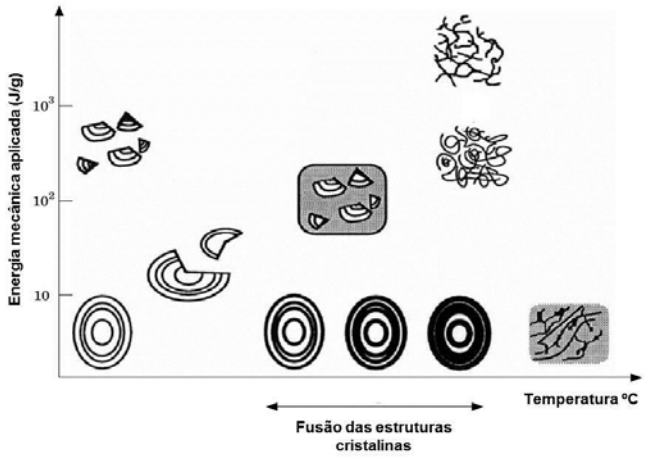

Fonte: Barron et al., 2001.

Embora seja um material promissor, a aplicação comercial do amido termoplástico é ainda limitada, devido à fragilidade e susceptibilidade à umidade dos materiais resultantes (MIRANDA; CARVALHO, 2011). Com o objetivo de substituir os polímeros convencionais por TPS, as desvantagens associadas a esse material devem ser superadas. Ainda, considerando a possibilidade de diversas aplicações, características específicas como rigidez, flexibilidade e força tornam-se necessárias (BELIBI et al., 2013).

Durante o processo de extrusão, os grânulos de amido são expostos a elevadas temperaturas e cisalhamento e sofrem alterações estruturais. Para que o amido se comporte como um material termoplástico, a adição de um plastificante é essencial (RODRIGUEZ-GONZALEZ; RAMSAY; FAVIS, 2004). Os plastificantes atuam reduzindo as forças intermoleculares atrativas entre as macromoléculas, principalmente ligações de hidrogênio, resultando em um aumento do volume livre entre as cadeias e tornando a matriz menos densa (REN et al., 2009; ALVES et al., 2007; PARRA et al., 2004).

A água é o plastificante mais popular em materiais a base de amido, entretanto amido termoplástico plastificado somente com água é frágil (LIU et al., 2009). Assim, existem relatos de diversos outros plastificantes que podem ser aplicados na obtenção de TPS, como a uréia, sacarose, glicerol e sorbitol (MALI et al., 2005; GALDEANO et al., 2009). Entre eles, o glicerol está entre os plastificantes mais utilizados (SHI et al., 2007a; MALI et al., 2004).

O amido termoplástico tende a exibir menor viscosidade quando maiores concentrações de plastificante são empregadas, o que melhora o fluxo do material e facilita seu processamento, assim como aumenta a flexibilidade do material final e reduz sua temperatura de transição vítrea (Tg), pois confere maior mobilidade molecular devido a sua ação na redução das interações entre as cadeias poliméricas. Com isso, é possível afirmar que a temperatura de transição vítrea de materiais a base de amido é dependente da concentração de plastificante (SOTHORNVIT et al., 2007; RODRIGUEZ-GONZALEZ; RAMSAY; FAVIS, 2004; VAN SOEST; VLIEGENTHART, 1997), assim como suas propriedades de barreira, uma vez que este têm grande afinidade pela água (MÜLLER; YAMASHITA; LAURINDO, 2008).

4 Poli (adipato co-tereftalato de butileno) (PBAT)

A combinação de unidades alifáticas e aromáticas na mesma cadeia de poliéster tem sido uma alternativa interessante na obtenção de novos produtos, combinando biodegradabilidade e alta *performance* (MÜLLER; KLEEBERG; DECKWER, 2001). Nesse contexto insere-se o poli (adipato co-tereftalato de butileno) (PBAT) produzido comercialmente pela combinação de ácido tereftálico, ácido adípico e 1,4-butanodiol (Figura 4) (WITT et al., 1995).

Figura 4 – Estrutura química do poli (adipato co-tereftalato de butileno) (PBAT).

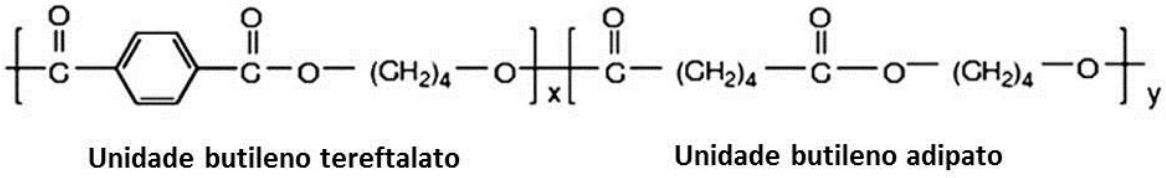

Fonte: FUKUSHIMA et al., 2012.

Nesse polímero, a susceptibilidade à hidrólise de sua parte aromática (PBT) é aumentada pela inclusão de componentes alifáticos (PBA) (Figura 4). Este poliéster sofre degradação inicial pela cisão hidrolítica das cadeias, onde as ligações éster são as mais susceptíveis, seguida pela degradação biológica (catalisada por enzimas) onde os oligômeros são metabolizados pelos microorganismos (MULLER et al., 2001; REN et al., 2009).

O PBAT apresenta boas propriedades mecânicas, térmicas e resistência às condições ambientais, características interessantes que favorecem sua utilização em blendas com amido termoplástico, de modo que a biodegradabilidade seja mantida e as propriedades das blendas sejam melhoradas (REN et al., 2009; RAQUÉZ et al., 2008).

5 Blendas Poliméricas

A composição com outros polímeros biodegradáveis de alto desempenho tem sido amplamente considerada como alternativa para superar as deficiências associadas ao amido termoplástico. Nesse caso, o amido também torna o preço dos polímeros biodegradáveis mais acessíveis, uma vez que é abundante e de baixo custo (MIRANDA; CARVALHO, 2011; REN et al., 2009).

O amido termoplástico pode ser associado a poliésteres e a outros materiais, como celulose ou silicatos, obtendo-se materiais multifásicos. Dessa associação, diferentes tipos de estruturas podem ser obtidos, através de diferentes técnicas de processamento (AVÉROUS, 2004) (Figura 5).

Figura 5 – Esquema de sistemas multifásicos a base de amido termoplástico – Processamento e estruturas.

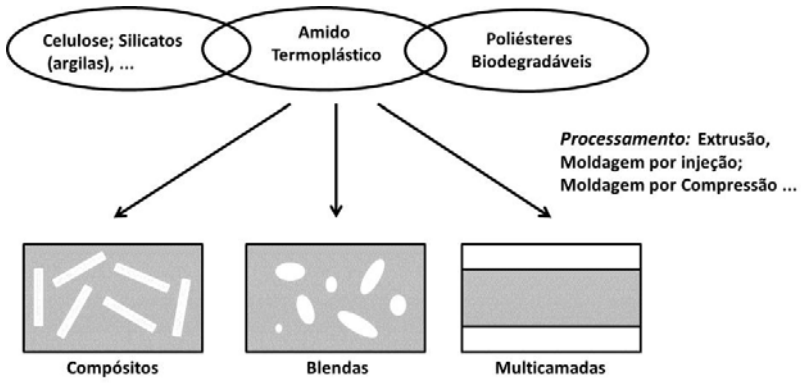

Fonte: Avérous, 2004.

6 Nanocompósitos

O amido termoplástico representa uma resposta promissora no desenvolvimento de materiais biodegradáveis, especialmente para embalagens (AVELLA et al., 2005). A adição de nanoargilas em materiais a base de amido representa uma alternativa ecologicamente favorável, naturalmente abundante e

econômica para superar as deficiências do TPS (CHIVRAC et al., 2010b; TANG; ALAVI; HERALD, 2008; AVÉROUS, 2004).

Nanocompósitos são materiais híbridos, nos quais pelo menos um de seus componentes está em escala nanométrica. Nanocompósitos a base de polímeros e nanoargilas, mesmo contendo concentrações reduzidas de nanosilicatos (< 5 % m/m), tem apresentado bons resultados na melhoria das suas propriedades térmicas, mecânicas e de barreira, assim como em sua biodegradabilidade e inflamabilidade (CORRÊA et al., 2011; TANG; ALAVI; HERALD, 2008; LEE; HANNA, 2008; PARK; KIM; HA, 2007; MCGLASHAN; HALLEY, 2003), quando comparados às matrizes puras, devido à grande área superficial dos nanosilicatos, em relação aos compósitos convencionais, o que resulta em maior interação entre a matriz polimérica e as nanopartículas (CHIVRAC; POLLET; AVÉROUS, 2009; CHIVRAC et al., 2008; OKAMOTO, 2005). A melhoria das propriedades com a inclusão de nanoargilas está relacionada à sua geometria e à área superficial, a qual está intimamente relacionada com seu grau de dispersão na matriz polimérica (CHIVRAC; POLLET; AVÉROUS, 2010a).

Nano-biocompósitos é uma nova classe de materiais híbridos compostos por materiais de reforço, em escala nanométrica, incorporados a uma matriz biodegradável. Essa combinação, com efeitos sinérgicos entre biopolímeros e nanopartículas, como as nanoargilas por exemplo, é uma das rotas mais inovadoras para melhorar as propriedades de materiais como o amido termoplástico (CHIVRAC et al., 2010b).

A incorporação de nanopartículas em uma matriz polimérica pode ser conduzida por meio de três técnicas principais: (a) polimerização *in-situ,* (b) intercalação em solvente e (c) intercalação no estado fundido ou *melt-blending.* No processo de *melt-blending,* tanto o polímero quanto a nanoargila são introduzidos simultaneamente em um dispositivo de mistura (extrusor, misturador interno, etc). Uma vez que as partículas individuais das nanoargilas são mantidas unidas por forças de Van der Waals, o cisalhamento produzido no processo é necessário para superar essas forças e promover sua dispersão na matriz polimérica. O grau de dispersão é um parâmetro importante nas propriedades finais do material (CHIVRAC; POLLET; AVÉROUS, 2009). O método de *melt-blending* tem a vantagem de não utilizar solventes e ser compatível com os processos atuais de

produção industrial, como extrusão, moldagem por injeção e moldagem por compressão (OKAMOTO, 2005; MOHANTY; NAYAK, 2012).

7 Sepiolita

Atualmente, as pesquisas envolvendo nano-biocompósitos a base de amido termoplástico tem sido focadas na utilização de silicatos lamelares, como a montmorilonita (CHIVRAC; POLLET; AVÉROUS, 2009; RAY; OKAMOTO, 2003). Entretanto, existem outros nanofilamentos de diferente estrutura, como a sepiolita, que tem apresentado bons resultados (CHIVRAC et al., 2010c).

Sepiolita é um silicato de magnésio de morfologia fibrosa, com formato semelhante a agulhas e caráter hidrofílico, formada pela alternância de blocos e canais microporosos finos de dimensões 0,37 x 1,06 nm^2, paralelos ao comprimento das fibras. Em sua estrutura, cada bloco é constituído basicamente de duas camadas tetraédricas de sílica, que estão encaixadas entre uma camada central octaédrica de magnésio (Figura 6) (CHIVRAC et al., 2010c).

Figura 6 – Estrutura da sepiolita.

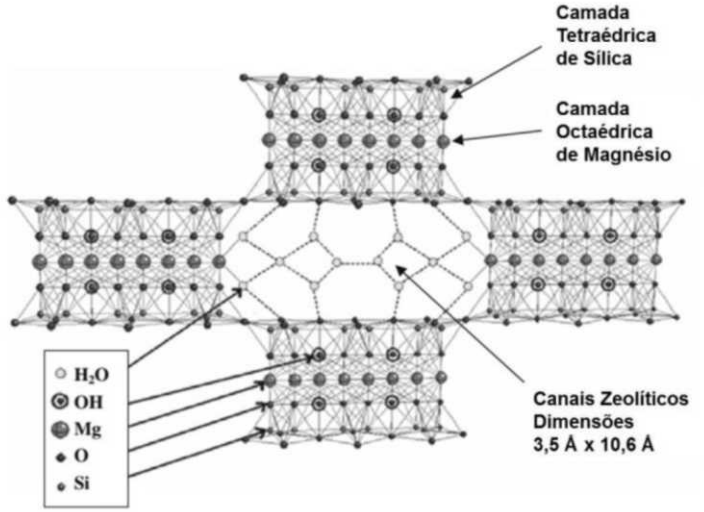

Fonte: Chivrac et al., 2010c.

O tamanho das fibras varia de 10-5000 nm de comprimento por 10-30 nm de largura e 5-10nm de espessura. Sua fórmula estrutural é Si12Mg8O30(OH)4(OH2)4.8H2O, indicando dois tipos de água presente. A água absorvida está ligada por ligações de hidrogênio na superfície externa (água zeolítica) ou no interior dos canais (água de cristalização) e a água que pode ser

identificada na estrutura da sepiolita, sendo chamada de água de constituição (DUQUESNE et al., 2007; CHEN et al., 2007).

A descontinuidade das lâminas de sílica que compõem a estrutura da sepiolita deve-se à presença de grupos silanol (Si-OH) nas bordas dos canais. Essa estrutura composta de canais aumenta a área superficial da sepiolita (maior que $300 m^2.g^{-1}$) e a presença de grupos silanol melhora a adesão interfacial entre a sepiolita e os polímeros, como o amido, devido à ocorrência de ligações de hidrogênio entre os grupos silanol da nanoargila e os grupos -OH das cadeias de amido (CHIVRAC et al., 2010c; CHEN et al., 2007).

A inclusão de sepiolita em matriz de amido termoplástico foi previamente avaliada por Chivrac e colaboradores (2010c). Em comparação com a montmorillonita, foi demostrado que a sepiolita resultou em materiais com maior resistência (maior tensão na deformação) e mais rígidos (maior módulo de Young), sendo esse comportamento atribuído à boa afinidade da sepiolita com as cadeias poliméricas de amido, representando assim, uma nanoargila com potencial para melhorar as propriedades do amido termoplástico.

8 Processamento

A obtenção de blendas e nanocompósitos poliméricos pode ser realizada pelo processo de mistura dos componentes em seu estado fundido. Essa etapa é normalmente realizada por meio de extrusão, processo mais utilizado no processamento de termoplásticos, ou com o auxílio de um misturador interno tipo Haake.

A extrusão representa uma alternativa interessante à tradicional técnica de *casting* para a produção de filmes a base de polissacarídeos, por ser um processo rápido, contínuo, livre de solventes e com ampla faixa operacional (permitindo variações das condições de temperatura e rotação) (LIU et al., 2009; SOTHORNVIT et al., 2007; THUNWALL; BOLDIZAR; RIGDAHL, 2006). É necessária uma grande quantidade de água para a completa gelatinização do amido pela técnica de *casting,* enquanto na extrusão, o processo pode ser conduzido com teores reduzidos de água, com aplicação de cisalhamento, temperatura e alta pressão.

Dentre todos os componentes do extrusor, a rosca é um dos mais importantes. Tem como função fundir, transportar, homogeneizar e plastificar o polímero. Devido ao seu movimento e consequente cisalhamento sobre o material, a rosca gera 80% da energia térmica e mecânica envolvida no processo de extrusão. A rosca deve ser projetada de tal forma que promova máxima eficiência, vazão constante, plastificação e homogeneização adequadas ao material (MANRICH, 2005).

Extrusão-sopro é um método que consiste na extrusão através de uma matriz anelar, sendo o material processado expandido devido ao aumento da pressão no interior do tubo com a injeção de ar comprimido (THUNWALL et al., 2008). Na parte externa da base do "balão", existe um sistema de resfriamento com ar frio jateado, ao longo do tubo (Figura 7). Os filmes tubulares são soprados de forma a atingir uma espessura fina e orientação desejada, sendo sua cristalinidade e orientação dependentes da temperatura e da taxa de resfriamento (MANRICH, 2005).

Figura 7 – Extrusão-sopro de filmes de amido/PBAT.

Um misturador interno tipo Haake também pode ser utilizado para a obtenção de blendas e compósitos poliméricos (Figura 8). Esse equipamento permite a seleção de rotores, velocidade e temperatura adequados a fornecer energia térmica e mecânica suficiente para a fusão das fases poliméricas

(desestruturação/ gelatinização no caso específico do amido). Ainda, permite registro da variação do torque no interior da mistura durante o processamento, fornecendo dados importantes sobre o comportamento das blendas no estado fundido.

Figura 8 – Misturador interno (Haake) e rotores tipo *roller.*

No entanto, misturas poliméricas homogêneas são difíceis de serem obtidas devido à imiscibilidade inerente à maioria dos polímeros, como no caso do amido termoplástico (hidrofílico) e do PBAT (hidrofóbico). Uma estratégia, nesse caso, para a obtenção de materiais compatíveis, seria a adição de um agente compatibilizante, que promove a compatibilização pela redução da tensão interfacial, reduzindo a tendência à coalescência da fase dispersa e aumentando a adesão interfacial (AKCELRUD, 2007).

9 Compatibilizantes

O amido, devido a seu caráter hidrofílico, tem pouca ou nenhuma compatibilidade com a maioria dos polímeros sintéticos disponíveis, devido à alta tensão interfacial entre um polímero não polar e um polar (WANG et al., 2007).

O papel do compatibilizante é controlar as propriedades de sistemas multifásicos. Para sua função ser desempenhada de forma eficiente, deve estar localizado na interface entre os domínios de fase das blendas imiscíveis. Os compatibilizantes atuam segundo dois mecanismos distintos: o mecanismo de

natureza termodinâmico, onde atua reduzindo a tensão interfacial entre as fases e o mecanismo de natureza cinética, onde o compatibilizante localizado na interface, reduz a aglomeração dos domínios por estabilização estérica. Ainda não está elucidado qual é o mecanismo dominante no processo de compatibilização de blendas poliméricas (MALIGER et al., 2006).

Entre os métodos utilizados para a compatibilização de blendas poliméricas, a extrusão reativa é uma técnica bastante utilizada e que combina a realização de reações químicas (síntese ou modificação polimérica) e extrusão (mistura, fusão, moldagem e obtenção de blendas) em um processo único, conduzido no interior do extrusor. Essa rota é ainda atrativa do ponto de vista da viabilidade comercial e de custos operacionais, pois permite o processamento/modificação química em apenas uma etapa (RAQUÉZ; NARAYAN; DUBOIS, 2008; MALIGER et al., 2006).

10 Ácidos Orgânicos

Com o objetivo de aumentar a compatibilidade entre amido termoplástico e poliésteres, compatibilizantes como o anidrido maleico (REN et al., 2009; RAQUÉZ et al., 2008) e metileno difenildiisocianato (MDI) (YU et al., 2007) tem sido utilizados para reduzir a tensão interfacial entre as fases. Entretanto, esses componentes podem ser tóxicos se ingeridos. Assim, ácidos carboxílicos, como os ácidos orgânicos, usados como aditivos em blendas biodegradáveis a base de amido termoplástico, representam uma alternativa atóxica, com vantagens evidentes de segurança e compatibilidade com os alimentos, quando o objetivo da produção de tais materiais é a embalagem alimentar (Da RÓZ et al., 2011; CARVALHO et al., 2005).

A modificação química do amido está diretamente relacionada com reações dos grupos hidroxílicos de sua cadeia. Em geral, a esterificação de polissacarídeos com ácidos orgânicos permite a modificação de sua natureza hidrofílica e de suas propriedades mecânicas e térmicas. Aditivos multifuncionais, como os ácidos policarboxílicos, também permitem a reação com um ou mais grupos hidroxílicos, via transesterificação, formando ligações cruzadas entre as cadeias de amido (CONTRERAS et al., 2008).

11 Ácido Cítrico

O ácido cítrico possui um grupo hidroxílico e três grupos carboxílicos em sua estrutura (Figura 9), sendo o componente ácido principal de frutas cítricas. É um aditivo multifuncional na indústria de alimentos, atuando como acidulante, antibacteriano, reforçador do efeito de antioxidantes ou como melhorador de sabor em sucos e refrigerantes (YUN; NA; YOON, 2006).

Ácido cítrico tem sido frequentemente aplicado em materiais à base de amido termoplástico. Diversos autores relataram a ocorrência de ligações éster entre as moléculas de ácido cítrico e as hidroxilas das cadeias de amido, tornando-o mais hidrofóbico (SHI et al., 2007b) ou ainda a realização de ligações cruzadas (transesterificação) entre cadeias de amido (REDDY; YANG, 2010). Ainda, o ácido cítrico pode formar fortes ligações de hidrogênio com o amido e, quando não participa das reações de esterificação, pode atuar como plastificante (SHI et al., 2008; HOLSER, 2008).

Olivato et al. (2011, 2012) mostraram que a adição de ácido cítrico em filmes soprados de amido/PBAT contribuiu para melhoria das propriedades térmicas, mecânicas e de barreira, observando-se melhores resultados com este componente em comparação com o anidrido maleico, na compatibilização das blendas.

Figura 9 – Estrutura química do ácido cítrico.

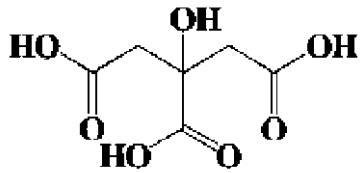

Adicionalmente, por se tratar de um ácido orgânico, atua na hidrólise acido-catalisada das ligações éter da cadeia do polissacarídeo, acelerando a dissolução dos grânulos de amido e facilitando seu processamento. Contudo, se não controlada, resulta em intensa redução de sua massa molecular, o que deteriora as propriedades mecânicas dos materiais produzidos.

A ação hidrolítica é catalisada pela umidade residual do amido e sua extensão depende da força do ácido utilizado, sua concentração e das condições de processo (CHABRAT et al., 2012; CARVALHO et al., 2005; WANG et al., 2009).

Miranda e Carvalho (2011) mostraram que a adição de ácido cítrico foi efetiva na melhoria da compatibilidade em blendas de amido termoplástico e polietileno. Wang et al.(2007) mostraram que o ácido cítrico foi eficiente em melhorar as propriedades mecânicas de blendas de amido termoplástico e polietileno de baixa densidade. A ação compatibilizante do ácido cítrico em blendas de TPS e poli (ácido lático) (PLA) também foi evidenciada por Chabrat e colaboradores (2012).

12 Ácido Tartárico

Ácido tartárico possui dois grupos hidroxílicos e dois grupos carboxílicos em sua estrutura (Figura 10) (YUN; NA; YOON, 2006). É um ácido orgânico de ocorrência natural, que faz parte da composição de frutas como banana, tamarindo e uvas, sendo sua concentração determinante nos níveis de acidez de vinhos. É comumente utilizado na indústria de alimentos, como aditivo em bebidas, entre outros (CHIN et al., 2012; YOON; CHOUGH; PARK, 2006).

Figura 10 – Estrutura química do ácido tartárico.

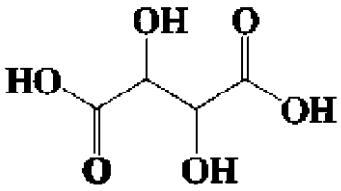

Por se tratar de um ácido dicarboxílico, é capaz de realizar reações de esterificação com as hidroxilas livres da molécula de amido, como demostrado por CHIN et al. (2012) (Figura 11).

Figura 11 – Esquema da reação de esterificação entre amido e ácido tartárico.

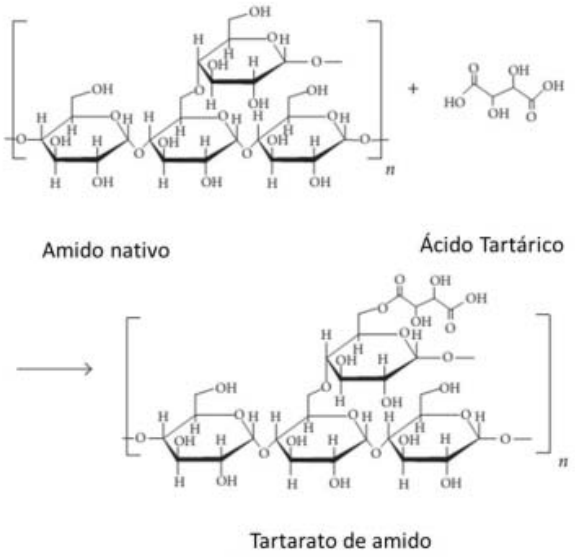

Yun e Yoon (2010) mostraram melhores propriedades mecânicas de filmes produzidos por *casting,* à base de amido e poli (álcool vinilico) adicionados de ácido tartárico, sendo estes resultados superiores aos observados para os filmes contendo apenas glicerol e semelhantes aos obtidos para a blenda contendo ácido cítrico. Esse fato aponta para a potencial utilização do ácido tartárico como compatibilizante em blendas contendo amido, por meio de reações de esterificação, tornando o amido mais hidrofóbico.

13 Ácido Málico

O ácido málico possui em sua estrutura química um grupo hidroxílico e dois grupos carboxílicos (Figura 12). De ocorrência natural em muitas frutas e plantas, é amplamente utilizado como aditivo na indústria de alimentos (YOON; CHOUGH; PARK, 2006).

Figura 12 – Estrutura química do ácido málico.

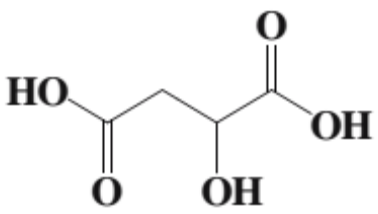

Yun, Na e Yoon (2006) mostraram que a inclusão de ácido málico foi eficiente no aumento da resistência máxima à tração e elongação de filmes contendo amido / poli (álcool vinílico) (PVA), produzidos por *casting.* Segundo os autores, efeito semelhante também foi observado para o ácido tartárico.

14 Referências

AKCELRUD, L. **Fundamentos da Ciência dos Polímeros.** Barueri, SP: Manole, 2007.

ALVES, V. D; MALI, S; BELEIA, A; GROSSMANN, M. V. E. Effect of glycerol and amylose enrichment on cassava starch films properties, **Journal of Food Engineering,** v. 78, p. 941-946, 2007.

AVELLA, M; VLIEGER, J. J ; ERRICO, M. E ; FISCHER, S; VACCA, P; VOLPE, M. G. Biodegradable starch/clay nanocomposite films for food packaging applications. **Food Chemistry,** v. 93, p. 467-474, 2005.

AVEROUS, L. Biodegradable multiphase systems based on plasticized starch: A review. **Journal of Macromolecular Science Part C - Polymer Reviews,** v. C44, n. 3, p. 231-274, 2004.

AVÉROUS, L; FRINGANT, C. Association between plasticized starch and polyesters: Processing and performance of injected biodegrdable systems. **Polymer Engineering and Science,** v. 41, p. 727-734, 2001.

AVEROUS, L; FRINGANT, C; MORO, L. Starch-based biodegradable materials suitable for thermoforming packaging. **Starch/Starke,** v. 53, p. 368-371, 2001.

BARRON, C; BOUCHET, B; DELLA VALLE, G ; GALLANT, D. J ; PLANCHOT, V. Microscopical study of the destructuring of waxy maize and smooth pea starches by shear and heat at low hydration. **Journal of Cereal Science,** v. 33, p. 289-300, 2001.

BELIBI, P. C; DAOU, T. J; NDJAKA; J-M. B; MICHELIN, L; BRENDLE, J; NSOM, B ; DURAND, B. Tensile and water barrier properties of cassava starch composite films reinforced by synthetic zeolite and beidellite. **Journal of Food Engineering,** v. 115, p. 339-346, 2013.

BORDES, P; POLLET, E; AVEROUS, L. Nano-biocomposites: Biodegradable polyester/nanoclay systems. **Progress in Polymer Science,** v. 34, p. 125-155, 2009.

CARVALHO, A. J. F; ZAMBOM, M. D; CURVELO, A. A. S; GANDINI, A. Thermoplastic starch modification during melt processing: Hydrolysis catalyzed by carboxylic acids. **Carbohydrate Polymers,** v. 62, p. 387-390, 2005.

CHABRAT, E; ABDILLAHI, H; ROUILLY, A; RIGAL, L. Influence of citric acid and water on thermoplastic wheat flour/poly(lactic acid) blends: Thermal, mechanical and morphological properties. **Industrial Crops and Products,** v. 37, p. 238-246, 2012.

CHEN, H; ZHENG, M; SUN, H; JIA, Q. Characterization and properties of sepiolite/polyurethane nanocomposites. **Materials Science and Engineering A,** v. 445-446, p. 725-730, 2007.

CHIN, S. F; PANG, S. C; LIM, L. S. Synthesis and characterization of novel water soluble starch tartarate nanoparticles. **ISRN - Materials Science,** v. 2012, p. 1-5, 2012.

CHIVRAC, F; POLLET, E; SCHMUTZ, M; AVEROUS, L. New approach to elaborate exfoliated starch-based nanobiocomposites. **Biomacromolecules,** v. 9, p. 896-900, 2008.

CHIVRAC, F; POLLET, E; AVEROUS, L. Progress in nano-biocomposites based on polysaccharides and nanoclays. **Materials Science and Engineering R,** v. 67, p. 1-17, 2009.

CHIVRAC, F; POLLET, E; AVEROUS, L. Shear induced clay organo-modification: application to plasticized starch nano-biocomposites. **Polymer Advanced Technologies,** v. 21, p. 578-583, 2010a.

CHIVRAC, F; POLLET, E; DOLE, P; AVEROUS, L. Starch-based nano-biocomposites: Plasticizer impact on the montmorillonite exfoliation process. **Carbohydrate Polymers,** v. 79, p. 941-947, 2010b.

CHIVRAC, F; POLLET, E; SCHMUTZ, M; AVEROUS, L. Starch nano-biocomposites based on needle-like sepiolite clays. **CarbohydratePolymers,** v. 80, p. 145-153, 2010c.

CONTRERAS, O. I. P; PERILLA, J. E. P; ENCISO, N. A. A. Revisión de lamodificación química delalmidóncon ácidos orgânicos. **RevistaIngenería e Investigación,** v. 28, n. 3, p. 47-52, 2008.

CORREA, M. C. S; BRANCIFORTI, M. C; POLLET, E; AGNELLI, J. A. M; NASCENTE, P. A. P; AVÉROUS, L. Elaboration and characterization of nano-biocomposites based on plasticized poly(hydroxybutyrate-co-hydroxyvalerate) with organo-modified montmorillonite. **Journal of Polymer and Environment,** v. 20, p. 283-290, 2011.

DA ROZ, A. L; ZAMBON, M. D; CURVELO, A. A. S; CARVALHO, A. J. F. Thermoplastic starch modified during melt processing with organic acids: The effect of molar mass on thermal and mechanical properties. **Industrial Crops and Products,** v. 33. p. 152-157, 2011.

DUQUESNE, E; MOINS, S; ALEXANDRE, M; DUBOIS, P. How can nanohybrids enhance polyester/sepiolite nanocomposite properties?**Macromolecular Chemistry and Physics,** v. 208, p. 2542-2550, 2007.

FUKUSHIMA, K; TABUANI, D; ABBATE, C; ARENA, M; FERRERI, L. Effect of sepiolite on the biodegradation of poly(lactic acid) and polycaprolactone. **Polymer Degradation and Stability,** v. 95, p. 2049-2056, 2010.

GALDEANO, M. C; GROSSMANN, M. V. E; MALI, S; BELLO-PEREZ, L. A; GARCIA, M. A; ZAMUDIO-FLORES, P. B. Effects of production process and plasticizers on stability of films and sheets of oat starch. **Materials Science and Engineering C,** v. 29, p. 492-498, 2009.

HOLSER, R. A. Thermal analysis of glycerol citrate/starch blends. **Journal of Applied Polymer Science,** v.110, p. 1498-1451, 2008.

LAROTONDA, F. D. S; MATSUI, K. N; SOLDI, V; LAURINDO, J. B. Biodegradable films made from raw and acetylated cassava starch. **Brazilian Archives of Biology and Technology,** v. 43, n. 3, p.477-484, 2004.

LEONEL, M; CEREDA, M. P. Caracterização fisico-química de algumas tuberosas amiláceas. **Ciência e Tecnologia de Alimentos,** v. 22, n. 1, p. 65-69, 2002.

LIU, H; XIE, F; YU, L; CHEN, L; LI, L. Thermal processing of starch-based polymers. **Progress in Polymer Science,** v. 34, p. 1348-1368, 2009.

MALI, S; GROSSMANN, M. V. E; YAMASHITA, F. Filmes de amido: produção, propriedades e potencial de utilização. **Semina: Ciências Agrárias,** v. 31, n. 1, p.137-156, 2010.

MALI, S; GROSSMANN, M. V. E; GARCIA, M. A. MARTINO, M. N; ZARITZKY, N. E. Barrier, mechanical and optical properties of plasticized yam starch films. **Carbohydrate Polymers,** v. 56, p. 129-135, 2004.

MALI, S; SAKANAKA, L. S; YAMASHITA, F; GROSSMANN, M. V. E. Water sorption and mechanical properties of cassava starch films and their relation to plasticizing effect. **Carbohydrate Polymers,** v. 60, p. 283-289, 2005.

MALIGER, R. B; McGLASHAN, S. A; HALLEY, P. J; MATTHEW, L. G. Compatibilization of starch-polyester blends using reactive extrusion. **Polymer Engineering and Science,** v. 46, n. 3, p. 248-263, 2006.

MANRICH, S. **Processamento de Termoplásticos: Rosca única, extrusão e matrizes, injeção e moldes.** São Paulo: Artliber Editora, 2005.

McGLASHAN, S. A; HALLEY, P. J. Preparation and characterization of biodegradable starch-based nanocomposite materials. **Polymer International,** v. 52, p. 1767-1773, 2003.

MIRANDA, V. R; CARVALHO, A. J. F. Blendas compatíveis de amido termoplástico e polietileno de baixa densidade compatibilizadas com ácido cítrico. **Polímeros: Ciência e Tecnologia,** v. 21, n. 5, p. 353-360, 2011.

MOHANTY, S; NAYAK, S. K. Biodegradable nanocomposites of poly(butylene adipate-co-terephthalate) (PBAT) and organically modified layered silicates. **Journal of Polymers and the Environment,** v. 20, p. 195-207, 2012.

MULLER, C. M. O; YAMASHITA, F; LAURINDO, J. B. Effect of compatibilizer distribution on the blends of starch/biodegradable polyesters. **Carbohydrate Polymers,** v. 72, p. 82-87, 2008.

MÜLLER, R-J; KLEEBERG, I; DECKWER, W-D. Biodegradation of polyesters containing aromatic constituents. **Journal of Biotechnology,** v. 86, p. 87-95, 2001.

OLIVATO, J. B; GROSSMANN, M. V. E; YAMASHITA, F; NOBREGA, M. M; SCAPIN, M. R. S; EIRAS, D; PESSAN, L. A. Compatibilisation of starch/poly(butylene adipate co-terephthalate) blends in blown films. **International Journal of Food Science and Technology,** v. 46, p. 1934-1939, 2011.

OLIVATO, J. B; GROSSMANN, M. V. E; YAMASHITA, F; EIRAS, D; PESSAN, L. A. Citric acid and maleic anhydride as compatibilizers in starch/poly(butylene adipateco-terephthalate) blends by one-step reactive extrusion. **Carbohydrate Polymers,** v. 87, p. 2614-2618, 2012.

OKAMOTO, M. Biodegradable polymer/layered silicate nanocomposites: A review. **Handbook of biodegradable polymeric materials and their applications,** v. 1, p. 1-45, 2005.

PARRA, D. F; TADINI, C. C; PONCE, P; LUGAO, A. B. Mechanical properties and water vapor transmission in some blends of cassava starch edible films. **Carbohydrate Polymers,** v. 58, p. 475-481, 2004.

PARK, H. M; KIM, G. H; HA, C. S. Preparation and characterization of biodegradable aliphatic polyester/thermoplastic starch/organoclay ternary hybrid nanocomposites. **Composite Interfaces,** v.14, n. 5-6, p. 427-438, 2007.

RAQUEZ, J. M; NARAYAN, R; DUBOIS, P. Recent advances in reactive extrusion processing of biodegradable polymer-based compositions. **Macromolecular Materials and Engineering,** v. 293, p. 447-470, 2008.

RAY, S. S; OKAMOTO, M. Polymer/layered silicate nanocomposites: a review from preparation to processing. **Progress in Polymer Science,** v. 28, p. 1539-1641, 2003.

REN, J; FU, H; REN, T; YUAN, W. Preparation, characterization and properties of binary and ternary blends with thermoplastic starch, poly(lactic acid) and poly(butylene adipate-co-terephthalate). **Carbohydrate Polymers,** v. 77, p. 576-582, 2009.

REDDY, N; YANG, Y. Citric acid cross-linking of starch films. **Food Chemistry,** v. 118, p. 702-711, 2010.

RODRIGUEZ-GONZALEZ, F. J; RAMSAY, B. A; FAVIS, B. D. Rheological and thermal properties of thermoplastic starch with high glycerol content. **Carbohydrate Polymers,** v. 58, p. 139-147, 2004.

SHI, R; LIU, Q; DING, T; HAN, Y; ZHANG, L; CHEN, D; TIAN, W. Ageing of soft thermoplastic starch with high glycerol content. **Journal of Applied Polymer Science,** v. 103, p. 574-586, 2007a.

SHI, R; ZHANG, Z; LIU, Q; HAN, Y; ZHANG, L ; CHEN, D ; TIAN, W. Characterization of citric acid/glycerol co-plasticized thermoplastic starch prepared by melt blending. **Carbohydrate Polymers,** v. 69, p. 748-755, 2007b.

SHI, R; BI, J; ZHANG, Z; ZHU, A; CHEN, D; ZHOU, X; ZHANG, L; TIAN, W. The effect of citric acid on the structural properties and cytotoxicity of the polyvinyl alcohol/starch films when molding at high temperature. **CarbohydratePolymers,** v. 74, p. 763-770, 2008.

SOUZA, R. C. R; ANDRADE, C. T. Investigação dos processos de gelatinização e extrusão de amido de milho. **Polímeros: Ciência e Tecnologia,** v. 10, n. 1, p. 24-30, 2000.

SOTHORNVIT, R; OLSEN, C. W; McHUGH, T. H; KROCHTA, J. M. Tensile properties of compression-molded whey protein sheets: Determination of molding condition and glycerol-content effects and comparison with solution-cast films. **Journal of Food Engineering,** v. 78, p. 855-860, 2007.

TANG, X; ALAVI, S; HERAL, T. J. Effects of plasticizers on the structure and properties of starch-clay nanocomposite films. **Carbohydrate Polymers,** v. 74, p. 552-558, 2008.

THARANATHAN, R. N. Starch - Value addition by modification. **Critical Reviews in Food Science and Nutrition,** v. 45, p. 371-384, 2005.

THUNWALL, M; BOLDIZAR, A; RIGDAHL, M. Extrusion processing of high amylose potato starch materials. **Carbohydrate Polymers,** v. 65, p. 441-446, 2006.

THUNWALL, M; KUTHANOVA, V; BOLDIZAR, A; RIGDAHL, M. Film blowing of thermoplastic starch. Carbohydrate Polymers, v. 71, 583-590, 2008.

VANDEPUTTE, G. E; DELCOUR, J. A. From sucrose to starch granule to starch physical behaviour: a focus on rice starch. **Carbohydrate Polymers,** v. 58, p. 245-266, 2004.

VAN SOEST, J. J. G; HELLEMAN, S. H. D; de WIT, D; VLIEGENTHART, J. F. G. Crystallinity in starch bioplastics. **Industrial Crops and Products,** v. 5, p. 11-22, 1996.

VAN SOEST, J. J. G; VLIEGENTHART, J. F. G. Crystallinity in starch plastics: consequences for material properties. **Trends in Biotechnology,** v. 15, p. 208-213, 1997.

YOON, S. D; CHOUGH, S. H; PARK, H. R. Effects of additives with different functional groups on the physical properties of starch/PVA blend film. **Journal of Applied Polymer Science,** v. 100, p. 3733-3740, 2006.

YU, L; DEAN, K; YUAN, Q; CHEN, L; ZHANG, X. Effect of compatibilizer distribution on the blends of starch/biodegradable polyesters. **Journal of Applied Polymer Science,** v. 103, p. 812-818, 2007.

YUN, Y. H; YOON, S. D. Effect of amylose contents of starches on physical properties and biodegradability of starch/PVA-blended films. **Polymer Bulletin,** v. 64, p. 553-568, 2010.

YUN, Y. H; NA, Y. H; YOON, S. D. Mechanical properties with the functional group of additives for starch/PVA blend film. **Journal of Polymers and the Environment,** v. 14, n. 1, p. 71-78, 2006.

WANG, N; YU, J; MA, X; WU, X. The influence of citric acid on the properties of thermoplastic starch/linear low-density polyethylene blends. **Carbohydrate Polymers,** v. 67, p. 446-453, 2007.

WANG, N; ZHANG, X; HAN, N; SHIHE, B. Effect of citric acid and processing on the performance of thermoplastic starch/montmorillonite nanocomposites. **Carbohydrate Polymers,** v. 76, p. 68-73, 2009.

WITT, U; MULLER, R. J; DECKWER, W. D. New biodegradable polyester-copolymers from commodity chemicals with favourable use properties. **Journal of Environmental Polymer Degradation,** v. 3, p. 215-223, 1995.

ZULLO, R; IANNACE, S. The effects of different starch sources and plasticizers on film blowing of thermoplastic starch: Correlation among process, elongational properties and macromolecular structure. **Carbohydrate Polymers,** v. 77, p. 376383, 2009.

CAPITULO 2 – EFFECT OF ORGANIC ACIDS AS ADDITIVES ON THE PERFORMANCE OF THERMOPLASTIC STARCH/POLYESTER BLOWN FILMS

ABSTRACT: The influence of citric acid (CA), malic acid (MA) and tartaric acid (TA) in starch/poly (butylene adipate co-terephthalate) blown films was evaluated by examining the barrier, structural and mechanical properties of the films. These properties were analysed in different relative humidities. Greater concentrations of TA and CA (1.5 %wt) produced films with improved tensile strength (6.8 ± 0.3 and 6.7 ± 0.3 MPa, respectively), reduced water vapour permeability and a more homogeneous structure. The compatibilising effect of MA was less efficient, as shown in the scanning electron microscopy (SEM) images. Changes in the relative humidity (RH) affected the elongation of the films, which reached values of 5.7 ± 0.5 at 33% RH and increased to 312.4 ± 89.5% at 53% RH. The FT-IR spectra showed no additional reactions caused by the incorporation of the additives, and the observed results are attributed to the esterification reactions and/or hydrolysis of the starch, producing films with interesting properties. This process represents an alternative to the use of non-biodegradable materials.

Keywords*:* Starch/PBAT films. Compatibilisers. Organic acids. Mechanical properties. Relative humidity.

1 Introduction

Efforts have been made to produce totally biodegradable packaging that exhibits a good performance to ensure market needs. Starch is an inexpensive polysaccharide that is obtained from renewable resources. Its use in packaging development has been extensively studied, and it can be transformed to a melted thermoplastic (TPS) by an extrusion process with the inclusion of plasticisers, such as glycerol, which is the most used (LIU et al., 2009; NABAR et al., 2005). Chemical modification by reactive extrusion using organic acids could be useful to obtain TPS with modified properties (CARVALHO et al., 2005). However, the mixture of the thermoplastic starch with another polymer is necessary to improve the properties of the final product (LU et al., 2009).

The main drawback of starch-based biodegradable films is their sensitivity to environmental conditions. Because of its high character hydrophilic, starch tends to absorb greater quantities of water under conditions of high relative humidity (MALI et al., 2005; GALDEANO et al., 2009). Blends containing TPS and biodegradable synthetic polyesters, such as poly (butylene adipate co-terephthalate)

(PBAT), are interesting for these applications because the polyester has good mechanical and barrier properties that could overcome the limitations of TPS (REN et al., 2009; RAQUEZ et al., 2008; NABAR et al., 2005).

Organic acids are naturally present in fruits and vegetables, and they are synthesised by microorganisms during the fermentation process (ESWARANANDAM et al., 2004). Citric acid has been used as an additive in corn starch films to promote crosslinking (REDDY and YANG, 2010), it has been used in TPS/PLA (polylactic acid) blends to improve the interaction between the polymeric phases and produce films with better properties (WANG et al., 2010) and it has been used in TPS/PVA (polyvinyl alcohol) blends to improve the compatibility of the polymeric phases and the mechanical stability of the materials (SHI et al., 2008).

In this context, it is expected that citric, malic and tartaric acids, which are polycarboxylic acids, will act to promote esterification (grafting) and transesterification reactions (cross-linking) between polymers, improving the compatibility between the starch chains (hydrophilic) and the PBAT (hydrophobic), which will add to the plasticising effect and acid hydrolysis of the starch. Consequently, the influence of citric acid (CA), malic acid (MA) and tartaric acid (TA) on the mechanical, structural and barrier properties of cassava starch/PBAT blown films produced by reactive extrusion were evaluated in this study. The influence of the relative humidity on the mechanical properties of the films was also investigated.

2 Experimental

2.1 MATERIALS

The films were produced with native cassava starch obtained from Indemil (Brazil), glycerol, which was used as a plasticiser, (Dinâmica, Brazil) and PBAT (poly(butylene adipate co-terephthalate)), supplied by BASF (Ludwigshafen, Germany) under the commercial name Ecoflex®. The tartaric acid, malic acid and citric acid were supplied by Sigma-Aldrich (Steinheim, Germany).

2.2 METHODS

2.2.1 Film Production

Pellets were processed using a laboratory single-screw extruder (model EL-25, BGM, Brazil) with a screw diameter (D) of 25 mm and a screw length of 28D. The components, PBAT, glycerol, acids and starch (in this order) were manually mixed at the time of extrusion and pelleted with a barrel temperature profile of 100/120/120/120°C from the feeding zone (zone 1) to the die zone (zone 4) at a screw speed of 40 rpm, using a die with six holes of 2 mm diameter. Then, the pellets were extruded again to produce films with a barrel temperature profile of 100/120/120/130°C for the four zones and 130°C for the 50 mm film-blowing die with internal air for the formation of the film "bubble" and a screw speed of 40 rpm was maintained.

All of the developed formulations contain the same concentration of starch/PBAT (a proportion of 55:45, respectively), corresponding to 90 %wt of the total, with the remaining 10 %wt contributed by glycerol and acids, as shown in Table 1, including a control formulation without acid.

Table 1 – Concentration of the organic acids and glycerol in the formulations.

Formulations	*Concentrations*[a]			
	TA	MA	CA	GLY
Control	0.0	0.0	0.0	10.00
TA0.375	0.375	0.0	0.0	9.625
TA0.75	0.75	0.0	0.0	9.25
TA1.5	1.50	0.0	0.0	8.50
MA0.375	0.0	0.375	0.0	9.625
MA0.75	0.0	0.75	0.0	9.25
MA1.5	0.0	1.50	0.0	8.50
CA0.375	0.0	0.0	0.375	9.625
CA0.75	0.0	0.0	0.75	9.25
CA1.5	0.0	0.0	1.50	8.50

a In relation to the total weight of the ternary mixture, the remainder 90 %wt corresponding to cassava starch/PBAT at a ratio of 55:45 wt.
TA=Tartaric acid; MA=Malic acid; CA=Citric acid; GLY=Glycerol.

The feed rate was maintained to ensure that the screw operated at full load, and the film thickness was controlled by the roll speed control and the air-flow rate. These parameters were adjusted for each formulation to maintain a thickness of 100–150 Mm.

2.2.2 Water Vapour Permeability (WVP)

The tests were conducted using the American Society for Testing and Materials ASTM E-96-95 (1996) standard with some modifications. Before the analysis, the samples were stored at 25°C and 53% RH for 48 hours. Each film sample was fixed in the circular opening of a permeation cell with a 60mm internal diameter, and silicone grease was applied to ensure that humidity migration occurred only through the film. The interior of the cell was filled with a magnesium chloride solution (MgCl2 / 32.8% RH), and the device was stored at 25°C in a desiccator to maintain a 42% RH gradient across the film. A saturated sodium chloride solution was used in the desiccator to provide 75% RH.

The samples were weighed every 3 hours during the 72 hours of testing time. Changes in the weight of the cell or mass gain *(m)* were plotted as a function of time *(t)*. The slope of the line was calculated by linear regression (R > 0.99), and the water vapour permeation ratio (WVPR) was obtained with Eq. 1:

$$WVPR = (m/t).(1/A) \qquad \textit{Eq. 1}$$

where *m/t* is the angular coefficient of the curve and *A* is the sample permeation area. The WVP (g/m.s.Pa) was calculated as follows:

$$WVP = WVPR.st/ps[(RH1-RH2)/100] \qquad \textit{Eq. 2}$$

where *st* is the mean sample thickness (m), *ps* is the water vapour saturation pressure at the assay temperature (Pa), *RH1* is the relative humidity of the desiccator and *RH2* is the relative humidity in the interior of the permeation cell. These tests were conducted in duplicate.

2.2.3 Weight Loss in Water

Samples were previously dried for three days in a desiccator containing anhydrous CaCl2 (0% RH). After weighing, the films were immersed in distilled water, maintaining a proportion of 30:1 (water/sample), for 48 hours at 25°C. The samples were then removed and dried at 105°C for 4 hours, and the weight of

the conditioned specimen after treatment was used to determine the % weight loss in water.

2.2.4 Mechanical Properties

A texture analyser, model TA.TX2 *plus* (Stable Micro Systems, Surrey-England) fitted with a 50 kg load cell, was used to determine the tensile properties of the films. The tensile tests were based on the ASTM standard D882-91 (1996). Ten samples of each formulation were cut in the longitudinal direction to a length of 50 mm and a width of 20 mm and fit to the tensile grips. The crosshead speed was set at 0.8 mm/s, and the initial distance between the grips was 30 mm. Before testing, the samples were conditioned at 23 ± 2°C and 53 ± 2% RH for 48 hours. The tensile strength (MPa) and elongation at break (%) were determined.

2.2.5 Scanning Electron Microscopy (SEM) Analysis

A scanning electron microscope FEI model Quanta 200 (FEI Company/Tokyo, Japan) was used to observe the fractured surface of the blown film samples. The samples were submerged in liquid nitrogen and then broken (cryogenic fracture).

Before coating with a gold layer, the samples were stored at 25°C in a desiccator with CaCl2 («0% RH) for 3 days. The coating was produced with a Sputter Coater (BAL-TEC SCD 050). Images were taken of the fractured surface at a magnification of 800x.

2.2.6 Fourier Transform Infrared Spectroscopy (FT-IR)

FT-IR analyses were conducted on the blown films from 4000 to 500 cm^{-1} with a spectral resolution of 4 cm^{-1}. A Perkin-Elmer Spectrum 2000 FT-IR with a Universal Attenuated Total Reflectance (UATR) Pike Miracle module was used. The samples were conditioned in a desiccator containing anhydrous calcium chloride (CaCl2) for 10 days before the analysis.

2.2.7 Statistical Analysis

The data were analysed using STATISTICA 7.0 software (Statsoft, Oklahoma), with analysis of variance (ANOVA) and Tukey's test at a 5% significance level.

3 Results and Discussion

3.1 Water Vapour Permeability (WVP)

The WVP results showed two different response profiles (Figure 1). An increase in the concentration of the citric and tartaric acids from 0.375 %wt to 0.75 %wt led to higher WVP values of the films. However, at a concentration of 1.5 %wt, the opposite effect was observed, and the WVP was reduced. The results suggest that in lower concentrations, both CA and TA are present in small quantities, insufficient to contribute to the cross-linking reactions.

Figure 1 – WVP of the films with TA, MA and CA in different concentrations.

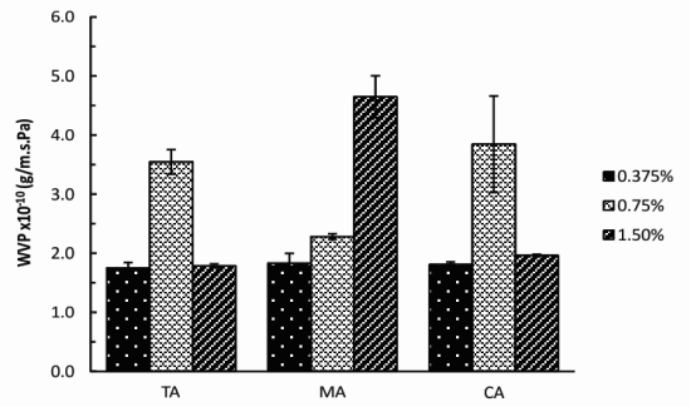

The reduction of the mobility of the polymeric chains, as a result of cross-linking reactions and making the diffusion of water across the film matrix more difficult, can be observed by the lower WVP results when greater concentrations (1.5 %wt) of these acids are used. In intermediary proportions (0.75 %wt), the hydrolytic actions of both CA and TA are more pronounced, resulting in films with greater molecular mobility and as consequence, more permeable to water.

A higher concentration of MA produced films with greater water vapour permeability, possibly because the difficulty in promote transesterification reactions than the other acids evaluated and because it may have contributed to the plasticising effect. The effects of plasticisers on the water vapour permeability of starch-based films have also been evaluated by other authors (MULLER et al., 2008; ALVES et al., 2007; PARRA et al., 2004).

3.2 WEIGHT LOSS IN WATER

Whereas that the control sample (without acids) exhibited a weight loss of 10.48 ± 0.41 % in water, the inclusion of organic acids in the formulations increased the weight loss of the films (Figure 2), causing the weight loss to reach greater values when the concentration of the acids was greater (1.5 %wt).

The organic acids may have promoted the acid hydrolysis of the starch during the film production process, making them more soluble. Moreover, the presence of free acids, which did not react with the polymeric molecules and are broadly soluble in water, could contribute to occurrence of these reactions during the test, which may have been responsible for the observed results. Yoon et al. (2006) observed that the inclusion of glycerol, succinic acid, malic acid and tartaric acid affects the properties of starch/PVA blends, increasing their water solubility, when greater concentrations of the additives are used.

Figure 2 – Weight loss in water (%) of the films with TA, MA and CA in different concentrations.

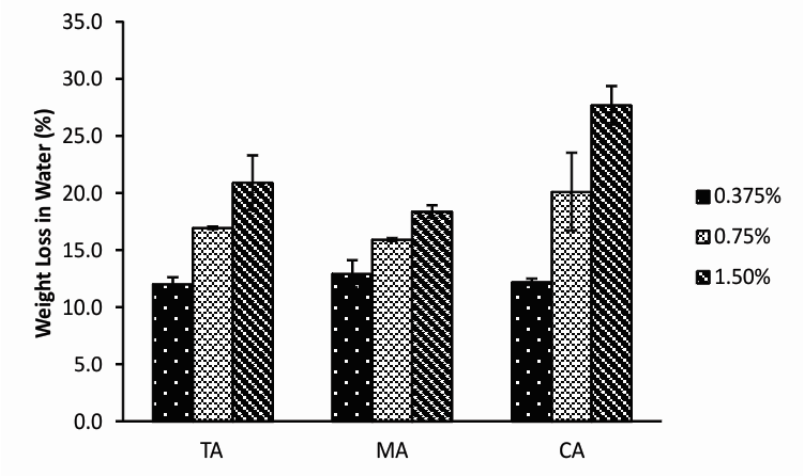

Crosslinking reactions between the polymeric chains may be indicated by the weight loss in water of the films, as described by Reddy and Yang (2010), who reported that starch films with added citric acid underwent crosslinking reactions, producing a denser structure that experienced reduced weight loss and water vapour permeability.

3.3 MECHANICAL PROPERTIES

The mechanical properties were affected by the inclusion of organic acids in the films. Figure 3 shows the tensile strength and elongation of the films that were previously conditioned in 53 ± 2% RH. A difference can be noted between the results observed for the CA and TA and those observed for the MA. More resistant films (higher tensile strength) were obtained when higher concentration of CA and TA (1.5 %wt) or intermediate concentrations of MA (0.75 %wt) were used. In the elongation results, the CA caused a remarkable reduction of this property when added in a concentration of 1.5 %wt.

Figure 3 – Tensile strength (MPa) and elongation at break (%) of the films with TA, MA and CA at different concentrations.

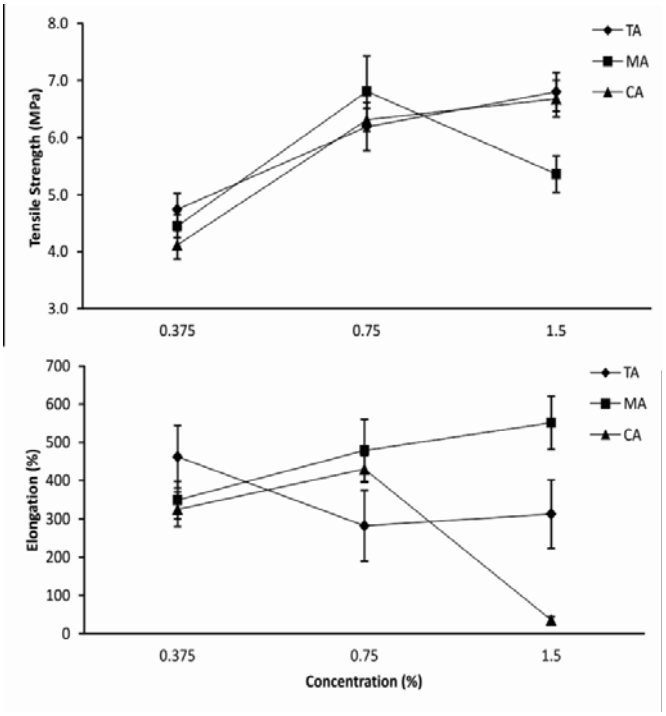

Multifunctional organic acids, such as CA, MA and TA, are able to interact with the hydroxyls of the starch, introducing new groups (carboxyls and esters) to their structure. These new groups represent new potential reactive points for crosslinking reactions, improving the compatibilisation between the polymeric molecules resulting in more resistant films. The action of the organic acids on the acid hydrolysis of starch molecules is known, and it has already been evaluated in other papers (Da ROZ et al., 2011; CARVALHO et al., 2005), which proves that increasing the concentration of acids leads to a reduction of the molecular weight of the starch chains. Consequently, the results shown in this work suggest a combination of these actions, in addition to the plasticising role of the organic acids reported in the study by Shi et al. (2007). This effect causes greater compatibilisation of the polymeric blends.

The citric and tartaric acids contribute to the production of a material with increase tensile strength and reduced elongation when their concentration in the starch/PBAT blend is increased. This result is most likely caused by crosslinking reactions, which interconnect the polymeric molecules and restrict their mobility, in agreement with the results of WVP. The effect of the citric acid and maleic anhydride in the starch/PBAT blends has already been discussed in a previous study (OLIVATO et al., 2012), and Shi et al. (2008) and Reddy and Yang (2010) also reported similar results with the inclusion of CA in starch-based materials.

Although both showed similar behaviour, the addition of CA caused a pronounced decrease in the elongation of the films (with 1.5 %wt), while TA did not significantly alter the results obtained at concentrations of 0.75 %wt or 1.5 %wt. This result shows that, beyond the crosslinking reactions, CA interacts with the polymeric molecules and produces strong hydrogen bonds (SHI et al., 2007). The proliferation of hydrogen bonds makes the movement of chains past each other more difficult, reducing the elongation as a consequence.

With the objective of evaluating the influence of the relative humidity on the mechanical properties, films were conditioned at three relative humidities (33, 53 and 75 ± 2% RH), and these results are shown in Figure 4. In general, as the RH was increased, the tensile strength was reduced for all film formulations. In other words, their mechanical properties deteriorated, and the films became fragile. Greater water content resulted in a pronounced plasticising effect, weakening the polymeric matrix. In the case of the films with added CA, TA and MA, the gain of

water favours acidolysis reactions, which may have been the cause of the lower tensile strength and higher elongation at break, which changed only slightly for the control films (containing only glycerol) as the RH increased.

Greater film tensile strengths were observed at lower relative humidities (33 ± 2%). Nevertheless, in these conditions, the materials are rigid and brittle, making their utilisation as packaging difficult. Galdeano et al. (2009) and Mali et al . (2005) found the same comportment in oat starch- and cassava starch-based films, respectively.

Figure 4 – Tensile strength (MPa) and elongation (%) of the analysed films at relative humidity of 33, 53 and 75% at formulations of TA1.5, MA1.5, CA1.5 and the control.

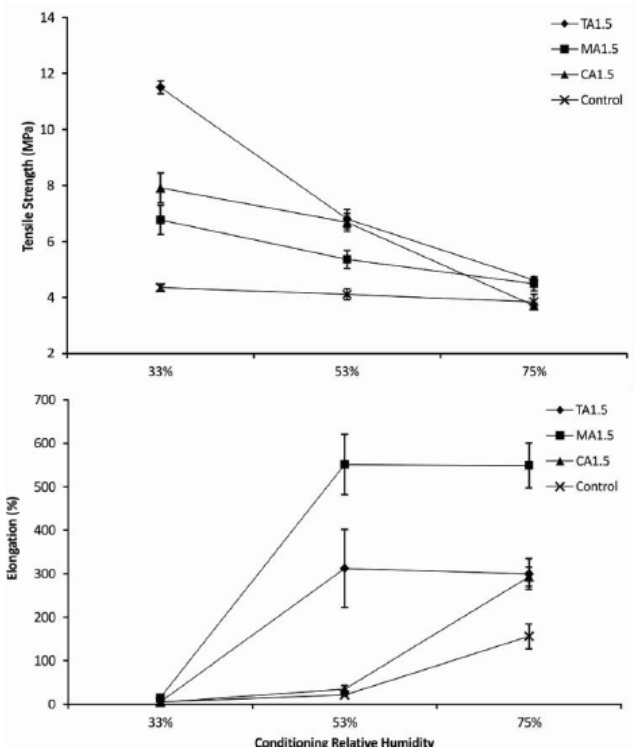

The role of water as a plasticiser produces materials with higher elongation, as observed at Figure 4. In this case, the behaviour of the acids were similar, regardless of the organic acid used, and it was observed that the water content in the films had no clear influence on the mechanical properties past an RH of 53 ± 2%, possibly because the maximum capacity of water absorption of the films was achieved.

3.4 SCANNING ELECTRON MICROSCOPY (SEM) ANALYSIS

The sample morphology was evaluated by scanning electron microscopy, and the resulting images are presented in Figure 5. In these images, it is possible to observe partially fragmented granules of starch in the control sample and the sample containing malic acid (MA1.5), although it is present in small quantities for this sample, which shows that the starch was not completely fragmented. Consequently, a continuous thermoplastic phase is not observed, interfering with the homogeneity of the blend.

Figure 5 – SEM images of fractures of the TA1.5, MA1.5, CA1.5 and Control samples. (Magnification, 800x).

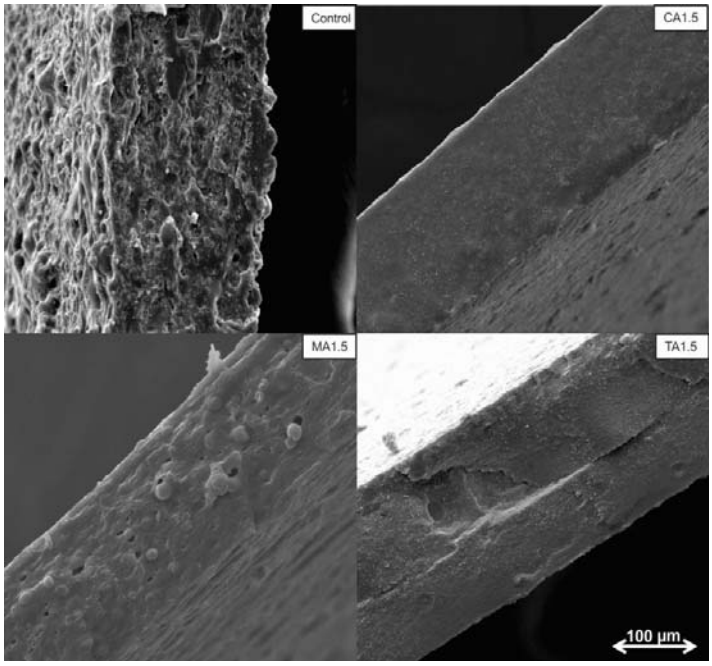

In the samples with citric acid (CA1.5) and tartaric acid (TA1.5), starch granules are not observed in the images (i.e., a visually homogeneous structure was formed). Therefore, we can conclude that both CA as TA acted as better compatibilisers than MA, producing a more uniform and smooth material, which was also indicated by in the improvement of their mechani cal properties. The effect of citric acid on the morphology of blends containing thermoplastic starch was already evaluated in previous works (OLIVATO et al., 2011; WANG et al., 2010).

When considering the dicarboxylic organic acids (TA and MA) and the polycarboxylic acid (CA), we should consider the possibility of intramolecular

hydrogen bonds (RODRIGUES, 2000). This phenomenon could explain the difference in the behaviour of these acids. Citric and tartaric acid have substitution in the carbonic chain, which makes more difficult for the molecule acquire the necessary conformation to form intramolecular hydrogen bonds (steric blocking), which is opposed to MA, that is able to perform intramolecular hydrogen bonds. This could explain the lower efficiency of MA in disrupting the starch granules and promoting esterification reactions. Also, the differences in the molar concentrations for the tested acids must be taken into consideration to explain the results.

This effect would compromise the mechanical properties of the blends because these intermolecular bonds retard the interaction of the acid with the other components of the film. However, some adjustments in the process parameters could be useful to provide the necessary energy for the complete fragmentation and melting of the starch. Wang et al. (2010) observed that the addition of greater quantities of CA to the starch/PLA blends improved both the plasticisation of the starch and the phase dispersion, leading to the production of more homogeneous blends, which could be attributed to acceleration of the fragmentation and dissolution of the starch granules by the acid.

3.5 FOURIER TRANSFORM INFRARED SPECTROSCOPY (FT-IR)

Figure 6 shows the FT-IR spectra (wave numbers between 1800 and 1000 cm^1) of the control starch/PBAT films and those with 1.5% of each organic acid. A peak at approximately 1715 cm^{-1}, produced by a carbonyl stretch attributed to esters, was observed for all of the samples. This visibility is a result of peak coalescence because of the ester bonds naturally present in the PBAT molecules, and also due those which were produced by the esterification and transesterification reactions that occurred during the reactive extrusion process. Consequently, it is not possible to obtain accurate information to discriminate the localisation of these chemical bonds.

The stretch vibrations of C-O in C-OH bonds are observed at 1150 cm^{-1}, and an increase of the peak intensity is noted when the organic acids are present. Similar behaviour is observed for the C-O bond stretching of the C-O-C group in the anhydroglucose ring at 1020 cm^{-1}, which is also amplified in the CA1.5, MA1.5 and TA1.5 samples, relative to the control. The peaks at approximately 1280

and 1123 cm^{-1} are characteristic of C-O in -O-C=O bonds, and a slight increase in their intensity could be observed in samples containing acids, of which CA exhibited the most visible peak. Similar spectra were obtained by Wang et al. (2010) and by Miranda and Carvalho (2011).

In general, all of the sample spectra are similar, showing that the results are produced by the acid hydrolysis of the glycosidic linkages and the esterification and transesterification reactions, whose definition was impaired by overlapping peaks. No additional reactions or modifications to the polymeric matrix could be observed.

Figure 6 – Comparison of FT-IR spectra for the control, MA1.5, TA1.5 and CA1.5.

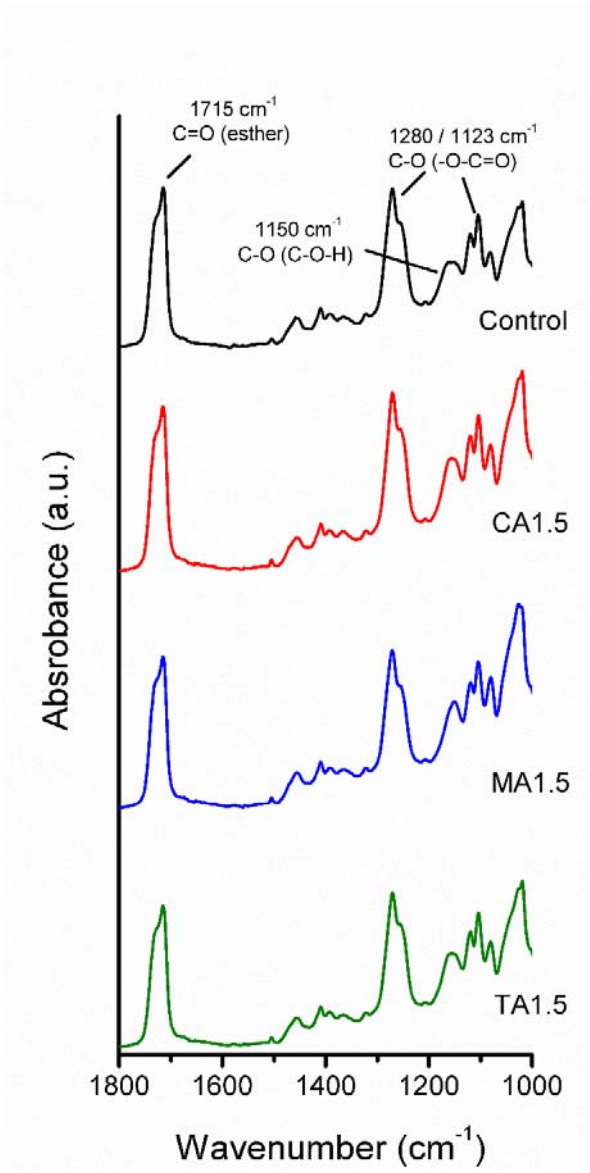

4 Conclusion

The inclusion of organic acids improved the properties of starch/PBAT films because they produced crosslinks that interconnect the polymeric chains, generating more resistant and less permeable films. In addition, organic acids contribute to starch hydrolysis, facilitating the destructuring and disruption of the granules, decreasing the material viscosity, improving the processing properties and producing a more homogeneous matrix, as observed in the scanning electron micrographs.

The increase in the relative humidity led the tensile strength to decrease and increment at elongation of the films because of the role of water as a plasticiser. Thus, biodegradable films with better properties could be produced. These films represent an alternative to synthetic packaging, but their limitations should be respected.

5 References

ALVES, V. D; MALI, S; BELEIA, A; GROSSMANN, M.V.E. Effect of glycerol and amylose enrichment on cassava starch films properties. **Journal of Food Engineering,** v. 78, p. 941-946, 2007.

AMERICAN SOCIETY FOR TESTING AND MATERIAL (ASTM). **Standard test methods for water vapor transmission of material.** E96-95, Philadelphia: ASTM, 1996.

AMERICAN SOCIETY FOR TESTING AND MATERIAL (ASTM). **Standard test methods for tensile properties of thin plastic sheeting**. D882-91, Philadelphia: ASTM, 1996.

CARVALHO, A. J. F; ZAMBON, M. D; CURVELO, A. A. S; GANDINI, A. Thermoplastic starch modification during melt processing: Hydrolysis catalyzed by carboxylic acids. **Carbohydrate Polymers,** v. 62, p. 387-390, 2005.

DA ROZ, A. L; ZAMBON, M. D; CURVELO, A. A. S; CARVALHO, A. J. F. Thermoplastic starch modified during melt processing with or ganic acids: The effect of molar mass on thermal and mechanical properties. **Industrial Crops and Products,** v. 33, p. 152-157, 2011.

ESWARANANDAM, S; HETTIARACHCHY, N. S; MEULLENET, J. F. Effect of malic and lactic acid incorporated soy protein coatings on the sensory attributes of whole apple and fresh-cut cantaloupe. **Journal of Food Science,** v. 71, p. 307-313, 2006.

GALDEANO, M. C; MALI, S; GROSSMANN, M.V.E; YAMASHITA, F; GARCIA, M. A. Effects of plasticizers on the properties of oat starch films. **Materials Science and Engineering C,** v. 29, p. 532-538, 2009.

LIU, H ; XIE, F ; YU, L ; CHEN, L ; LI, L. Thermal processing of starch-based polymers. **Progress in Polymer Science,** v. 34, p. 1348-1368, 2009.

LU, D. R; XIAO, C. M; XU, S. J. Starch-based completely biodegradable polymer materials. **Express Polymer Letters,** v. 3, n. 6, p. 366-375, 2009.

MALI, S; SAKANAKA, L. S; YAMASHITA, F; GROSSMANN, M. V. E. Water sorption and mechanical properties of cassava starch films and their relation to plasticizing effect. **Carbohydrate Polymers,** v. 60, p. 283-289, 2005.

MIRANDA, V. R; CARVALHO, A. J. F. Blendas compatíveis de amido termoplástico e polietileno de baixa densidade compatibilizadas com ácido cítrico. **Polímeros,** v. 21, p. 353-360, 2011.

MULLER, C. M. O; YAMASHITA, F; LAURINDO, J. B. Evaluation of the effects of glycerol and sorbitol concentration and water activity on the water barrier properties of cassava starch films through a solubility approach. **Carbohydrate Polymers,** v. 72, p. 82-87, 2008.

NABAR, Y; RAQUEZ, J. M ; DUBOIS, P ; NARAYAN, R. Production of starch foams by twin-screw extrusion: effect of maleated poly(butylene adipate-co-terephthalate) as a compatibilizer. **Biomacromolecules,** v. 6, p. 807-817, 2005.

OLIVATO, J. B; GROSSMANN, M. V. E; YAMASHITA, F; NOBREGA, M. M; SCAPIN, M. R. S; EIRAS, D; PESSAN, L. A. Compatibilisation of starch/poly(butylene adipate co-terephthalate) blends in blown films. **International Journal of Food Science and Technology,** v. 46, p. 1934-1939, 2011.

OLIVATO, J. B; GROSSMANN, M. V. E; YAMASHITA, F; EIRAS, D; PESSAN, L. A. Citric acid and maleic anhydride as compatibilizers in starch/poly(butylene adipate-co-terephthalate) blends by one-step reactive extrusion. **Carbohydrate Polymers,** v. 87, p. 2614-2618, 2012.

PARRA, D. F; TADINI, C. C; PONCE, P; LUGAO, A. B. Mechanical properties and water vapor transmission in some blends of cassava starch edible films. **Carbohydrate Polymers,** v. 58, p. 475-481, 2004.

RAQUEZ, J. M; NABAR, Y; SRINIVASAN, M; SHIN, B. Y; NARAYAN, R; DUBOIS, P. Maleated thermoplastic starch by reactive extrusion. **Carbohydrate Polymers,** v. 74, p. 159-169, 2008.

REDDY, N; YANG, Y. Citric acid cross-linking of starch films. **Food Chemistry,** v. 118, p. 702-711, 2010.

REN, J; FU, H; REN, T; YUAN, W. Preparation, characterization and properties of binary and ternary blends with thermoplastic starch, poly(lactic acid) and poly(butylene adipate-co-terephthalate). **Carbohydrate Polymers,** v. 77, p. 576-582, 2009.

RODRIGUES, J. A. R. Ligações de hidrogênio fortes em ácidos dicarboxílicos e diaminas aromáticas. **Química Nova,** v. 23, p. 812-817, 2000.

SHI, R; BI, J; ZHANG, Z; ZHU, A; CHEN, D; ZHOU, X; ZHANG, L; TIAN, W. The effect of citric acid on the structural properties and cytotoxicity of the polyvinyl alcohol/starch films when molding at high temperature. **Carbohydrate Polymers,** v. 74, p. 763-770, 2008.

SHI, R; ZHANG, Z; LIU, Q; HAM, Y; ZHANG, L; CHEN, D; TIAN, W. Characterization of citric acid/glycerol co-plasticized thermoplastic starch prepared by melt blending. **Carbohydrate Polymers,** v. 69, p. 748-755, 2007.

YOON, S; CHOUGH, S; PARK, H. Effects of additives with different functional groups on the physical properties of starch/PVA blend film. **Journal of Applied Polymer Science,** v. 100, p. 3733-3740, 2006.

YUN, Y., NA, Y., YOON, S. Mechanical properties with the functional group of additives for starch/PVA blend film. **Journal of Polymers and the Environment,** v. 14, n. 1, p. 71-78, 2006.

WANG, N; ZHANG, X; HAN, N; FANG, J. Effects of water on the properties of thermoplastic starch poly(lacticacid) blend containing citric acid. **Journal of Thermoplastic Composite Materials,** v. 23, p. 19-34, 2010.

CAPITULO 3 – MIXTURE DESIGN APPLIED FOR THE STUDY OF THE TARTARIC ACID EFFECT ON STARCH/POLYESTER FILMS

ABSTRACT: Tartaric acid (TA), a dicarboxylic acid, can act as a compatibiliser in starch/polyester blends. A mixture design was proposed to evaluate the effect of TA on the properties of starch/poly (butylene adipate co-terephthalate) (PBAT) blown films plasticised with glycerol. The interaction between the starch/PBAT and the TA has a positive effect on the tensile strength and puncture force. Additionally, greater proportions of TA increased Young's modulus. The starch+PBAT/TA and Gly/TA interactions contributed to a reduction in the water vapour permeability of the films. The inclusion of TA did not change the crystallinity of the samples. Formulations with intermediate proportions of TA (0.8g/100 g) were shown to produce the best compatibilising effect. This was observed by DMA analysis as a consequence of the perfect equilibrium between the contributions of TA as a compatibiliser and in the acidolysis of starch, resulting in films with a tensile strength of 5.93MPa, a possible alternative to non-biodegradable packaging.

Keywords*:* Starch. Tartaric acid. Glycerol. Mixture design. Blown films.

1 Introduction

Starch has been the focus of several studies whose objective has been to take this biodegradable, inexpensive, and abundant material, obtained from renewable resources and create packaging (LU; XIAO; XU, 2009). During the extrusion process, the granular structure of starch is disrupted by the combination of temperature and shear forces and, in the presence of a plasticiser, forms a melted material called thermoplastic starch (TPS) (AVEROUS et al., 2001).

The use of pure TPS in packaging materials is limited by its low mechanical resistance, the deterioration of its mechanical properties when exposed to environmental conditions (mostly in high humidity conditions) and the difficult processing due to its inherently high viscosity (CONTRERAS et al., 2008; YOON et al., 2006). A proposed alternative that could potentially overcome these deficiencies is to blend TPS with good performance biodegradable polyesters, such as PBAT (poly (butylene adipate co-terephthalate).

The melting and mixing of TPS with PBAT result in an immiscible blend with high interfacial tension between the phases (TAGUET; HUNEAULT; FAVIS, 2009). A compatibiliser could be added to interact with the starch hydroxyl to improve the adhesion between the polymeric phases, producing blends with improved properties (REN et al., 2009; OROZCO et al., 2009).

In previous studies (OLIVATO et al., 2012 a,b) we observed that multifunctional organic acids, such as citric, malic and tartaric acids, could improve the compatibility between the polymeric phases, producing structurally more homogeneous blends with better mechanical properties. These acids have the added advantage of health safety when the objective is food packaging, once they are non-toxic and non-volatile (Da ROZ et al., 2011). Tartaric acid was also evaluated by Yun, Na and Yoon (2006), resulting in starch/PVA films with improved properties.

Using a mixture design and low concentrations of PBAT (<40 %wt), this paper aims to evaluate the influence of TA, glycerol as a plasticiser, and a third component represented by a starch+PBAT mixture, on the mechanical, thermal and barrier properties of blown-films obtained by reactive extrusion.

2 Experimental

2.1 MATERIALS

Native cassava starch was obtained from Indemil (Paranavaí, PR/Brazil) (amylose 20.8 ± 0.6% wt), PBAT (Poly (butylene adipate co-terephthalate)), was supplied by BASF (Ludwigshafen, Germany); glycerol, supplied by Dinâmica (Diadema, SP/Brazil) and tartaric acid, supplied by Sigma-Aldrich (Steinheim, Germany).

2.2 METHODS

2.2.1 Mixture Design

A mixture design, with constraints on the lower and upper levels of each component (determined from previous tests), was used for the development of the films. Table 1 shows the concentration (in real values and as pseudo-components) of each component in the different samples. The components of the blends were the tartaric acid (TA), glycerol (Gly) and the third component was represented by a mixture of cassava starch and PBAT (starch+PBAT) in a proportion of 55:45, respectively. Two replicates of the T5 sample (T5.1 and T5.2) were used.

Table 1 – Concentrations of the components in the film formulations according to the mixture design.

Samples	*Components*			*Pseudo-components*		
	Starch+PBAT [c] (% wt)	**Glycerol (% wt)**	**Tartaric acid (% wt)**	***x1***		
C	88.0	12.0	0.0	0.3	0.7	0.0
T1	87.0	11.9	1.1	0.0	0.6	0.4
T2	89.5	9.9	0.5	0.8	0.0	0.2
T3	87.5	11.9	0.5	0.2	0.6	0.2
T4	89.0	9.9	1.1	0.6	0.0	0.4
T5 [b]	88.3	10.9	0.8	0.4	0.3	0.3

[a] ***Xi=Ci-a/1-Zai*** was used to calculate the pseudo-components values were **xi** = starch+PBAT, ***X2*** = glycerol and ***X3*** = tartaric acid (TA), ***c*** is the real concentration and ***a,*** is the lower limit of each component in the mixture design.
Two replicates of the T5 sample were performed.
Mixture of cassava starch and PBAT (starch+PBAT) in a proportion of 55:45, respectively.

The mechanical properties and water vapour permeability of the films were analysed with STATISTICA 7.0 software (Statsoft, Tulsa/USA) using data modelling and analysis of the surface contours of the mixture design. Quadratic models (Eq. 1) better fit the results.

$$y = \beta_1 X_1 + \beta_2 X_2 + \beta_3 X_3 + \beta_{12} X_1 X_2 + \beta_{13} X_1 X_3 + \beta_{23} X_2 X_3 \qquad Eq.\ 1$$

where *y* = dependent variable, *β* = regression coefficient for each component, *x1* = starch+PBAT, *x2* = glycerol and *x3* = tartaric acid.

2.2.2 Film Production

All components of the formulations (Table 1) were manually miXed at the time of eXtrusion and processed to produce pellets using a laboratory single-screw eXtruder (model EL-25, BGM, São Paulo, Brazil) with a screw diameter (D) of 25 mm and a screw length of 28D. A barrel temperature profile of 100/120/120/120°C from the feed zone (zone 1) to the die zone (zone 4) was used. The screw speed was set to 40 rpm using a die with siX 2 mm diameter holes. The pellets were then eXtruded, using the same equipment, to obtain the films. The barrel temperature profile was set to 100/120/120/130°C and 130°C for the 50 mm film-blowing die and screw speed was set to 40 rpm. The feed rate was maintained to ensure that the screw operated at full load. The film thickness (maintained between 80-100 um) was controlled via roll speed control and the air flow.

2.2.3. Water Vapour Permeability (WVP)

The tests were conducted using ASTM method E-96-95 (1996) with some modifications. Before analysis, the samples were stored at 25 °C and 53% RH for 48 hours. Each film sample was fiXed in the circular opening of a permeation cell with a 60 mm internal diameter using silicone grease to ensure that humidity migration occurred only through the film. The interior of the cell was filled with a magnesium chloride solution (MgCl2 / 32.8% RH) and the device was stored at 25°C in a desiccator containing a saturated sodium chloride solution that provided 75% RH and maintained a 42% RH gradient across the film. The samples were weighed every 3 hours during the 72 hour testing time. Changes in the weight of the cell or mass gain (m) were plotted as a function of time (t). The slope of the line was calculated by linear regression (R > 0.99). The water vapour permeation ratio (WVPR) was obtained with Eq. 2:

$$WVPR = (m/t).(1/A) \qquad Eq.\ 2$$

where *m/t* is the angular coefficient of the curve and *A* is the sample permeation area. The WVP (g.Pa. $s^{-1}.m^{-1}$) was calculated using Eq. 3:

$$WVP = WVPR.st/ps[(RH_1-RH_2)/100] \qquad Eq.\ 3$$

where *st* is the mean sample thickness (m), *ps* is the water vapour saturation pressure at the assay temperature (Pa), *RHi* is the relative humidity of the desiccator and *RH2* is the relative humidity of the interior of the permeation cell. The tests were conducted in duplicate.

2.2.4 Mechanical Properties

A texture analyser model TA.XT2i (Stable Micro Systems, Surrey/England) fitted with a 50 kg load cell was used to conduct the tensile and puncture tests of the films. Tensile tests were based on the ASTM method D882-91 (1996). Ten samples from each formulation were cut along the longitudinal direction

(50 mm in length and 20 mm in width) and fit in the tensile grips. The crosshead speed was set at 0.8 mm/s and the initial distance between the grips was 30 mm. The tensile strength (MPa), elongation at break (%) and Young's modulus (MPa) were determined.

Puncture tests were performed using 10 samples from each formulation. These were fixed in an appropriate apparatus that allowed exposure to 35 mm of the sample. The perforation was conducted using a cylindrical probe 3.0 mm in diameter at a speed of 0.4 mm/s, which pierced perpendicular to the sample. The puncture force (N) was determined (GONTARD et al., 1993). Before all tests, the samples were conditioned at 23 ± 2°C and 53 ± 2% RH for 48 hours.

2.2.5 Dynamical-mechanical analysis (DMA)

A Dynamical Mechanical Analyser (DMA-Q800, TA Instruments, USA) was used to determine the storage modulus (MPa) and loss factor (tan 5) of the blown films. The samples were subjected to a sinusoidal strain in traction mode and scanned from -50°C to 100°C with a heating rate of 3°C/min and fixed frequency of 1 Hz. Glass transition temperatures (Tg) were expressed as the temperature of the tan 5 peaks. For clarity, the analysis was done for samples C, T1 and T5, which contained different levels of tartaric acid.

2.2.6 X-ray Diffraction (XRD)

X-ray patterns of the samples were taken using an XPert PRO (Panalytical, Philips) machine with Cu(ka) radiation (^=1.5406 A) operating at room temperature, 30 mA and 40 kV. The scanned region ranges from 2ϑ = 3.0-70.0°, with a step size of 0.01° and dwell time of 4.0. The relative crystallinity index (CI) was estimated from the relative areas of crystalline and amorphous regions, according to the relationship described by Muller et al. (2009). For clarity, the analysis is shown for samples C, T1 and T5, which contained different levels of TA.

3 Results and Discussion

3.1 Modelling of Mixture Design

Compatibilised blends containing starch/polyester produce films with improved mechanical and barrier properties that represent a potential substitute for plastic packaging available today (NABAR et al., 2005; YU et al., 2007). In Table 2, the regression coefficients of the models adjusted for the mechanical and barrier properties are listed. The presented determination coefficients (R^2) that are higher than 0.70 indicate good fit with experimental data, except in the case of elongation (R^2 = 0.474), whose model cannot be considered for prediction purposes.

Table 2 – Regression coefficients for the mechanical and barrier properties

Coefficients	*Properties*				
	Tensile strength	Elongation	Young's modulus	Puncture force	WVP
β_1	3.39*	197.71	29.61*	2.02*	9.11*
β_2	8.41*	960.79*	50.16*	13.28*	4.25*
β_3	-16.97*	-3016.43*	142.76*	-52.34*	32.23*
β_{12}	-4.35*	-794.25*	-19.99	-18.59*	13.02*
β_{13}	41.37*	6229.25*	8.24	93.35*	-45.57*
β_{23}	16.06*	3235.63*	-246.78*	64.77*	-27.70*
R^2	*0.775*	*0.474*	*0.834*	*0.918*	*0.890*

β1 = Starch+PBAT, β2 = Gly (glycerol), β3 = TA (tartaric acid), β12 = Interaction starch+PBAT/Gly, β12 = Interaction starch+PBAT/TA, β23 = Interaction Gly/TA.
Gly = glycerol and TA = tartaric acid.
* Significant effects (p<0.05).

The influence of the components on the mechanical resistance of the films were evaluated based on modelling coefficients for the tensile strength and puncture force, which both showed similar effects. The inclusion of tartaric acid exerted a negative effect on the tensile strength (£3 -16.97) and the puncture force (63 -52.34), i.e., when the concentration of TA increases, the film's tensile strength and puncture force were reduced. On the other hand, the interaction between the mixture of starch/PBAT and TA *(6 13)* had a more significant positive effect on the response, producing more resistant films (Table 2). This can also be observed in Figure 1; for tensile strength, improved results were obtained when intermediate concentrations of glycerol and TA are used (calculated value of 5.93 MPa).

Figure 1 – Surface contour map showing the effect of the starch+PBAT, glycerol (Gly) and tartaric acid (TA) on the tensile strength (MPa), in terms of pseudo-components. The experimental area is delimitated by the shown sample points.

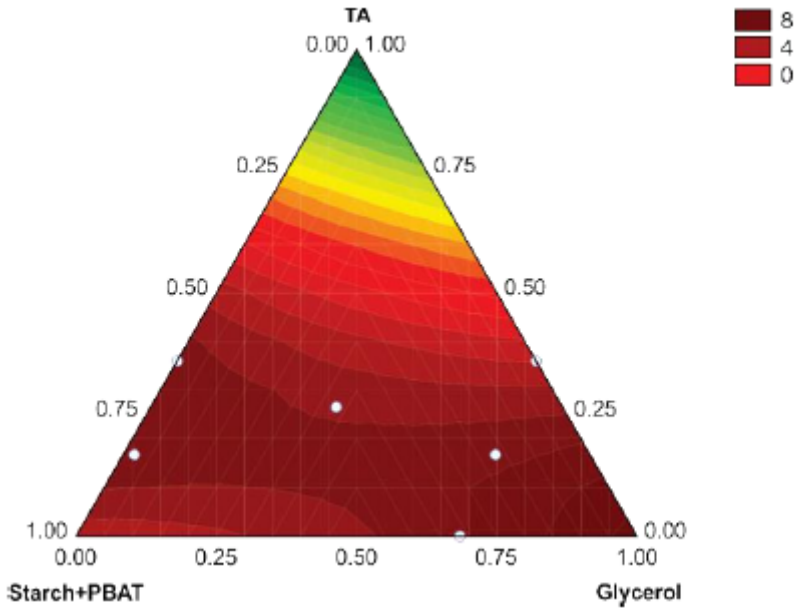

Young's modulus or elastic modulus is related to film rigidity. Higher values of Young's modulus indicate a more rigid material. The resultant Young's moduli for the starch/PBAT films ranged from 29.95 to 74.87 MPa (Figure 2). A positive effect was seen by the addition of TA (63 142.76). The films were more rigid when increased amounts of TA were used. At the same time, the antagonistic interaction of Gly/TA (623 -246.78) results in more flexible films as a consequence of the plasticising role of the glycerol together with the TA action as a plasticiser. These components interpose themselves between the starch molecules and reduce the attractive intermolecular forces. This behaviour was also observed for citric acid in thermoplastic starch films (SHI et al., 2007; GARCIA et al., 2011; OLIVATO et al., 2011).

Figure 2 – Surface contour map showing the effect of the starch+PBAT, glycerol (Gly) and tartaric acid (TA) on the Young's modulus (MPa), in terms of pseudo-components. The experimental area is delimitated by the shown sample points.

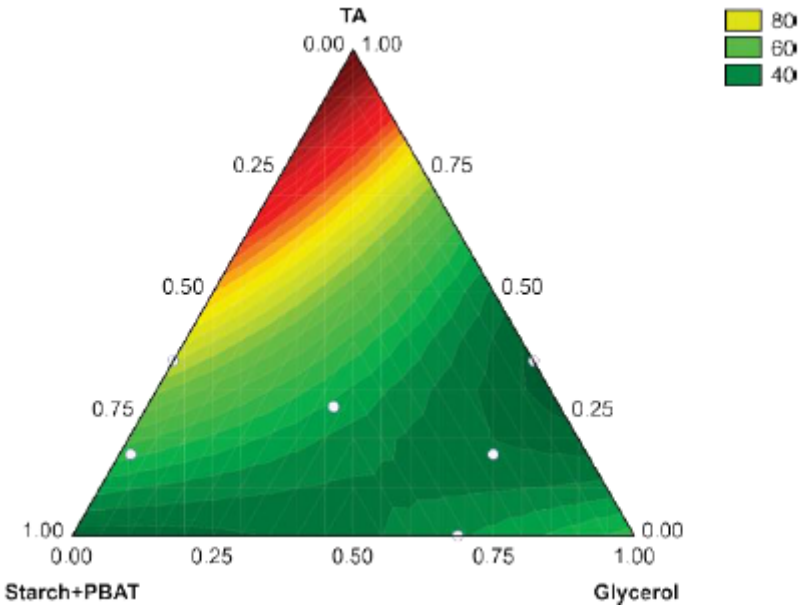

Ayoub and Rizvi (2009) observed that the utilisation of greater concentrations of glycerol reduces the crosslink reaction efficacy. This is because the intermacromolecular distances increase and the possibility of creating macro radical combinations is reduced, which also could be responsible for the negative effect observed with the Gly/TA interaction on Young's modulus. Additionally, Wang et al. (2009), studying starch/montmorillonite nanocomposites, observed that citric acid (3 wt. %) contributed to starch granule disruption and facilitated the penetration of the plasticiser within the film, resulting more flexible films.

The results from mechanical testing allow us to observe different and concomitant roles of TA when added to starch/PBAT blends. Organic dicarboxylic acids, such as TA, are able to promote crosslinking reactions (transesterification), connecting the starch chains together and restraining their molecular mobility, with the overall effect being to reinforce the film matrix (OLIVATO et al., 2012a). This function can be evidenced by the positive effect of the starch+PBAT/TA interaction on the tensile strength and puncture force (Table 2), where more resistant and more rigid films (positive effect of TA on Young's modulus) were seen. The reinforcing effect could additionally be caused by the TA reaction with the hydroxyl group on the starch (grafting). This would reduce the hydrophilic character and improve their

compatibility with PBAT, promoting enhanced stress transference within the polymeric matrix.

Residual TA, which did not participate in esterification and/or transesterification reactions, can cause starch acidolysis, which factors into viscosity control of the molten thermoplastic starch. As shown by Da Roz et al. (2011), the addition of organic acids during thermoplastic starch melting results in a reduction of molecular weight. The acid hydrolysis of starch resulted in more brittle films when higher proportions of TA were used (negative effect on tensile strength and puncture force) (Figure 1, Table 2).

3.2 WATER VAPOUR PERMEABILITY (WVP)

To use starch films for food packaging, in place of synthetic plastics, it is important to minimise water vapour permeability in order to avoid the moisture transference between the packaged material and the atmosphere (GONTARD; GUILBERT; CUQ, 1992). The WVP of the films ranged from $6.44x10^{-10}$ to $8.80x10^{-10}$ $g.s^{-1}.m^{-1}.Pa^{-1}$ and are lower than those found for cassava starch/glycerol films, which reach WVP values of $3.20 \pm 0.20x10^{-9}$ (ALVES et al., 2007). The improvement was promoted by the inclusion of PBAT, which added a hydrophobic character to the films. The results, however, are closer to those of our previous works (OLIVATO et al., 2011) and also to those of Wang et al. (2009), who observed a WVP of $2.0x10^{-10}$ $g.s^{-1}.m^{-1}.Pa^{-1}$ for starch/montmorillonite nanocomposites containing citric acid, and to the results obtained by Pelissari et al. (2009), which ranged from $0.62 \pm 0.15x10^{-10}$ to $1.39 \pm 0.15 \ x10^{-10}$ $g.s^{-1}.m^{-1}.Pa^{-1}$ for cassava starch/chitosan films.

The WVP increased (positive effect on the response) when the proportions of any component in the blends was increased (Table 2). According Wang and Padua (2005), the permeability of a material is strongly influenced by the hydrophobic or hydrophilic nature of its components. For hydrophilic molecules, the inclusion of higher proportions of glycerol or TA resulted in a greater affinity of the polymeric matrix for water, contributing to an increase in the WVP (Figure 3). Similar results were observed by Galdeano et al. (2009) in oat starch films and Parra et al. (2004) for cassava starch samples.

Figure 3 – Surface contour map showing the effect of the starch+PBAT, glycerol (Gly) and tartaric acid (TA) in the WVP (g/s.m.Pa), in terms of pseudo-components. The experimental area is delimitated by the shown sample points.

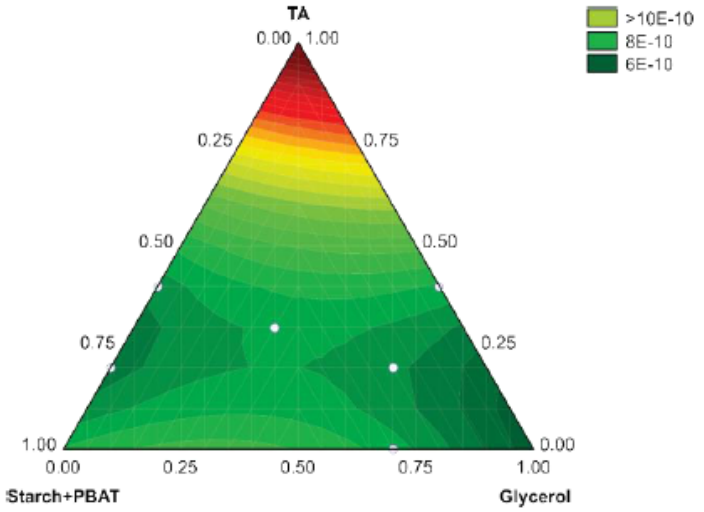

Considering the component interactions, a reduction in WVP was promoted by the *613* (Starch+PBAT/TA) and *623* (Gly/TA) interactions (Table 2). The role of TA as a compatibiliser, through transesterification reactions and/or single esterification reactions with starch hydroxyls (which formed a more hydrophobic starch), could contribute to the WVP decrease (Figure 3). Ren et al. (2009) observed that the reaction of the compatibiliser with the starch -OH group (ester bonds) causes the "coating" of the hydrophilic centres of the starch by a hydrophobic layer. This could be making the starch more compatible with PBAT, thus decreasing WVP.

Possible reactions between tartaric acid and glycerol should also be considered. The availability of both molecules acting as plasticisers was reduced and, as a consequence, the diffusion of water through the film matrix became more difficult. Raquez et al. (2008), studying melt-blends of TPS/PBAT, also reported the occurrence of glycosylation reactions during the process of reactive extrusion. This was also the case when decreasing the glycerol available to act as a plasticiser.

3.3 X-RAY DIFFRACTION (XRD)

Similar X-ray patterns were obtained for samples C, T1 and T5 (Figure 4). For all the samples, the peaks identified at 29=13.1° and 19.8° are due to the crystallisation of the starch induced by processing (type VH). No residual native

crystallinity was observed in the films, leading to the conclusion that complete starch melting occurred. Van Soest et al. (1996) found similar results for TPS processed at temperatures lower than 180°C. Moreover, the peaks at 29=17.6° and 23.2° are related to the PBAT crystallinity, which is in agreement with those observed by Raquez et al. (2008) for thermoplastic starch/PBAT blends.

Figure 4 – X-ray diffractograms for samples C (withouth TA), T1 (1.1%wt TA) and T5 (0.8%wt TA). Relative crystallinity index (CI) was calculated and is indicated on the plots.

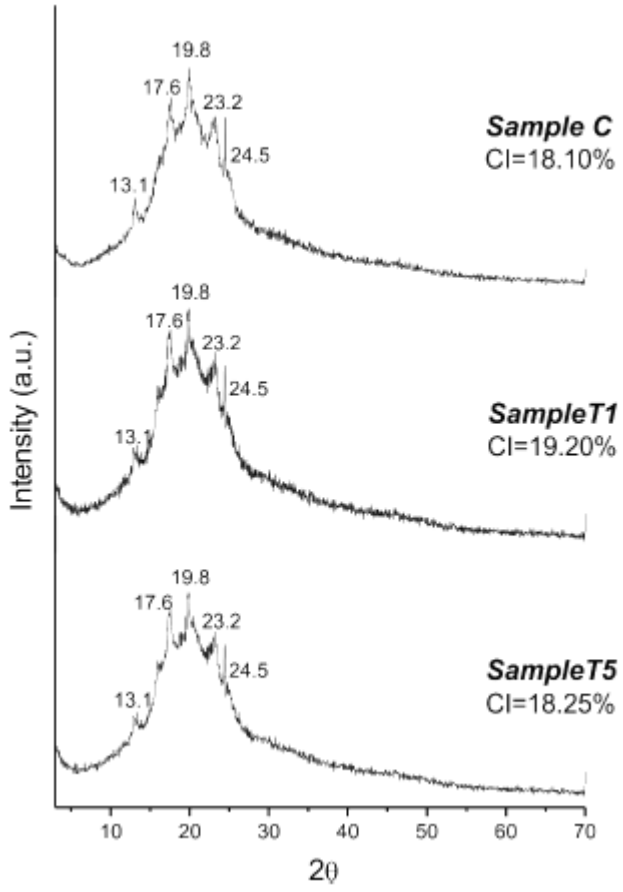

Shi et al. (2007) observed that starch has its crystallinity reduced when citric acid is added. However, in this work, the inclusion of tartaric acid did not change the crystallinity index (CI) of the films, as can be observed in Figure 4. The sample T1 has a slightly greater CI (19.2%) and the C sample, without acid, had a CI of 18.1%, which is similar to those of the T5 sample (18.25%).

3.4 DYNAMICAL MECHANICAL ANALYSIS (DMA)

The viscoelastic response of the material can be studied using a temperature sweep at a fixed frequency by dynamical mechanical analysis (DMA). The storage modulus is related to the potential energy stored by the material under deformation and is closely related to the load bearing capacity of the material (MOHANTY et al., 2006; VAIDYA et al., 1995). The higher storage modulus was obtained for sample T5 (Figure 5), indicating an increase in the viscoelastic stiffness, which could be a consequence of the more pronounced compatibiliser effect of the TA, at intermediate proportions. Sample T1 was similar to sample C, i.e., without acid.

Figure 5 – Storage modulus (MPa) for samples C (withouth TA), T1 (1.1 %wt TA) and T5 (0.8%wt TA).

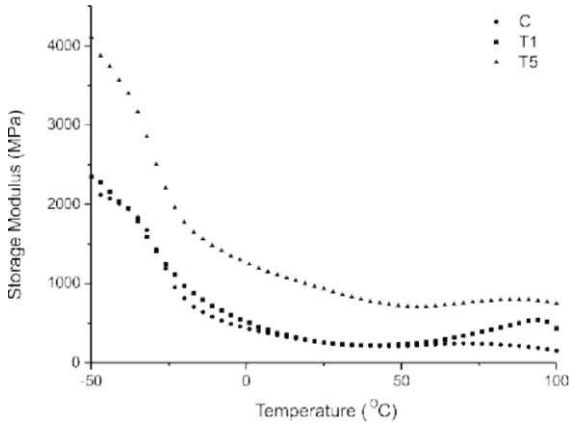

Liang and Williams (1992) observed that poor adhesion between the co-continuous phases in blends results in a lower storage modulus. With the addition of a compatibiliser the adhesion is improved and results in a greater storage modulus. Comparing the results of our work, it is possible to conclude that sample T5 contained the better proportion of TA for the compatibiliser effect.

Loss factor (tan 5) is the ratio between the loss and storage modulus. Their peaks are usually used as an indicator of glass transition temperature (Tg) for materials (VAIDYA et al., 1995). Tan 5 curves for the samples (Figure 6) reveal two thermal relaxations, characteristic of an immiscible blend. The first transition, at approximately -25°C, is attributed to the glass transition temperature of the PBAT rich phase and the second one, above room temperature, corresponds to the glass transition temperature (Tg) of the TPS rich phase.

Figure 6 – Loss factor (tan δ) for samples C (withouth TA), T1 (1.1%wt TA) and T5 (0.8%wt TA).

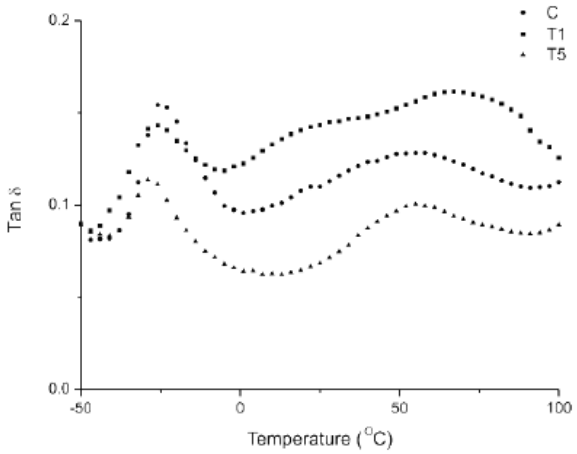

The Tg of the samples with TA, in general, showed a slight decrease when compared to the control (C), except for T1, whose loss factor curves showed a broadening of the glass transition of TPS. This could be attributed to the higher proportion of TA in the sample favouring acidolysis reactions and resulting in starch chains with several molecular weights, i.e., polymeric chains with various sizes and consequently different molecular mobility. The reduction of Tg with the inclusion of TA could be related to its behaviour as a compatibiliser, improving the interaction between the polymeric phases (WANG et al., 2010), and potentially due to its role as a plasticiser and promoter of acidolysis (SHI et al., 2007; MANI; BHATTACHARYA, 2001).

4 Conclusions

The proposed mixture design was efficient for evaluating the influence of tartaric acid in starch/ PBAT blown films. TA proved to be a good compatibiliser at intermediate levels (0.8 g/100 g), improving the interfacial interaction between the polymeric phases and the transference of stress in the films. This resulted in greater resistance and more rigid materials. TA also acted as a plasticiser and in the acidolysis of the starch; however, it did not change the crystallinity of the films.

In conclusion, TA contributes to the improvement of the mechanical and barrier properties of films in which adequate concentrations is necessary to reach the optimal properties, as shown in the DMA analysis. Thus, the obtained

biodegradable films containing reduced proportions of PBAT show good performance and represent an interesting alternative to non-biodegradable packaging.

5 References

ALVES, V. D; MALI, S; BELEIA, A; GROSSMANN, M. V. E. Effect of glycerol and amylose enrichment on cassava starch film properties. **Journal of Food Engineering,** v. 78, p. 941-946, 2007.

AMERICAN SOCIETY FOR TESTING AND MATERIAL (ASTM). **Standard test methods for water vapor transmission of material.** E96-95, Philadelphia: ASTM, 1996.

AMERICAN SOCIETY FOR TESTING AND MATERIAL (ASTM). **Standard test methods for tensile properties of thin plastic sheeting**. D882-91, Philadelphia: ASTM, 1996.

AVEROUS, L ; FRINGANT, C ; MORO, L. Starch-based biodegradable materials suitable for thermoforming packaging. **Starch/Starke,** v. 53, p. 368-371, 2001.

AYOUB, A. S; RIZVI, S. S. H. An overview on the technology of cross-linking of starch for nonfood applications. **Journal of Plastic Film and Sheeting,** v. 25, p. 25-44, 2009.

CONTRERAS, O. I. P; PERILLA, J. E. P; ENCISO, N. A. A. A review of using organic acids to chemically modify starch. **Revista Ingenería e Investigación,** v. 2, n. 3, p. 47-52, 2008.

DA ROZ, A. L; ZAMBON, M. D; CURVELO, A. A. S; CARVALHO, A. J. F. Thermoplastic starch modified during melt processing with organic acids: The effect of molar mass on thermal and mechanical properties. **Industrial Crops and Products,** v. 33, p. 152-157, 2011.

GALDEANO, M. C; MALI, S; GROSSMANN, M. V. E; YAMASHITA, F; GARCIA, M. A. Effects of plasticizers on the properties of oat starch films. **Materials Science and Engineering C,** v. 29, p. 532-538, 2009.

GARCIA, P. S; GROSSMANN, M. V. E; YAMASHITA, F; MALI, S; DALL'ANTONIA, L. H; BARRETO, W. J. Citric acid as multifunctional agent in blowing films of starch/PBAT. **Química Nova,** v. 34, p. 1507-1510, 2011.

GONTARD, N; GUILBERT, S; CUQ, J. L. Edible wheat gluten films: influence of the main process variables on film properties using response surface methodology. **Journal of Food Science,** v. 57, p. 190-195, 1992.

GONTARD, N; GUILBERT, S; CUQ, J. Water and glycerol as plasticizer affect mechanical and water vapor barrier properties of an edible wheat gluten film. **Journal of Food Science,** v. 58, n. 1, p. 206-211, 1993.

LIANG, Z; WILLIAMS, H. L. Dynamic mechanical properties of polypropylene-polyamide blends: Effect of compatibilization. **Journal of Applied Polymer Science,** v. 44, p. 699-717, 2003.

LU, D. R; XIAO, C. M; XU, S. J. Starch-based completely biodegradable polymer materials. **Express Polymer Letters,** v. 3, n. 6, p. 366-375, 2009.

MANI, R; BHATTACHARYA, M. Properties of injection molded blends of starch and modified biodegradable polyesters. **European Polymer Journal,** v. 17, p. 515-526, 2001.

MOHANTY, S; VERMA, S. K; NAYAK, S. K. Dynamic mechanical and thermal properties of MAPE treated jute/HDPE composites. **Composites Science and Technology,** v. 66, p. 538-547, 2006.

MULLER, C. M. O; LAURINDO, J. B; YAMASHITA, F. Effect of cellulose fibers on the crystallinity and mechanical properties of starch-based films at different relative humidity values. **Carbohydrate Polymers,** v. 77, p. 293-299, 2009.

NABAR, Y; RAQUEZ, J. M ; DUBOIS, P ; NARAYAN, R. Production of starch foams by twin-screw extrusion: effect of maleated poly(butylene adipate-co-terephthalate) as a compatibilizers. **Biomacromolecules,** v. 6, p. 807-817, 2005.

OLIVATO, J. B; GROSSMANN, M. V. E; YAMASHITA, F; NOBREGA, M. M; SCAPIN, M. R. S; EIRAS, D; PESSAN, L. A. Compatibilisation of starch/poly(butylene adipate co-terephthalate) blends in blown films. **International Journal of Food Science and Technology,** v. 46, p. 1934-1939, 2011.

OLIVATO, J. B; GROSSMANN, M. V. E; BILCK, A. P; YAMASHITA, F. Effect of organic acids as additives on the performance of thermoplastic starch/polyester blown films. **Carbohydrate Polymers,** v. 90, p. 159-164, 2012a.

OLIVATO, J. B; GROSSMANN, M. V. E; YAMASHITA, F; EIRAS, D; PESSAN, L. A. Citric acid and maleic anhydride as compatibilizers in starch/poly (butylene adipate-co-terephthalate) blends by one-step reactive extrusion. **Carbohydrate Polymers,** v. 87, p. 2614-2618, 2012b.

OROZCO, V. H; BROSTOW, W; CHONKAEW, W; LOPEZ, B. L. Preparation and characterization of poly(lactic acid)-g-maleic anhydride + starch blends. **Macromolecules Symposium,** v. 277, p. 69-80, 2009.

PARRA, D. F; TADINI, C. C; PONCE, P; LUGAO, A. B. Mechanical properties and water vapor transmission in some blends of cassava starch edible films. **Carbohydrate Polymers,** v. 58, p. 475-481, 2004.

PELISSARI, F. M; GROSSMANN, M. V. E; YAMASHITA, F; PINEDA, E. A. G. Antimicrobial, mechanical and barrier properties of cassava starch-chitosan films incorporated with oregano essential oil. **Journal of Agriculture and Food Chemistry,** v. 57, p. 7499-7504, 2009.

REN, J; FU, H; REN, T; YUAN, W. Preparation, characterization and properties of binary and ternary blends with thermoplastic starch, poly(lactic acid) and

poly(butylene adipate-co-terephthalate). **Carbohydrate Polymers,** v. 77, p. 576-582, 2009.

RAQUEZ, J. M; NABAR, Y; NARAYAN, R ; DUBOIS, P. In-situ compatibilization of maleated thermoplastic starch/polyester melt-blends by reactive extrusion. **Polymer Engineering and Science,** v. 48, p. 1747-1754, 2008.

SHI, R; ZHANG, Z; LIU, Q; HAM, Y; ZHANG, L ; CHEN, D ; TIAN, W. Characterization of citric acid/glycerol co-plasticized thermoplastic starch prepared by melt blending. **Carbohydrate Polymers,** v. 69, p. 748-755, 2007.

SHI, R; BI, J; ZHANG, Z; ZHU, A; CHEN, D; ZHOU, X; ZHANG, L; TIAN, W. The effect of citric acid on the structural properties and cytotoxicity of the polyvinyl alcohol/starch films when molding at high temperature. **Carbohydrate Polymers,** v. 74, p. 763-770, 2008.

TAGUET, A; HUNEAULT, M. A; FAVIS, B. D. Interface/morphology relationships in polymer blends with thermoplastic starch. **Polymer,** v. 50, p. 5733-5743, 2009.

VAIDYA, U.R; BHATTACHARYA, M ; ZHANG, D. Effect of processing conditions on the dynamic mechanical properties of starch and anhydride functional polymer blends. **Polymer,** v. 36, p. 1179-1188, 1995.

VAN SOEST, J. J. G; HULLEMAN, S. H. D; DE WIT, D; VLIEGENTHART, J. F. G. Crystallinity in starch bioplastics. **Industrial Crops and Products,** v. 5, p. 11-22, 1996.

YOON, S; CHOUGH, S; PARK, H. Effects of additives with different functional groups on the physical properties of starch/PVA blend film. **Journal of Applied Polymer Science,** v. 100, p. 3733-3740, 2006.

YU, L; DEAN, K; YUAN, Q; CHEN, L; ZHANG, X. Effect of compatibilizer distribution on the blends of starch/biodegradable polyesters. **Journal of Applied Polymer Science,** v. 103, p. 812-818, 2007.

YUN, Y; NA, Y; YOON, S. Mechanical properties with the functional group of additives for starch/PVA blend film. **Journal of Polymers and the Environment,** v. 14, n. 1, p. 71-78, 2006.

WANG, N; ZHANG, X; HAN, N; SHIHE, B. Effect of citric acid and processing on the performance of thermoplastic starch/montmorillonite nanocomposites. **Carbohydrate Polymers,** v. 76, p. 68-73, 2009.

WANG, N; ZHANG, X; HAN, N; FANG, J. Effects of water on the properties of thermoplastic starch poly(lactic acid) blend containing citric acid. **Journal of Thermoplastic Composite Materials,** v. 23, p. 19-34, 2010.

WANG, Q; PADUA, G. W. Properties of zein films coated with drying oils. **Journal of Agricultural and Food Chemistry,** v. 53, n. 9, p. 3444-3448, 2005.

CAPITULO 4 – PHYSICAL AND STRUCTURAL CHARACTERISATION OF STARCH/POLYESTER BLENDS WITH THE ADDITION OF TARTARIC ACID

ABSTRACT: Starch/PBAT blends were produced by reactive extrusion with tartaric acid (TA) as additive. The effect of TA, glycerol and starch+PBAT, based in a constraint mixture design, in the mechanical, optical and structural properties of the films were evaluated. Tartaric acid is able to act as compatibiliser and as a concomitant role, promotes acid hydrolysis of the starch chains. Both functions explain the results of the films resistance and opacity. TA reduced weight loss in water. Scanning electron microscopy (SEM) images showed that TA causes reduction of the interfacial tension between the polymeric phases and more homogeneous films were obtained. Nuclear magnetic resonance (^{13}C CPMAS) and Fourier transform infrared spectroscopy (FT-IR) suggest that tartaric acid is able to react with hydroxyls of the starch, by esterification / transesterification reactions, which confirms their role as compatibiliser, producing materials with better properties and adequate to use in food packaging.

Keywords: Nuclear magnetic resonance (NMR). Fourier transform infrared spectroscopy (FT-IR). Scanning electron microscopy (SEM). Tartaric acid. Starch/PBAT blends.

1 Introduction

Synthetic polymers, produced from petrochemicals, are a significant source of environmental pollution. Growing ecological concerns have resulted in the emergence of biodegradable plastics as alternative materials to petroleum-based polymers (CHALEAT et al., 2008; AVEROUS, 2004).

There is a strong interest for bio-based and/or biodegradable polymers. The reasons for this include the reduced costs and abundance of the biomass and the biodegradability, with the objective to reduce the waste disposal into the environment (HUNEAULT; LI, 2012).

Thermoplastic starch represents an abundant, renewable and low-cost alternative to synthetic plastics, but have some disadvantages as deficient mechanical properties (crystallisation due to ageing and plasticisation by water adsorption) and hygroscopic character (HUNEAULT; LI, 2012; AVEROUS; FRINGANT; MORO, 2001).

As a possibility to overcome the thermoplastic starch drawbacks, a blend with good performance polyester could be interesting (YANG et al., 2008). In

this direction and with the aim to conserve the biodegradability of the final material, poly (butylene adipate co-terephthalate) (PBAT) represents a promisor material, considering their good mechanical and barrier properties (REN et al., 2009; AVEROUS; DIGABEL, 2006;). However, as most synthetic polymers, PBAT is hydrophobic and thermodynamically immiscible with hydrophilic starch, making necessary the utilisation of a compatibiliser capable to act improving the interfacial adhesion between the polymeric phases and resulting in blends with adequate morphology and improved mechanical properties (MOAD, 2011; MALIGER et al., 2006).

The most important processing method for thermoplastic materials is probably extrusion, which film blowing is a commonly used method for producing self-supporting plastic films (THUWALL et al., 2006). Reactive extrusion combines the thermo-mechanical energy necessary to disrupt/melt the polymeric matrix with chemical reactions in a single and continuous process with absence of solvents.

Starch could be chemical modified by reactive extrusion using different process. Esterification with carboxylic acids as citric acid (SHI et al., 2007, 2008; WANG et al., 2007, 2009, 2010), formic acid (DIVERS et al., 2004), ascorbic acid (CARVALHO et al., 2005) has been studied to produce more hydrophobic starch esters and also to promote transesterification reactions. Taking into consideration health safety, the use of organic acids seems advantageous once they are non-toxic and used as adjuvants in food products.

Tartaric acid proved to be a good compatibiliser for starch/PBAT blends (OLIVATO et al., 2012; 2013). Based on this, by one-step reactive extrusion using tartaric acid (TA) as compatibiliser, this work had the objective to evaluate structural and physical properties of starch/PBAT blends with formulations based in a constraint mixture design.

2 Experimental

2.1 MATERIALS

Native cassava starch was supplied by Indemil (Paranavaí, Brazil), PBAT (poly (butylene adipate co-terephthalate)), by BASF (Ludwigshafen, Germany), glycerol by Dinâmica (Diadema, Brazil) and tartaric acid by Sigma-Aldrich (Steinheim, Germany).

2.2 EXPERIMENTAL DESIGN

With the aim to observe the effect of TA in the properties of the starch/PBAT, a constraint mixture design was proposed with proportions of TA ranging from 0 to 1.1 g.100g^{-1}. The glycerol maximum content was established in 12.0 g.100g^{-1} and the third component was represented by a mixture of starch and PBAT, keeping a proportion of 55:45 between the phases, respectively. Table 1 shows the complete experiment.

The films produced by this experiment were evaluated for their mechanical properties, opacity and weight loss in water. These results were analysed with STATISTICA 7.0 software (Statsoft, Tulsa/USA), using data modelling (Scheffa's canonical polynomial models) and analysis of the surface contours of the mixture design.

Table 1 – Components and pseudo-components according to constraint mixture design in starch/PBAT blends formulations.

Samples	*Components*			*Pseudo-components*[a]		
	Starch+PBAT[b] (% wt)	Glycerol (% wt)	Tartaric acid (% wt)	x_1	x_2	x_3
C	88.0	12.0	0.0	0.3	0.7	0.0
T1	87.0	11.9	1.1	0.0	0.6	0.4
T2	89.5	9.9	0.5	0.8	0.0	0.2
T3	87.5	11.9	0.5	0.2	0.6	0.2
T4	89.0	9.9	1.1	0.6	0.0	0.4
T5	88.3	10.9	0.8	0.4	0.3	0.3

a $xi = ci - ai / 1-\Sigma ai$ was used to calculate the pseudo-components values, were *x1* = starch+PBAT, *x2* = glycerol and *x3* = tartaric acid (TA), *ci* is the real concentration and *ai* is the lower limit of each component in the mixture design.
b Mixture of cassava starch and PBAT (starch+PBAT) in a proportion of 55:45, respectively.

2.3 FILM PRODUCTION BY REACTIVE EXTRUSION

The formulations were processed using a laboratory single-screw extruder (model EL-25, BGM, São Paulo, Brazil) with a screw diameter (D) of 25 mm and a screw length of 28D, using a barrel temperature profile of 100/120/120/120°C. The screw speed was set to 40 rpm using a die with six 2 mm diameter holes. This first step resulted in a production of pellets, which were then extruded to obtain the films. The same equipment was set at barrel temperature profile of 100/120/120/130°C and 130°C for the 50 mm film-blowing die and screw speed of 40 rpm. The film thickness (maintained between 80-100 um) was controlled via roll speed control and the air flow.

2.4 FILM CHARACTERIZATION

2.4.1 Tensile test

A texture analyser model TA.XT2i (Stable Micro Systems, Surrey/England) was used to perform the tensile tests of the materials. Tensile tests were based on the ASTM method D882-91 (1996), using ten samples from each formulation and crosshead speed set at 0.8 mm/s. The tensile strength (MPa) was determined.

2.4.2 Opacity

Opacity was determined by means of colorimeter (BYK Gardner-USA) at a 10° angle and illuminant D65 (day light), according to Hunterlab methods (Hunter Associates Laboratory, 1997). The opacity of the samples was calculated as the ratio between the opacity of a sample placed under a black pattern and the opacity of a sample placed under a white pattern. The opacity results were expressed as relation of the thickness, using an arbitrary scale (0 - 1%.um^{-1}). The determinations were performed in triplicate.

2.4.3 Weight Loss in Water

This test was conducted according Reddy and Yang (2010), with some modifications. Samples were previously desiccated for three days in a desiccator containing anhydrous CaCl2 (0% RH). After weighing, the films were immersed in distilled water, maintaining a proportion of 30:1 (water/sample), for 48 hours at 25°C. The samples were then removed and dried, using the same conditions described above. The weight of the conditioned specimen after treatment was used to determine the % weight loss in water.

2.4.4 Scanning Electron Microscopy (SEM)

A scanning electron microscope FEI model Quanta 200 (FEI Company/Tokyo, Japan) was used to observe the cryogenic (under liquid nitrogen) fractured surface of the blown film samples. The samples were previously gold coated with a Sputter Coater (BAL-TEC SCD 050). Images were taken of the fractured surface at magnification of 1600x.

2.4.5 Fourier Transform Infrared Spectroscopy (FT-IR)

FT-IR analyses were conducted on the blown films from 4000 to 500 cm^{-1} with a spectral resolution of 4 cm^{-1}. A Perkin-Elmer Spectrum 2000 FT-IR with a Universal Attenuated Total Reflectance (UATR) Pike Miracle module was used. The samples were conditioned in a desiccator containing anhydrous calcium chloride (CaCb) for 10 days before the analysis.

2.4.6 Spectroscopy 13C Solid-State Cross-Polarisation/Magic Angle Spinning Nuclear Magnetic Resonance (13C CPMAS NMR).

The solid state 13C CPMAS NMR spectra were obtained on a Mercury 300BB spectrometer, operating at 300MHz for carbon-13. The CPMAS conditions were, spectral width: 75,000 Hz; acquisition time: 0.05 s; pulse width 90.0°, recycle delay 3 s and number of transients 712.

3 Results and Discussion

3.1 Mixture Design

The results of tensile strength, weight loss in water and opacity were analysed and models were adjusted to the data (Table 2). While the first two showed satisfactory adjustment (R^2 = 0.8), the last one must be used with caution due its low R^2. Tartaric acid is able to act as compatibiliser, by means of esterification/transesterification reactions with the polymeric chains, which restrain their mobility. As a concomitant role, promotes acid hydrolysis of the starch chains. Both functions explains the results of the films resistance, which is influenced mostly by the effect of the interaction starch+PBAT/TA (P13) that increase the films resistance and the opposite negative effect of TA ((3 3 -16.97), which, when used in greater concentrations, causes an excessive hydrolysis of the starch and becomes prejudicial to the tensile strength of the material. Similar results, in relation to the mechanical properties, were fully discussed in our previous works (OLIVATO, 2012; 2013).

The opacity of the films was influenced positively by all the components, with almost no difference between the effects (Table 2). This shows an increment of opacity values with greater concentrations of the evaluated components. The same behaviour was observed for Pelissari et al. (2012) in the study of starch/chitosan films, for the glycerol and starch effects.

Table 2 – Results of film properties and regression coefficients according the mixture design.

Samples		Tensile Strength (MPa)	Opacity (%.μm^{-1})	Weight Loss in Water (%)
C		5.88 ± 0.20	0.39 ± 0.01	14.33 ± 0.81
T1		2.99 ± 0.09	0.40 ± 0.01	26.97 ± 4.20
T2		5.70 ± 0.24	0.43 ± 0.01	25.22 ± 1.26
T3		5.78 ± 0.09	0.39 ± 0.01	26.35 ± 3.91
T4		5.60 ± 0.10	0.43 ± 0.02	30.37 ± 1.48
T5		5.51 ± 0.14	0.42 ± 0.02	28.40 ± 3.16
Coefficients[a]	β_1	3.39*	0.42*	8.07
	β_2	8.41*	0.35*	6.47
	β_3	-16.97*	0.41	-55.09*
	β_{12}	-4.35*	0.08	34.02*
	β_{13}	41.37*	0.06	195.45*
	β_{23}	16.06*	0.15	185.13*
	R^2	0.78	0.60	0.79

a Model: y = β1x1 + β2x2 + β3x3 + β12x1x2 + β13x1x3 + β23x2x3, where *x1* = starch+PBAT, *x2* = glycerol and *x3* = tartaric acid (TA), **β1** = starch+PBAT, **β2** = Gly (glycerol), **β3** = TA (tartaric acid), **β12** = interaction starch+PBAT/Gly, **β13** = interaction starch+PBAT/TA, **β23** = interaction Gly/TA.
* Significant effects (p<0.05).

Olivato et al. (2011) observed that greater concentrations of citric acid could increase the opacity of the films based on starch/PBAT, by acting as compatibiliser, reducing the interfacial tension between the polymeric phases, which will result in a more dense structure, consequently more opaque. These results (increase of opacity with increase in concentration) were also observed for TA (P3) in this work.

Figure 1 – Surface contour for the effect of the components in the weight loss in water (%) of the films, in terms of pseudo-components. The experimental area is delimitated by the shown sample points.

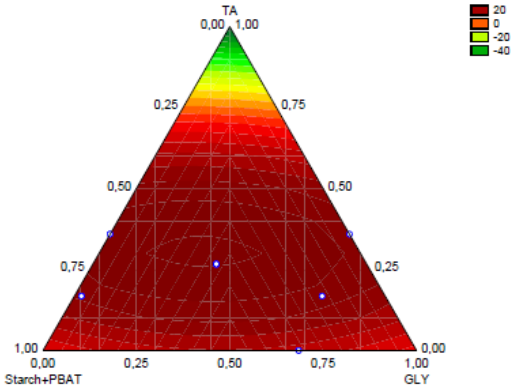

The addition of greater proportions of TA is responsible for reducing the weight loss in water of the films (negative effect of (3). The inclusion of carboxyl groups in the starch chains, with subsequent transesterification reactions, was capable to improve the resistance to the dissolution of the materials, fact also showed by Reddy and Yang (2010) for cross-linked starch and in accordance with the results of Table 2. Considering the hydrolytic action of TA, a significant positive effect on the response was observed for the interaction between starch+PBAT/TA ((13). Based on these different effects, it is possible to observe that intermediary proportions between the components will results in greater weight loss in water of the films (Figure 1).

3.2 MORPHOLOGY (SEM IMAGES)

In Figure 2 are shown SEM images of the samples C, T1 and T5, which containing different levels of TA. The addition of TA, independent of the concentration, changes the morphology of the starch/PBAT blends.

Figure 2 – SEM images for the fractures of the samples C (left), T1 (centre) and T5 (right). Magnification 1600x.

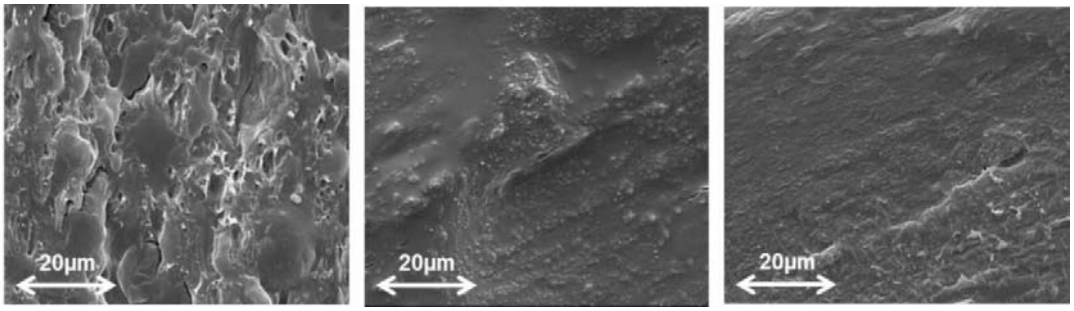

It is well defined that thermoplastic starch and PBAT form an immiscible blend, with high interfacial tension. This makes necessary the addition of compatibilisers capable to act in the interface to obtain stable blends, with good properties (REN et al., 2009; RAQUEZ et al., 2008; KONING et al., 1998). In the fracture of the sample without TA (Figure 2 - left) it is possible to observe empty spaces between the phases which reflect the high interfacial tension, typical structure of a two-phase polymer blend. With the inclusion of TA (Figure 2, centre and right), the compatibility between the phases is improved, resulting in reduction of the interfacial tension which is responsible for a more homogeneous films.

The influence of citric acid in starch/PLA blends was studied by Wang et al. (2010) and a structure that is more homogeneous and with improved dispersion between the phases was achieved in the presence of this acid. In addition, Shi and co-workers (2008) related better compatibility between PVA and starch with the addition of citric acid. These results are in accordance to those presented in this work for tartaric acid.

3.3 FOURIER TRANSFORM INFRARED SPECTROSCOPY (FT-IR)

Considering the FT-IR spectra for the formulations C, T1, T3 and T5 shown at Figure 3, no additional peaks were observed when TA was included in the formulation, resulting in very similar spectra.

Figure 3 – FT-IR spectra of the starch/PBAT films with and without tartaric acid.

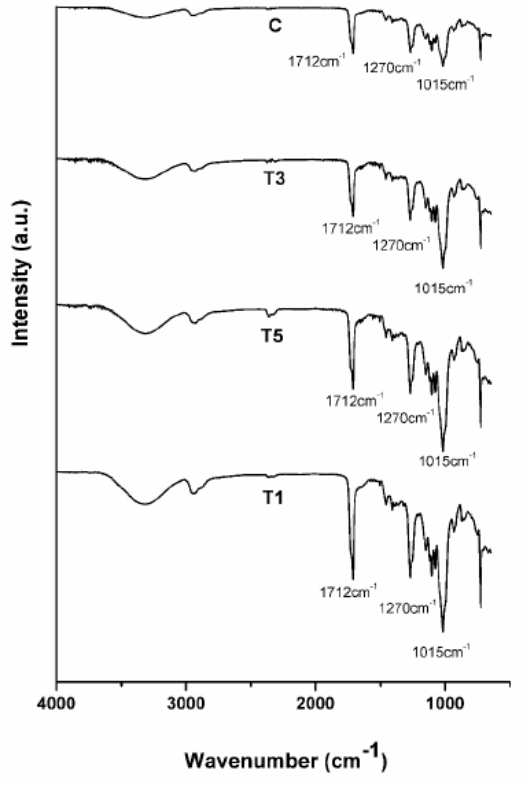

As a characteristic of the starch structure, all the formulations showed C-O bond stretching of C-O-C groups in anhydroglucose ring in 1015cm^{-1}. Also, peaks for C-O stretching in C-OH bonds could be observed in 1100 cm^{-1} and 1080cm^{-1} (WANG et al., 2007; 2009). Characteristic peak in 1270cm^{-1} represents the C-O in O-C=O bonds present in the PBAT structure, even as out of plane deformation of benzene ring, with peaks in 725 cm^{-1}and angular deformation of CH2 bonds in 1450 cm^{-1} and 1408 cm^{-1} (NOBREGA et al., 2012; OLIVATO et al., 2012).

The most probable action of TA, as compatibiliser in starch/PBAT blends, includes esterification reactions, introducing new groups in the starch chains (carboxyl groups), which are potential reactive points, or also transesterification reactions. Characteristic carboxyl peak for these materials is represented in 1712 cm^{-1}. Is possible to observe an increase of this peak when greater proportions of TA are used (Figure 3), which suggests that esterification reactions occurred during the reactive extrusion. In a similar way, FT-IR results observed by Shi et al. (2007) using citric acid in starch films suggests that esterification reactions happened during the melt blending, resulting in an increase of the C=O peaks.

However, the peak referent to ester function is a result of the coalescence between the mentioned ester bonds and those resulting of the polyester (PBAT) present in the formulation. This fact makes more difficult to obtain precise information concerning the esterification/transesterification reactions promoted by TA in starch/PBAT blends.

3.4 13C CPMAS NMR

The 13C CPMAS NMR spectra of samples without TA (C) and with 1.1 g.100g^{-1} TA (T1) are shown at Figure 4, with all the resonances pointed. The resonance peaks at õ 174, 165, 134, 130, 64, 34, 26 ppm were attributed to PBAT molecule, which chemical structure, detaching the different carbon, is presented in Figure 5. Cranston et al. (2003) observed similar values to those.

Figure 4 – ^{13}C CPMAS spectra for the samples without TA (C) and with 1.1 g.100g^{-1} TA (T1).

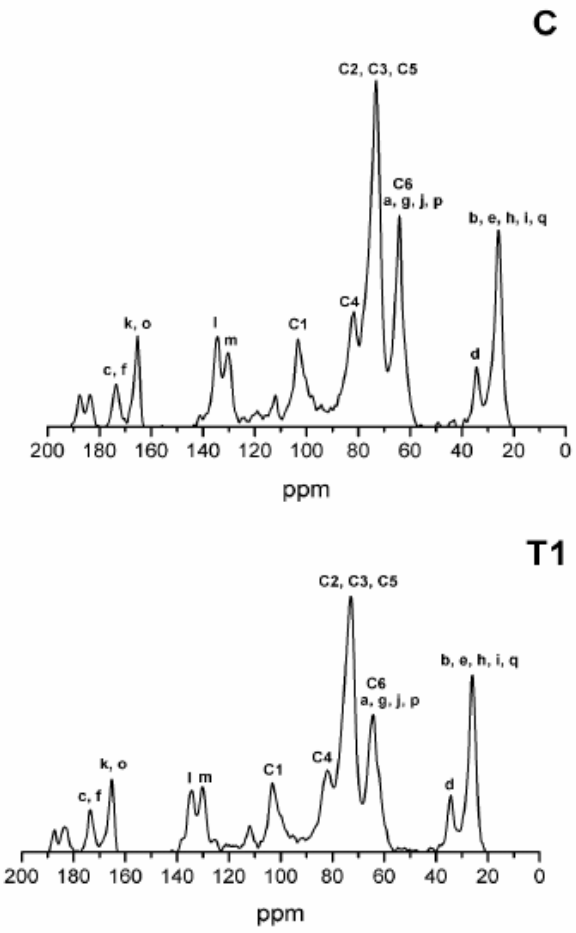

Figure 5 – PBAT (poly (butylene adipate co-terephthalate) chemical structure, with assignment of all carbons with resonance peaks shown at Figure 4.

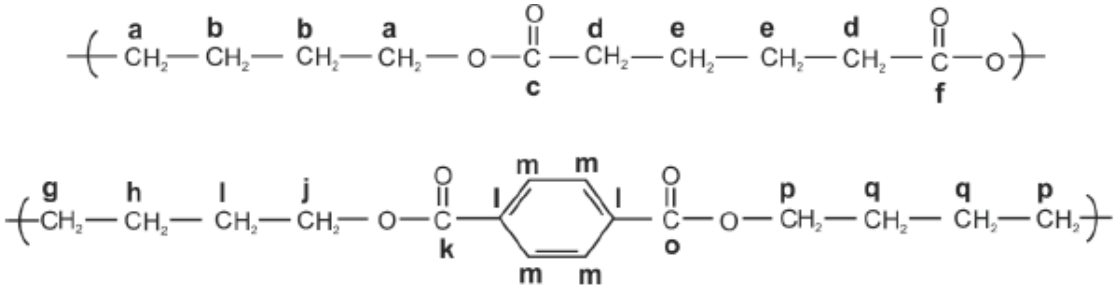

Starch macromolecules are formed by anhydroglucose units connected by a 1-4 linkages in amylose chains and also by a 1-6 in branches in amylopectin (MOAD, 2011). Figure 6 represents the structure of a unit of anhydroglucose, with the identification of all carbons. Figure 4 shows that carbon C(1) presents a resonance in 5 103 ppm; C(4) in 5 82 ppm; C(2), C(3), C(5) in 5 72.9 ppm and C(6) in 5 63 ppm. Bathista et al. (2012) found similar 13C CPMAS spectra for mango starch and Veregin et al. (1986) revealed the broadening for all resonances when the samples were previously dried. Taking this in consideration, we could explain the difficulty of reveal the doublet associated to C(1) carbons for glucose structure in the asymmetric unit, for example, for cassava starch used in this work.

Figure 6 – Anhydroglucose unit structure with assignment of all carbons and resonance peaks shown at Figure 4.

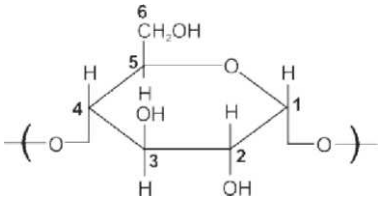

The results discussed along the manuscript indicates that TA would be capable to promote esterification reactions with the -OH of starch. Based on this, it be expected that the signal of an ester carbon would appear when TA was incorporated in the formulation. However, PBAT also produces resonances in this region and caused some difficulty in characterise the modification occurring in the starch. Thus, considering the spectra, no chemical shifts or additional peaks were observed in the formulation containing tartaric acid (T1), only a shoulder being identified in the region of 5 185 ppm, corresponding to a carbon localised in a

carbonyl of carboxylic acid, probably due unreacted TA. The ratio between the area of the signal 5 174 ppm and the area of the 5 130 ppm, a carbon that does not change in the process, was then used to identify the esterification reaction. These reactions promoted by TA increased the ratio 5 174 / 5 130 from 0.60 for C sample to 1.11 for T1 sample.

Considering that the esterification reactions occur preferentially at C(6) of the anhydroglucose units of starch (RAQUEZ et al., 2008), it would be expected that the ratio 5 63 / 5 130 would be reduced in the sample with TA. Therefore, for C sample the ratio 5 63 / 5 130 result in 2.74 whereas for T1 sample resulted in 2.13.

In conclusion, these results could prove the occurrence of esterification reactions, which improved the compatibility between starch and PBAT and explains the effects of TA observed in the mechanical, optical and structural properties of starch/PBAT films.

4 Conclusions

Starch/PBAT blends compatibilised by tartaric acid were successfully produced by one-step reactive extrusion, with formulations based in a constraint mixture design. Tartaric acid was able to act as compatibiliser between the polymeric phases and resulting in more homogeneous blends, as could be observed by scanning electron microscopy (SEM) images. The analysis of data modelling showed that the interaction between the polymers and TA increased the films resistance. All the components (TA, GLY and starch+PBAT) positively contributed to the films opacity and the increase of TA content reduces their weight loss in water. Esterification reactions promoted by TA were well characterised by FT-IR and 13C CPMAS NMR as an evidence of their reaction with the starch, making them more compatible with PBAT phase and resulting in blends with better mechanical properties.

5 References

AMERICAN SOCIETY FOR TESTING AND MATERIAL (ASTM) (1996). **Standard test methods for tensile properties of thin plastic sheeting.** D882-91. Philadelphia: ASTM.

AVEROUS, L. Biodegradable multiphase systems based on plasticized starch: A review. **Journal of Macromolecular Science C,** v. 44, p. 231-274, 2004.

AVEROUS, L; FRINGANT, C; MORO, L. Starch-based biodegradable materials suitable for thermoforming packaging. **Starch/Starke,** v. 53, p. 368-371, 2001.

AVÉROUS, L; DIGABEL, F. L. Properties of biocomposites based on lignocellulosic fillers. **Carbohydrate Polymers,** v. 23, p. 480-493, 2006.

BATHISTA, A. L. B. S; SILVA, E. O; TAVARES, M. I. B; PRADO, R. J. Solid-state NMR to evaluate the molecular changes in the mango starch after 8 years of storage. **Journal of Applied Polymer Science,** v. 126, p. 123-126, 2012.

CARVALHO, A. J. F; ZAMBON, M. D; CURVELO, A. A. S; GANDINI, A. Thermoplastic starch modification during melt processing: Hydrolysis catalyzed by carboxylic acids. **Carbohydrate Polymers,** v. 62, p. 387-390, 2005.

CRANSTON, E; KAWADA, J; RAYMOND, S; MORIN, F. G; MARCHESSAULT, R. H. Cocrystallization model for synthetic biodegradable poly(butylene adipate-co-butylene terephthalate). **Biomacromolecules,** v. 4, p. 995-999, 2003.

DIVERS, T; PILLIN, I; FELLER, J. F; LEVESQUE, G; GROHENS, Y. Starch modification, destructuration and hydrolysis during O-formylation. **Starch/Starke,** v. 56, p. 389-398, 2004.

HUNEAULT, M. A; LI, H. Preparation and properties of extruded thermoplastic starch/polymer blends. **Journal of Applied Polymer Science,** v. 126, p. 96-108, 2012.

HUNTER ASSOCIATES LABORATORY. **Universal Software version 3.2: User manual.** United States: Reston, 2012.

KONING, C; DUIN, M. V; PAGNOULLE, C; JEROME, R. Strategies for compatibilization of polymer blends. **Progress in Polymer Science,** v. 23, p. 707-757, 1998.

MALIGER, R. B; McGLASHAN, S. A; HALLEY, P. J; MATTHEW, L. G. Compatibilization of starch-polyester blends using reactive extrusion. **Polymer Engineering and Science,** v. 46, p. 248-263, 2006.

MOAD, G. Chemical modification of starch by reactive extrusion. **Progress in Polymer Science,** v. 36, p. 218-237, 2011.

NOBREGA, M. M; OLIVATO, J. B; MULLER, C. M. O; YAMASHITA, F. Biodegradable starch-based films containing saturated fatty acids: thermal, infrared

and raman spectroscopic characterization. **Polímeros - Ciência e Tecnologia,** v. 22, p. 467-474, 2012.

PELISSARI, F. M; YAMASHITA, F; GARCIA, M. A; MARTINO, M. N; ZARITZKY, N. E; GROSSMANN, M. V. E. Constrained mixture design applied to the development of cassava starch-chitosan blown films. **Journal of Food Engineering,** v. 108, p. 262-267, 2012.

OLIVATO, J. B; NOBREGA, M. M; MULLER, C. M. O; SHIRAI, M. A; YAMASHITA, F; GROSSMANN, M. V. E. Mixture design applied for the study of the tartaric acid effect on starch/polyester films. **Carbohydrate Polymers,** v 92, p. 1705-1710, 2013.

OLIVATO, J. B; GROSSMANN, M. V. E; BILCK, A. P; YAMASHITA, F. Effect of organic acids as additives on the performance of thermoplastic starch/polyester blown films. **Carbohydrate Polymers,** v. 90, p. 156-164, 2012.

OLIVATO, J. B; GROSSMANN, M. V. E; YAMASHITA, F.; NOBREGA, M. M; SCAPIN, M. R. S; EIRAS, D; PESSAN, L. A. Compatibilisation of starch/poly (butylene adipate co-terephthalate) blends in blown films. **International Journal of Food Science and Technology,** v. 46, p. 1934-1939, 2011.

RAQUEZ, J. M; NABAR, Y; SRINIVASAN, M; SHIN, B. Y; NARAYAN, R ; DUBOIS, P. Maleated thermoplastic starch by reactive extrusion. **Carbohydrate Polymers,** v. 74, p. 159-169, 2008.

REDDY, N; YANG, Y. Citric acid cross-linking of starch films. **Food Chemistry,** v. 118, p. 702-711, 2010.

REN, J; FU, H; REN, T; YUAN, W. Preparation, characterization and properties of binary and ternary blends with thermoplastic starch, poly (lactic acid) and poly(butylene adipate-co-terephthalate). **Carbohydrate Polymers,** v. 77, p. 576-582, 2009.

SHI, R; ZHANG, Z; LIU, Q; HAN, Y; ZHANG, L ; CHEN, D ; TIAN, W. Characterization of citric acid/glycerol co-plasticized thermoplastic starch prepared by melt blending. **Carbohydrate Polymers,** v. 69, p. 748-755, 2007.

SHI, R; BI, J; ZHANG, Z; ZHU, A; CHEN, D; ZHOU, X; ZHANG, L; TIAN, W. The effect of citric acid on the structural properties and cytotoxicity of the polyvinyl alcohol/starch films when molding at high temperature. **Carbohydrate Polymers,** v. 74, p. 763-770, 2008.

VEREGIN, R. P; FYFE, C. A; MARCHESSAULT, R. H; TAYLOR, M. G. Characterization of the crystalline A and B starch polymorphs and investigation of starch crystallization by high-resolution 13C CP/MAS NMR. **Macromolecules,** v. 19, p. 1030-1034, 1986.

YANG, S; LIU, C; WU, J; KUO, J; HUANG, C. Improving the processing ability and mechanical strength of starch/poly(vinyl alcohol) blends through plasma and acid modification. **Macromolecular Symposium,** v. 272, p. 150-155, 2008.

WANG, N; YU, J; MA, X; WU, Y. The influence of citric acid on the properties of thermoplastic starch/linear low-density polyethylene blends. **Carbohydrate Polymers,** v. 67, p. 446-453, 2007.

WANG, N; ZHANG, X; HAN, N; BAI, S. Effect of citric acid and processing on the performance of thermoplastic starch/montmorillonite nanocomposites. **Carbohydrate Polymers,** v. 76, p. 68-73, 2009.

WANG, N; ZHANG, X; HAN, N; JIANMING, F. Effects of water on the properties of thermoplastic starch poly(lactic acid) blend containing citric acid. **Journal of Thermoplastic Composite Materials,** v. 23, p. 19-34, 2010.

CAPITULO 5 – STARCH/POLYESTER FILMS: SIMULTANEOUS OPTIMISATION OF THE PROPERTIES FOR THE PRODUCTION OF BIODEGRADABLE PLASTIC BAGS

ABSTRACT: Blends of starch/polyester have been of great interest in the development of biodegradable packaging. Analysis techniques for multiple responses optimisation (Desirability) was used to evaluate the properties of tensile strength, perforation force, elongation and seal strength of cassava starch/poly(butylene adipate-co-terephthalate) (PBAT) blown films produced via a one-step reactive extrusion using tartaric acid (TA) as a compatibiliser. Maximum results for all the properties were set as more desirable, and an optimal formulation was obtained that contained (55:45) starch/PBAT (88.2%wt), glycerol (11.0%wt) and TA (0.8%wt). With the film obtained from this formulation, biodegradable plastic bags were produced and analysed according to the standard method of the Associação Brasileira de Normas Técnicas (ABNT). The bags exhibited a 45% failure rate in free-falling dart impact tests, a 10% of failure rate in dynamic load tests and no failure in static load tests; these results satisfy the specifications of the standard. Thus, the biodegradable plastic bags developed with an optimised formulation could be useful as an alternative to those made from non-biodegradable materials if the nominal capacity declared for this material is considered.

Keywords*:* Starch/PBAT blends. Tartaric acid. Extrusion. Desirability. Biodegradable bags.

1 Introduction

The global consumption of plastics in 2002 was of 120 million tons, and Brazil was responsible by 4200 tons of this total. The packaging sector is responsible for the greatest utilisation of plastics, which corresponds to more than a third of the Brazilian consumption (CANEVAROLO et al., 2010). The plastic bags provided by markets, which are resistant and convenient represent a large portion of all the plastic bags produced and supplied to consumers (SHARP; HOJ; WHELLER, 2010). These data show the inherent need for the development of alternatives for the substitution, or at least the partial substitution, of this type of packaging with another material that is ecologically favourable and that exhibits properties similar to those of synthetic plastics.

Starch is a polysaccharide formed by units of D-glucose and two different macromolecules: amylose, which possesses an essential linear structure, with a few branches, and amylopectin, which possesses a highly branched structure (AVEROUS, 2004). In the presence of plasticisers, at high temperature and under

shear, starch tends to melt and flow, which enables its use in injection and blown film extrusion equipment. This property makes starch similar to most of the synthetic conventional polymers, with the additional advantages of being abundant, renewable, inexpensive and biodegradable (MOAD, 2011; MATTA Jr et al., 2011; YU; WANG; MA, 2005).

Thermoplastic starch (TPS) alone is not adequate for use in packaging because is fragile and sensitive to environmental conditions (KALAMBUR and RIZVI, 2006). To overcome this difficulty, several researchers have focused on the development of blends that contain TPS added to biodegradable polyesters, such as PBAT (poly(butylene adipate-co-terephthalate) and PLA (polylactic acid) (OLIVATO et al., 2012a; WANG; WU; MA, 2007; RAQUEZ et al., 2008). In these cases, the use of additives (compatibilisers) capable of acting at the interface and improving the adhesion between the polymeric chains is necessary. This adhesion is impaired by the differences between the hydrophilic starch and the hydrophobic polyester. In this context, tartaric acid (TA) can be added. TA is an organic acid naturally present in fruits, mostly in grapes, that can act as plasticiser or acidifier or can be used to promote esterification/transesterification reactions between polymers (REN et al., 2009; ESWARANANDAM et al., 2006; YOON; CHOUGH; PARK, 2006).

Reactive extrusion is useful in the modification of the properties of starch and in the production of TPS blended with other materials. This process is industrially viable and continuous and offers the advantage of being a good mixing device, especially for high-viscosity systems such as TPS (MOAD, 2011). Films produced by blown extrusion are typically evaluated for their mechanical properties, including their tensile strength, elongation and perforation force.

Systems that provide a multiplicity of responses require data processing, with the aim of obtaining the best combination of factors that estimate the best possible combination of responses (CARNEIRO et al., 2005). The technique of desirability represents a way to achieve this goal through the analysis of all data together, where each parameter is converted into a normalised function with a value of 0 (less desirable) to 1 (more desirable), according to the method proposed by Derringer and Suich (1980).

This work is aimed at the production of cassava starch/PBAT biodegradable films by a one-step reactive extrusion, where TA is added as a compatibiliser, and the analysis of the mechanical results using the technique of

desirability. Additionally, the optimal conditions found using this technique were used to produce a blown film, which was characterised and used to produce plastic bags with properties similar to those made from synthetic plastics currently available in the market.

2 Experimental

2.1 MATERIALS

Native cassava starch was supplied by Indemil (Paranavaí, PR/Brazil), and the polyester PBAT (poly(butylene adipate-*co*-terephthalate)) was supplied by BASF (Ludwigshafen, Germany) under the commercial name Ecoflex®. Glycerol supplied by Dinâmica (Diadema, SP/Brazil) and TA supplied by Sigma-Aldrich (Steinheim, Germany) were also used.

2.2 METHODS

2.2.1 Experimental Design

To evaluate the influence of glycerol as a plasticiser and TA as a compatibiliser in starch/PBAT blends, a mixture design was proposed, as shown at Table 1, in which the third component of the ternary mixture is represented by starch+PBAT in a 55:45 (wt) proportion.

Table 1 – Concentration of the components in the formulations according to a mixture design.

Samples	*Components (%)*			*Pseudo-components**		
	Starch+PBAT (55:45)	Glycerol	Tartaric acid	x_1	x_2	x_3
C	88.0	12.0	0.0	0.3	0.7	0.0
T1	87.0	11.9	1.1	0.0	0.6	0.4
T2	89.5	9.9	0.5	0.8	0.0	0.2
T3	87.5	11.9	0.5	0.2	0.6	0.2
T4	89.0	9.9	1.1	0.6	0.0	0.4
T5	88.3	10.9	0.8	0.4	0.3	0.3

* To calculate the pseudo-components' values, the equation $xi = ci\text{-}ai / 1\text{-}\Sigma ai$ was used, where $x1$ = starch+PBAT, $x2$ = glycerol and $x3$ = tartaric acid; ci is the actual concentration; and ai is the lower limit of each component in the mixture design.

After a polynomial model was fit to the response, its simultaneous optimisation was conducted using the technique of Desirability according to the method described by Derringer and Suich (1980), which parameters were defined as more desirable (1) and less desirable (0) with base of the obtained results of the tested formulations (Table 2). The STATISTICA 7.0 software package (Statsoft, Tulsa/USA) was used to analyse data and plot the graphics of the properties of the films.

Table 2 – Maximum and minimum results obtained for the tested formulations used as reference in the simultaneous optimisation of the responses.

Parameters	*Higher Limit*	*Lower Limit*
Seal Strength (N)	720.27 (1)	188.51 (0)
Tensile Strength (MPa)	6.81 (1)	2.65 (0)
Elongation (%)	736.68 (1)	176.92 (0)
Puncture Force (N)	24.36 (1)	10.99 (0)

* Values in parentheses are the Desirability.

2.2.2 Blown Film Extrusion

Pellets were produced using a laboratory single-screw extruder (model EL-25, BGM, São Paulo, Brazil) with a screw diameter (D) of 25 mm and a screw length of 28D according the mixture design shown in Table 1. The barrel temperature profile was maintained at 100/120/120/120°C from the feeding zone (zone 1) to the die zone (zone 4). The screw speed was 40 rpm, and a die with six 2 mm diameter holes was used. The pellets were subsequently re-extruded using the same extruder to obtain blown films with a barrel temperature profile of 100/120/120/130°C and 130°C for the 50 mm film-blowing die and a screw speed of 40 rpm. The feed rate was maintained to ensure that the screw operated at full load. The film thickness was controlled via the roll-speed control and the air flow and was maintained between 100 and 150 um.

2.2.3 Characterisation and Mechanical Analysis

A model TA.XT2i texture analyser (Stable Micro Systems, Surrey/England) fitted with a 50 kg load cell was used to perform the tensile, seal and puncture tests on the films. The tensile tests were based on ASTM standard method D882-00 (2001). Ten samples of each formulation were cut in the longitudinal direction with a length of 50 mm and a width of 20 mm and were fit to the tensile grips. The crosshead speed was set at 0.8 mm/s, and the initial distance between the grips was 30 mm. The tensile strength (MPa) and elongation at break (%) were determined.

The puncture tests were performed based on ASTM standard method F1306-90 (2002) with 10 samples of each formulation, which were fixed in an appropriate dispositive that allowed exposure of 35 mm of the sample. The perforation was realised using a cylindrical probe with a diameter of 3.0 mm and a speed of 0.4 mm/s, which was used to perpendicularly pierce the sample. The puncture force (N) was determined.

Seal strength (N) was measured based on standard method ASTM F88-00 (2001) using 10 samples of each formulation that were 80 mm long and 25 mm wide. The samples were fixed into the tensile grips of the equipment, and the sealing area was positioned in the centre, perpendicular to the direction of traction. All the formulations were sealed in a hot-bar sealer, in which the temperature (140°C) and the time (3 sec) were kept constant. The sample was then submitted to traction with a crosshead speed of 1.0 mm/s until the seal was disrupted. Before all of the tests, the samples were conditioned at 23 ± 2°C and 53 ± 2% RH for 48 hours.

The mechanical properties and seal strength were evaluated to obtain an optimised formulation according to the Desirability technique. Tensile strength, elongation, puncture force and seal strength were specified as the maximum levels desirable (Table 2). The formulation T5 (closer to the optimal formulation) was then used to produce plastic bags, which were submitted to free-falling dart impact tests, static load tests and dynamic load tests performed at the Centre for Research and Development of Packages (Centro de Pesquisa e Desenvolvimento de Embalagens, CETEA/ITAL), Campinas/SP/BR, according parameters specified in the ABNT NBR 14937:2010 standard (2010).

To determine the bags' dynamic load strength, ten samples that contained 1 kg loads (declared as the nominal capacity) were tested in a vertical harmonic oscillation simulator operated with displacement amplitude of 100 ± 2 mm and at a frequency of 1 ± 0.1 Hz for 100 ± 2 sec. The static load strength tests were performed with five samples that contained 1 kg and were suspended by their handles in a tubular support for 120 ± 1 min. For both tests, the results are expressed as the presence or absence of failure (visual rupture with size > 10 mm).

Twenty specimens with diameters of 125 ± 2 mm were used to determine the material's falling dart strength, in which a dart with a polished surface and spherical tip diameter of 38 ± 1 mm and a weight of 60.0 ± 0.3 g was positioned 660 mm from the specimen such that it impacted the centre of the specimen during free fall. The results are expressed as the occurrence of a rupture of any size after the dart impact.

2.2.4 Scanning Electron Microscopy (SEM) Analysis

An FEI model Quanta 200 scanning electron microscope (FEI, Tokyo, Japan) was used for the observations of the fractured surface of the film-blown samples. The samples were submerged in liquid nitrogen and then broken (cryogenic fracture). Before being coated with a gold layer, the samples were stored at 25°C in a desiccator with CaCl2 («0% RH) for 3 days. The coating was applied using a sputter coater (BAL-TEC SCD 050). Images were taken of the fractured surface at 800x and 1600x magnification.

3 Results and Discussion

3.1 Analysis of the Results and the Simultaneous Optimisation

The diagram shown in Figure 1 presents the curves with the response observed for each variable analysed with the values of the other variables fixed. Each line shows the individual behaviour of the variables for each property analysed keeping constant the other variables. The results of all the properties used as reference in the Desirability technique are shown at Table 2.

Figure 1 – Desirability diagram based on the parameters of seal strength (N), tensile strength (MPa), elongation (%) and puncture force (N).

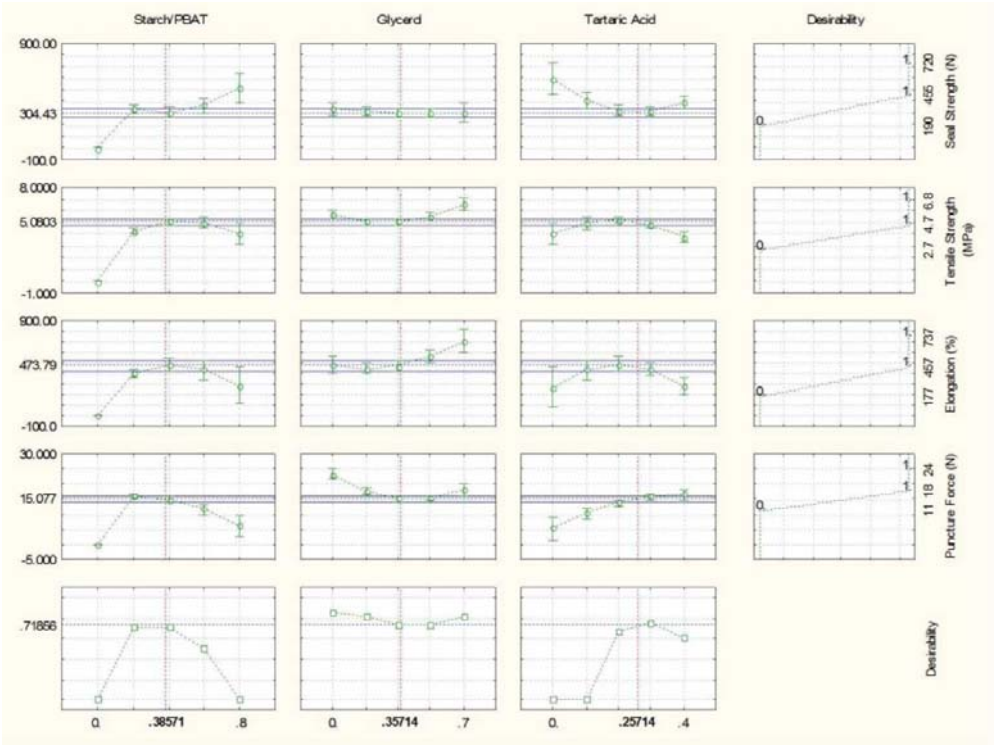

The ability to seal a flexible film is one of the most important properties of the materials used in flexible packaging; it is essential to the integrity of the packaging and to guarantee the shelf-life of the packaged product (OLIVEIRA et al., 2006). The results of sealing strength varied from 190 to 720 N (Table 2). The glycerol content had little influence on this property, and a greater sealing strength to traction was observed when low concentrations of tartaric acid (TA) were used.

The puncture force is a quality parameter for materials used in the packaging of products with tips, edges and other protrusions that might damage the packaging (SARANTOPOULOS et al., 2002). The puncture force was observed to increase with the use of greater proportions of TA in the films, whereas for glycerol, the opposite effect was observed in which higher levels of glycerol resulted in films with a lower puncture force (Figure 1). The plasticiser action of glycerol, which is expected to reduce the intermolecular forces between the polymer chains, is responsible for this result, as also reported by other authors (PARRA et al., 2004; CUQ et al., 1997). This plasticiser action also contributes to an increase in the elongation of the films because of the higher molecular mobility promoted by the addition of the plasticiser.

Tartaric acid, a dicarboxylic acid, induces acid hydrolysis of the starch chains, which reduces the molecular weight of the starch and consequently changes its melting temperature and viscosity, critical properties in the processing of thermoplastic starch. The inclusion of TA also results in more flexible films (higher elongation) (Da ROZ et al., 2011). Furthermore, the use of TA as an additive could allow the interaction of this component with the hydroxyl groups of the starch molecules, which promotes esterification/transesterification reactions that interconnect the polymer chains and improve the material's resistance, as observed in our previous works (OLIVATO et al., 2012b).

Taking this into consideration, a comparison of the results shown in Figure 1 for the tensile strength and elongation of films, indicate that better results were achieved for both properties at intermediate concentrations, which produce more resistant and flexible films. These results show that, at these proportions, a balance exists between hydrolytic action and crosslinking promoted by the TA. Thus, the compatibiliser action of TA in the films improves the interaction between the starch and hydrophobic PBAT, as evidenced by the SEM images in Figure 2.

Figure 2 – SEM images of fractured samples C (left) and T5 (right) at 800x magnification.

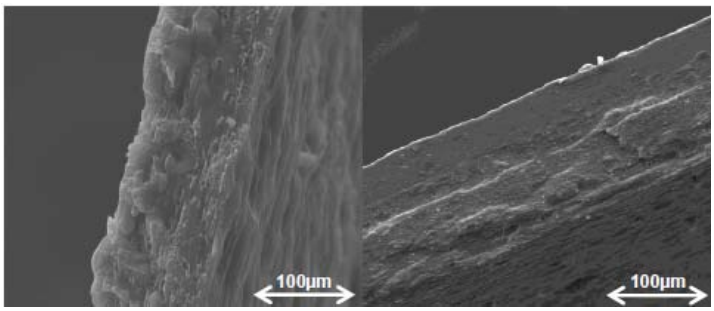

The SEM image of the C sample (without TA) shows starch granules that have not been completely disrupted (Figure 3) and are distributed throughout the film polymer matrix, which has resulted in a non-homogeneous structure (Figure 2). With the addition of TA (sample T5), the disruption of starch granules is facilitated, and the compatibility between the polymer phases is improved, which has resulted in films with a continuous and more homogeneous matrix. Similar results were obtained by Miranda and Carvalho (2011), who compatibilised blends that contained

thermoplastic starch and low-density polyethylene using citric acid, and by Olivato et al. (2011), who included citric acid in blends of starch/PBAT.

Figure 3 – SEM image of fractured sample C at 1600x magnification. The arrows indicate granules of starch not completely disrupted.

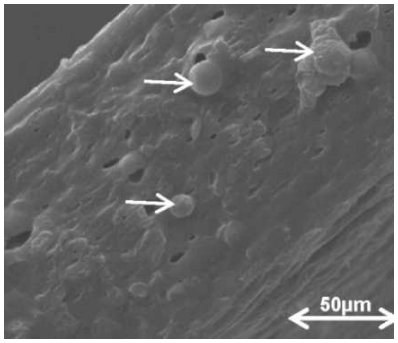

Based on the diagram shown in Figure 1, when the global Desirability (last line of the diagram) is considered, changes in both the TA concentration and the fraction that contains starch+PBAT influenced significantly the results of Desirability, and the use of intermediate concentrations of these components were observed to result in formulations with optimised properties. Thus, the Desirability function has resulted in values (pseudo-components data) that correspond to 0.386 for the mixture starch+PBAT (88.2% wt), 0.357 for glycerol (11.0% wt) and 0.257 for TA (0.8% wt). This composition therefore represents the most desirable formulation (expressed by the vertical line in the diagram).

3.2 Evaluation of the Properties of Plastic Bags Made with the Selected Film

The T5 formulation was closer to the theoretical values obtained by the Desirability function and was used for the production of films for biodegradable plastic bags (Figure 4). The results obtained for the analysis of these bags with respect to the free-falling dart impact strength, the static load strength and the dynamic load strength are shown in Table 3.

Figure 4 – Biodegradable plastic bags developed using the T5 formulation.

According to standard ABNT NBR 14937:2010 (2010), the fail tolerance is 50% in the free-falling dart impact strength test and 20% in the static load strength and dynamic load strength tests. Based on these tolerances, the developed sample meets the requirements set in the standard, once the bags produced with the optimised formulation (T5) exhibited a 45% failure rate in the free-falling dart impact strength test, a 10% failure rate in the dynamic load strength test and no failure in tests of static load strength. We therefore conclude that the developed bags are suitable for commercial use, taking into account the declared nominal capacity declared of this material.

The Supermarket Plastic Bags Analysis Report (Relatório de Análise em Sacolas Plásticas de Supermercados) was published by INMETRO on 24/06/2007, in which samples of plastic bags available in 18 different markets in Brazil were evaluated in accordance with current legislation. Among the results for the strength tests that simulate common consumer usage of packing and loading store-bought goods, 75% of the brands analysed were considered not in accordance.

Table 3 – Results of strength tests of plastic bags produced using the optimised formulation (T5).

Test		***Results***
Free-falling dart impact strength	Rupture (%)	45
Static load strength	Failure (%)	0
Dynamic load strength	Failure (%)	10

A comparison of these results to those obtained in the present work indicates that the starch-based bags are a viable and environmentally friendly alternative to synthetic packaging currently available on the market considering the

nominal capacity declared for each material. However, more research is needed to reduce the sensitivity of starch-based materials to environmental conditions, which remains a challenge even with blends that contain polyester, which has represented a major advance in this direction.

4 Conclusion

The addition of TA improved the compatibility between the polymeric phases and resulted in blends with a more homogeneous structure and a continuous matrix, as evidenced by SEM images. Additionally, the TA contributed to the increase in the films puncture strength and, at intermediate concentrations, resulted in materials with a higher tensile strength and elongation. These improvements are possibly due to the role of TA in promoting crosslinking and acid hydrolysis of starch molecules, which together are responsible for such effects.

The Desirability method was effective in the combined optimisation of mechanical properties and heat-sealing strength and resulted in an optimised formulation that corresponded to a blend of starch/PBAT (88.2% wt), glycerol (11.0% wt) and TA (0.8% wt).

The biodegradable plastic bags produced with formulation T5 (closest to the optimal formulation) and analysed according to the ABNT NBR 14937:2010 standard satisfied the requirements specified in this standard. Taking also into consideration the nominal specified load, these bags represent an alternative to non-biodegradable plastic bags currently sold for the packaging of low-weight products, which do not require a material of high mechanical strength.

5 References

AMERICAN SOCIETY FOR TESTING AND MATERIALS (ASTM). **Standard test methods for tensile properties of thin plastic sheeting.** D882-00, Philadelphia: ASTM, 2001.

AMERICAN SOCIETY FOR TESTING AND MATERIALS (ASTM). **Standard test method for slow rate penetration resistance of flexible barrier films and laminates.** F1306-90, Philadelphia: ASTM, 2002.

AMERICAN SOCIETY FOR TESTING AND MATERIALS (ASTM). **Standard test method for seal strength of flexible barrier materials.** F88-00, Philadelphia: ASTM, 2001.

ABNT NBR 14937:2010. **Sacolas plásticas tipo camiseta - Requisitos e métodos de ensaio.** Associação Brasileira de Normas Técnicas (ABNT), 20l0.

AVEROUS, L. Biodegradable multiphase systems based on plasticized starch: A review. **Journal of Macromolecular Science Part C - Polymer Reviews,** v. C44, n. 3, p. 231-274, 2004.

CANEVAROLO Jr, S. V. **Ciência dos Polímeros.** São Paulo: Artliber, 2010.

CARNEIRO, R. J; SILVA, R. S. S. F; BORSATO, D; BONA, E. Gradients methods for simultaneous optimizations: case studies for food systems. **Semina: Ciências Agrárias,** v. 26, p. 353-362, 2005.

CUQ, B; GONTARD, N; CUQ, J; GUILBERT, S. Selected functional properties of fish myofibrillar protein-based films as affected by hydrophilic plasticizers. **Journal of agricultural and Food Chemistry,** v. 45, p. 622-626, 1997.

DA ROZ, A. L; ZAMBON, M. D; CURVELO, A. A. S; CARVALHO, A. J. F. Thermoplastic starch modified during melt processing with organic acids: The effect of molar mass on thermal and mechanical properties. **Industrial Crops and Products,** v. 33, p. 152-157, 2011.

DERRINGER, G; SUICH, R. Simultaneous optimization of several response variables. **Journal of Quality Technology,** v. 12, p. 214-219, 1980.

ESWARANANDAM, S; HETTIARACHCHY, N. S; MEULLENET, J. F. Effect of malic and lactic acid incorporated soy protein coatings on the sensory attributes of whole apple and fresh-cut cantaloupe. **Journal of Food Science,** v. 71, p. 307-313, 2006.

KALAMBUR, S; RIZVI, S. S. H. An overview of starch-based plastic blends from reactive extrusion. **Journal of Plastic Film and Sheeting,** v. 22, p. 39-58, 2006.

MATTA JUNIOR, M. D; SARMENTO, S. B. S; SARANTOPOULOS, C. I. G. L; ZOCCHI, S. S. Propriedades de barreira e solubilidade de filmes de amido de ervilha associado com goma xantana e glicerol. **Polímeros: Ciência e Tecnologia,** v. 21, n. 1, p. 67-72, 2011.

MIRANDA, V. R; CARVALHO, A. J. F. Blendas compatíveis de amido termoplástico e polietileno de baixa densidade compatibilizadas com ácido cítrico. **Polímeros: Ciência e Tecnologia,** v. 21, p. 353-360, 2011.

MOAD, G. Chemical modification of starch by reactive extrusion. **Progress in Polymer Science,** v. 36, p. 218-237, 2011.

OLIVATO, J. B; GROSSMANN, M. V. E; YAMASHITA, F; NOBREGA, M. M; SCAPIN, M. R. S; EIRAS, D; PESSAN, L. A. Compatibilisation of starch/poly(butylene adipate co-terephthalate) blends in blown films. **International Journal of Food Science and Technology,** v. 46, p. 1934-1939, 2011.

OLIVATO, J. B; GROSSMANN, M. V. E; YAMASHITA, F; EIRAS, D; PESSAN, L. A. Citric acid and maleic anhydride as compatibilizers in starch/poly (butylene adipate-co-terephthalate) blends by one-step reactive extrusion. **Carbohydrate Polymers,** v. 87, p. 2614-2618, 2012a.

OLIVATO, J. B; GROSSMANN, M. V. E; BILCK, A. P; YAMASHITA, F. Effect of organic acids as additives on the performance of thermoplastic starch/polyester blown films. **Carbohydrate Polymers,** v. 90, p. 159-164, 2012b.

OLIVEIRA, L. M; SARANTOPOULOS, C. I. G. L; CUNHA, D. G; LEMOS, A. B.

Embalagens termoformadas e termoprocessáveis para produtos cárneos processados. **Polímeros: Ciência e Tecnologia,** v. 16, p. 202-210, 2006.

PARRA, D. F; TADINI, C. C; PONCE, P; LUGAO, A. B. Mechanical properties and water vapor transmission in some blends of cassava starch edible films. **Carbohydrate Polymers,** v. 58, p. 475-481, 2004.

Programa de Análise de Produtos: INMETRO. 2012. Available at: <http://www.inmetro.gov.br/consumidor/prodAnalisados.asp?texto=&ordem=titulo&pa g ina=6>. Accessed on 05 march 2012.

RAQUEZ, J. M; NABAR, Y; SRINIVASAN, M; SHIN, B. Y; NARAYAN, R. DUBOIS, P. Maleated thermoplastic starch by reactive extrusion. **Carbohydrate Polymers,** v. 74, p. 159-169, 2008.

REN, J; FU, H; REN, T; YUAN, W. Preparation, characterization and properties of binary and ternary blends with thermoplastic starch, poly(lactic acid) and poly(butylene adipate-co-terephthalate). **Carbohydrate Polymers,** v. 77, p. 576-582, 2009.

SARANTOPOULOS, C. I. G. L; OLIVEIRA, L. M; PADULA, M; COLTRO, L; ALVES, R. M. V; GARCIA, E. E. C. **Embalagens plásticas flexíveis: Principais polímeros e avaliação de propriedades.** 1 ed. Campinas: CETEA/ITAL, 2002. 265 p.

SHARP, A; HOJ, S; WHELLER, M. Proscription and its impact on anti-consumption behaviour and attitudes: the case of plastic bags. **Journal of Consumer Behaviour,** v. 9, p. 470-484, 2010.

YOON, S; CHOUGH, S; PARK, H. Effects of additives with different functional groups on the physical properties of starch/PVA blend film. **Journal of Applied Polymer Science,** v. 100, p. 3733-3740, 2006.

YU, J; WANG, N; MA, X. The effects of citric acid on the properties of thermoplastic starch plasticized by glycerol. **Starch/Starke,** v. 57, p. 494-504, 2005.

WANG, N; YU, J; MA, X. Preparation and characterization of thermoplastic starch/PLA blends by one-step reactive extrusion. **Polymer International,** v. 56, p. 1440-1447, 2007.

CAPITULO 6 – MORPHOLOGY AND PROPERTIES OF STARCH/POLYESTER NANO-BIOCOMPOSITES BASED IN SEPIOLITE CLAY

ABSTRACT: Nano-sized filler incorporation in thermoplastic starch/polyester blends could be an alternative to improve their properties. TPS/PBAT nano-biocomposites were elaborated with two proportions between the polymeric phases and the influence of sepiolite nanoclays in the mechanical, thermal and structural properties of the blends was evaluated. SEM images confirm a good dispersion of sepiolite clay, with low occurrence of small aggregates in polymeric matrix. Wide angle X-ray diffraction showed no significant alteration in the crystal structure of PBAT and starch induced by sepiolite clay. The addition of sepiolite slightly affected the thermal degradation of the nano-biocomposites, but showed higher torque values with greater nanoclay proportions. Mechanical tests showed an increase in the matrix stiffness, with Young's module of 102.1 ± 4.2 MPa (80:20 TPS/PBAT) and 117.1 ± 5.3 MPa (50:50 TPS/PBAT), thanks to sepiolite, which represent a promising nanofiller for TPS based materials.

Keywords*:* Nano-biocomposites. Sepiolite; Thermoplastic starch. Poly (butylene adipate co-terephthalate). Biodegradable polymer.

1 Introduction

There has been a growing interest in the use of biodegradable polymers for packaging materials, in order to reduce the environmental pollution caused by plastic wastes. Starch is a renewable, biodegradable and abundant alternative that is able to be processed to produce thermoplastic starch (TPS) using high temperature, shear and with the addition of plasticisers, as glycerol and water (ALTSKAR et al., 2008; ARVANITOYANNIS et al., 1998; VAN SOEST et al., 1996).

Poor water resistance and low strength are limiting factors for the use of materials only from TPS, and hence it is often blended with other polymers, as PBAT, a fully biodegradable synthetic plastic, producing biodegradable blends (PARK et al., 2002). Also, starch can reduce the cost of the finished product compared with synthetics alone, as well as providing biodegradable characteristics (DEAN; YU; WU, 2007; WILHELM et al., 2003).

Extensive studies are currently addressing the evaluation of nanoclays to develop polymer nanocomposites with enhanced mechanical, thermal and barrier properties. The nanofillers from natural clay minerals are often incorporated to improve the matrix properties, due to their availability, versatility, and low environmental and health concerns (CHANG et al., 2012).

It is well known that the reinforcement of polymeric matrixes with inorganic fillers, of different structure, composition, and morphology, depends on the interactions established between both components (DARDER et al., 2006). Thus, the clay sepiolite tends to be compatible with starch, based in their chemical structure, which contains silanol groups that interact with the hydroxyl groups of starch with the formation of hydrogen bonds (CHIVRAC et al., 2010).

Taking this into account, sepiolite nanoclay, a hydrated magnesium silicate with microfibrous morphology (needle-like shape) and particle size of 2-10um length range, was considered in this paper. Their structure is based on an alternation of blocks and tunnels (0.36 nm x 1.1 nm) that grow in the fiber direction. The discontinuity of the silica sheets occurs due the presence of silanol groups (Si-OH) at the edges of the channels, which are the tunnels opened to the external surface of the sepiolite particles (DARDER et al., 2006; GARCIA-LOPEZ, et al., 2010).

Generally, it is believed that fibrous fillers are more easily dispersible than platelet-like fillers. The interaction of primary particles of fibrous silicates, as sepiolite, is weaker than those of layered silicates, as montmorillonite, due their relatively small contact surface. Consequently a better dispersion of the nanoclays can be obtained in the polymer nanocomposites and an improvement of the mechanical properties can be expected (GARCÍA-LOPEZ et al., 2010; BILLOTI et al., 2009).

Blending polymers, a multiphase system is created and sphere-shape, ellipsoid-shaped or fibre-shaped dispersed phases can be obtained, taking into account the processing conditions, the miscibility and viscosity of the polymer phases and also in the amounts of each phase at final blend. These characteristics are determinant in the performance of the blends (SCHWACH; AVÉROUS, 2004).

With the aim to observe the morphology and the influence of sepiolite on the properties of the blends, TPS/PBAT nano-biocomposites were elaborated with two proportions between the polymeric phases. Finally, the influences of sepiolite nanoclays in the mechanical, thermal and structural properties of the nano-biocomposites were evaluated.

2 Experimental

2.1 MATERIALS

Nano-biocomposites were produced with native cassava starch obtained from Indemil (Paranavaí, Brazil), glycerol (99.5 % purity) kindly supplied by Novance (Paris, France), PBAT (poly(butylene adipate co-terephthalate)) supplied by BASF (Ludwigshafen, Germany) under the commercial name Ecoflex® and sodium sepiolite supplied by Tolsa (Madrid, Spain) under the commercial name of Pangel® S9, with a cationic exchange capacity (CEC) of 150 uequiv g^{-1}.

2.2 THERMOPLASTIC STARCH (TPS) PREPARATION

As an initial step to obtain TPS, starch/glycerol dry-blends were prepared. In this process, native cassava starch was dried overnight at 70°C in a ventilated oven. The dried starch was then introduced in a turbo-mixer with the slowly addition of glycerol, under stirring at 1700 rpm, until a homogenous mixture was achieved. The mixture was dried at 170°C in a ventilated oven for 40 minutes. After this process, the dry-blend was added of water and processed in a counter-rotating internal batch mixer, Rheomix OS (Haake, USA), at 70°C for 20 minutes with a rotor speed of 150 rpm, to obtain TPS, using a formulation containing 54 %wt of cassava starch, 23 %wt of glycerol and 23 %wt of water. A masterbatch (TPS + 10 %wt sepiolite) was also produced by the same processing conditions, with incorporation of sepiolite clay into the TPS and used to obtain the nano-biocomposites with PBAT, according to the proposed formulations.

2.3 BLENDS AND NANO-BIOCOMPOSITES PRODUCTION

The blends and nano-biocomposites were produced by mixing PBAT and TPS directly and also using the TPS+sepiolite masterbatch in a counter-rotating internal batch mixer Rheomix OS (Haake, USA), at 130°C for 20 minutes and 150 rpm. The melt-blended mixtures were then compression moulded at 130°C for 12 minutes with a pressure of 20 MPa in a Scientific hot press (Labtech Engineering Company, Muang, Thailand). Two proportions between the polymeric phases were

tested, 50:50 and 80:20 TPS/PBAT, containing 0, 1, 3 and 5 %wt of sepiolite clay. Along the text, these samples were designated as XX/YY/Z, where X is the proportion of TPS, Y the proportion of PBAT at the blend and Z is the %wt of sepiolite clay. Materials containing virgin PBAT, TPS and these added of 3 %wt of sepiolite were also produced to observe the behaviour of the nanofiller in the pure matrices. All the samples were conditioned at 53 ± 2% relative humidity and 25 ± 2°C for 20 days before the analysis.

2.4 CHARACTERISATION

2.4.1 Mechanical Properties

Tensile strength, elongation at break and Young's modulus were determined according ASTM D638-03 using a universal testing machine MTS 2/M (Minnesota, USA) at a strain rate of 50 mm/min. Five samples at each formulation were tested.

2.4.2 Scanning Electron Microscopy (SEM)

A scanning electron microscope FEI model Quanta 200 (FEI Company, Tokyo, Japan) was used to observe the cryogenic fractured surface of the samples. The blends were stored at 25°C in a desiccator with CaCl2 («0% RH) for 3 days and after coated with a gold layer by Sputter Coater (BAL-TEC SCD 050). The images were taken at magnification of 2000x and 4000x.

With the aim to observe the morphology of the immiscible polymeric phases, both samples, 50/50/0 and 80/20/0, were subjected to solvent extraction. For 50/50/0, TPS phase was extracted by stirring a sample at room temperature for 4 hours in solution of DMSO/HCl (8M) and for the 80/20/0 sample, PBAT phase was extracted at same conditions, but using chloroform (99.5%). After dried, the samples were subjected to the same treatments described before to observe the SEM images.

2.4.3 Thermogravimetric Analysis (TGA)

The thermal stability of the PBAT, TPS, their blends and the nano-biocomposites was determined by TGA, using a Q5000 equipment (TA Instruments, New castle, USA); approximately 5 mg of sample was scanned from 25°C to 700°C at 20°C/min under air atmosphere (flow rate 10 ml/min).

2.4.4 Wide Angle X-Ray Diffraction (WAXD)

Wide angle X-Ray diffraction analysis were carried out using a D8 Advance (Bruker, Massachussets, USA) diffractometer with CuKa radiation source (A = 0.1546 nm) and operating at 40 kV and 40 mA. Samples were scanned of 2 *d* from 5-50° at scanning rate of 0.9°/min.

2.4.5 Melt Viscosity Analysis

All the nano-biocomposites and also the TPS/PBAT blends were processed in the internal batch mixer Rheomix OS (Haake, USA), recording the torque curves against residence time. These data were used to evaluate the melt behavior of the blends during the process and the influence of the clay loading.

2.4.6 Statistical Analysis

The data were analysed using STATISTICA 7.0 software (Statsoft, Oklahoma), with analysis of variance (ANOVA) and Tukey's test at a 5% significance level.

3 Results and Discussion

3.1 Mechanical Properties

Table 1 shows the mechanical properties for all samples. Thermoplastic starch (TPS) is characterised by poor mechanical properties when no additive and/or modification of the matrix are considered. The inclusion of 3 %wt of

sepiolite (TPS/S) resulted in an increase greater than 300% in Young's modulus, also increasing the tensile strength (150%), while maintaining the elongation of the materials. Chivrac et al. (2010) observed similar results with the incorporation of natural sepiolite (3 %wt) in thermoplastic wheat starch, reporting the good performance of this nanoclay in starch materials.

Aliphatic-aromatic copolyesters, as PBAT, combine biodegradation and desirable physical properties. Some interactions between the carbonyl groups of PBAT and hydroxyl groups of the sepiolite clay could result in more resistant materials (FUKUSHIMA et al., 2012). A slightly increase of Young's modulus and tensile strength was observed with 3 %wt of sepiolite in PBAT matrix, which also resulted in reduction of the % elongation of the materials (PBAT/S).

The properties of nanocomposites are strongly dependent on the amount of nanofiller and their dispersion state. The improvement of the mechanical properties, with the inclusion of nanofillers, is mostly resulting of good dispersion and the strong interface interaction between the filler and the polymer (DUQUESNE et al., 2007; CHEN et al., 2007).

Considering the 50:50 TPS/PBAT nano-biocomposites, the inclusion of higher amounts of sepiolite did not altered the tensile strength of the materials, moreover resulted in more rigid materials, reaching 117.1 ± 5.3 MPa of Young's modulus with the inclusion of 5 %wt of sepiolite (50/50/5). Also for these materials, a reduction of the elongation at break was observed, probably due the formation of some clay aggregates.

Table 1 – Mechanical properties of TPS, PBAT and the nano-biocomposites based on sepiolite clay.

Sample	*Tensile strength (MPa)*	*Elongation at break (%)*	*Young's modulus (MPa)*
TPS	2.3 ± 0.4	55.7 ± 20.3	51.7± 11.1
TPS/S	3.6 ± 0.6	60.0 ± 15.4	179.2 ± 50.9
PBAT	12.7 ± 0.5	> 600	41.0 ± 1.3
PBAT/S	14.0 ± 1.1	569.7 ± 30.1	57.9 ± 3.6
50/50/0	6.2 ± 0.2 [a]	284.1 ± 16.6 [a]	52.4 ± 1.1 [c]
50/50/1	5.3 ± 0.1 [a]	120.5 ± 17.2 [b]	58.0 ± 2.1 [b]
50/50/3	5.4 ± 0.2 [a]	54.9 ± 17.2 [c]	69.5 ± 2.3 [d]
50/50/5	5.6 ± 0.3 [a]	15.1 ± 1.7 [d]	117.1 ± 5.3 [a]
80/20/0	3.2 ± 0.2 [b]	37.1 ± 2.4 [a]	49.2 ± 0.7 [c]
80/20/1	3.2 ± 0.1 [b]	25.6 ± 1.9 [a]	72.2 ± 4.7 [b,c]
80/20/3	3.4 ± 0.2 [a,b]	25.4 ± 2.0 [a]	82.3 ± 7.9 [a,b]
80/20/5	4.0 ± 0.1 [a]	27.8 ± 5.7 [a]	102.1 ± 4.2 [a]

[a,b,c] Means in the same column, considering the same proportion between the polymeric phases, with different letters differ significantly (Tukey's Test; $p < 0.05$).

For the nano-biocomposites produced with 80:20 of TPS/PBAT (Table 1), the sepiolite contributed to increase the matrix stiffness, with highest modulus of 102.1 ± 4.2 MPa with 5 %wt of nanoclay. A reinforcement effect was also recorded for the nano-biocomposites, with an increment in the tensile strength dependent of the concentration of sepiolite, showing greater values (4.0 ± 0.1 MPa) for the 80/20/5 formulation. In relation to the elongation at break, no significant difference was observed, even with the inclusion of 5 %wt of sepiolite.

The results of mechanical properties suggest that sepiolite was more compatible with TPS, due their hydrophilic character, and was preferentially localised at this phase. Therefore, greater proportion of TPS makes easier the sepiolite dispersion and their contribution to improve the mechanical properties becomes more evident. With the increase of PBAT phase (50:50 blends), sepiolite remains localised in the TPS phase, and as the TPS proportion is reduced, the dispersion of the nanofillers is difficult and more aggregates must be formed, making difficult the improvement of the mechanical properties of these nano-biocomposites.

3.2 THERMOGRAVIMETRIC ANALYSIS (TGA)

The degradation temperatures of virgin PBAT, TPS and nano-biocomposites have been measured by thermogravimetric analysis (TGA) with results showed at Figures 1, 2 and Table 2.

Figure 1 – TG and DTG curves for PBAT, PBAT/S, TPS and TPS/S.

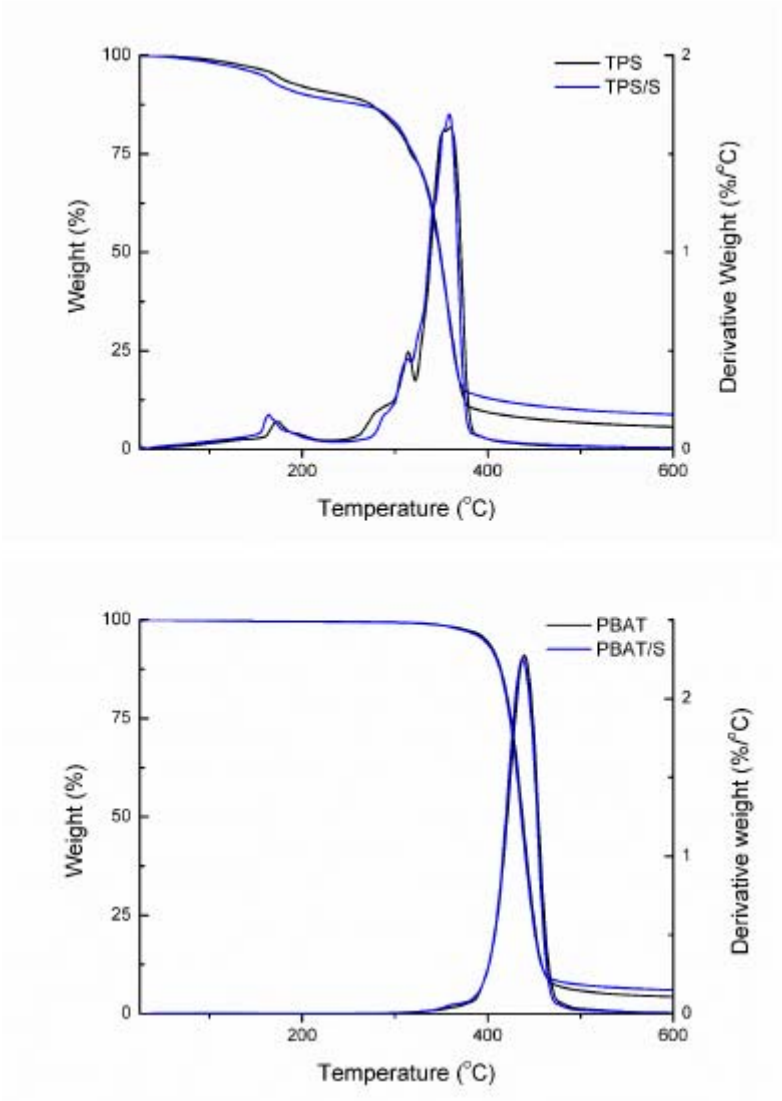

Neat PBAT exhibits a single degradation process with degradation temperature of 439°C, with no significant changes with the incorporation of 3 %wt of sepiolite, registering 437°C for this sample (Figure 1). Fukushima et al. (2012) observed a little increase in the thermal stability of PBAT with the inclusion of nanoclays, including sepiolite, independently of the clay content. Mohanty and Nayak (2012) showed that organically modified montmorillonite, as C30B, was efficient to improve the thermal stability of PBAT, due their ability to act as a heat barrier as well as assisting in char formation during thermal decomposition (RAY; OKAMOTO, 2003).

Figure 2 – TG and DTG curves for samples 50/50/0, 50/50/5, 80/20/0 and 80/20/5.

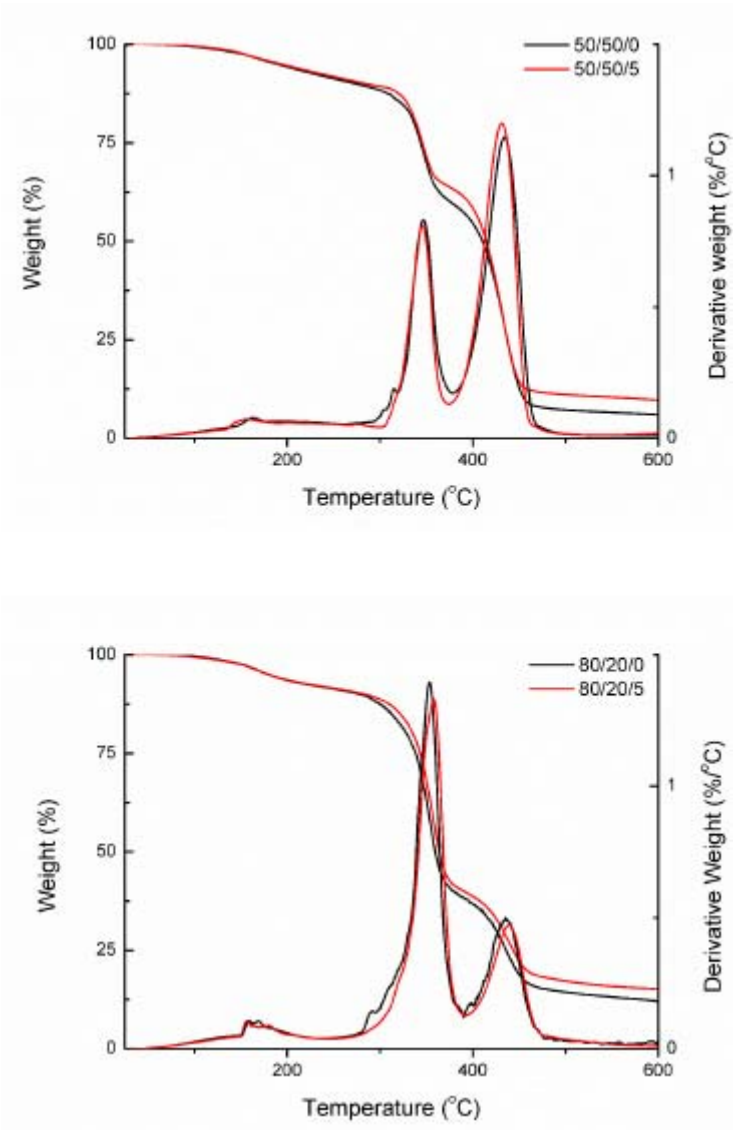

For pristine TPS matrix is possible to observe three different degradation processes, at 170°C, 283°C and 360°C. The first step corresponds to the water loss, the second, to the glycerol volatilisation and the last one to amylose and amylopectin thermal degradation (NAYAK, 2010; CHIVRAC et al., 2010). TPS/S also exhibits three degradation process at 163°C, 287°C and 358°C, showing that the inclusion of sepiolite marginally increases the thermal degradation of TPS matrix.

For samples 50/50/0 and 80/20/0 (Figure 2) were observed four steps of thermal degradation around 163°C, 310°C, 336°C and 432°C, a combination to those observed for PBAT and TPS (Table 2). The addition of 5%wt of sepiolite (50/50/5 and 80/20/5) slightly affected the thermal degradation of the nano-biocomposites, but resulted in the absence of the thermal degradation around 300

°C, correspondent to the glycerol volatilisation, probably due some interaction between glycerol and hydroxyl groups on the sepiolite clays.

Table 2 – Degradation temperatures and residue (%) for the nano-biocomposites.

Samples	Degradation temperatures (ºC)				Residue (%)
50/50/0	163.1	315.6	346.1	432.8	---
50/50/5	158.1	---	345.3	432.2	4.47
80/20/0	169.2	292.5	353.1	435.2	---
80/20/5	181.5	---	357.9	439.8	5.65

The increase of degradation temperatures for the nano-biocomposites with the inclusion of 5 %wt of sepiolite was more evident when the proportion 80:20 TPS/PBAT was analysed, as a result of the better compatibility and dispersion of sepiolite in TPS matrix. Nayak (2010) studied the inclusion of organo-modified montmorillonite (as C30B and C20A) and found that the presence of clay increased the degradation temperatures of PBAT/TPS biodegradable polymer, which is in accordance to the present work.

3.3 Scanning Electron Microscopy (SEM)

Figure 3 shows the SEM images for 50:50 and 80:20 TPS/PBAT blends, after phase extraction. Previous researches reported that the co-continuity occurs at the phase inversion point, when the proportions between the polymeric phases are approximately in equal amounts. However, the influences of the interfacial tension, the shape of the dispersed component and the process conditions (as stress level and matrix viscosity) are quite important to obtain a co-continuous structure (SCHWACH; AVÉROUS, 2004, WALIA et al., 2000; WILLEMSE et al., 1999).

Figure 3 – SEM images of the fractures of samples 50/50/0 (a) and 80/20/0 (b) after phase extraction. Magnification 2000x.

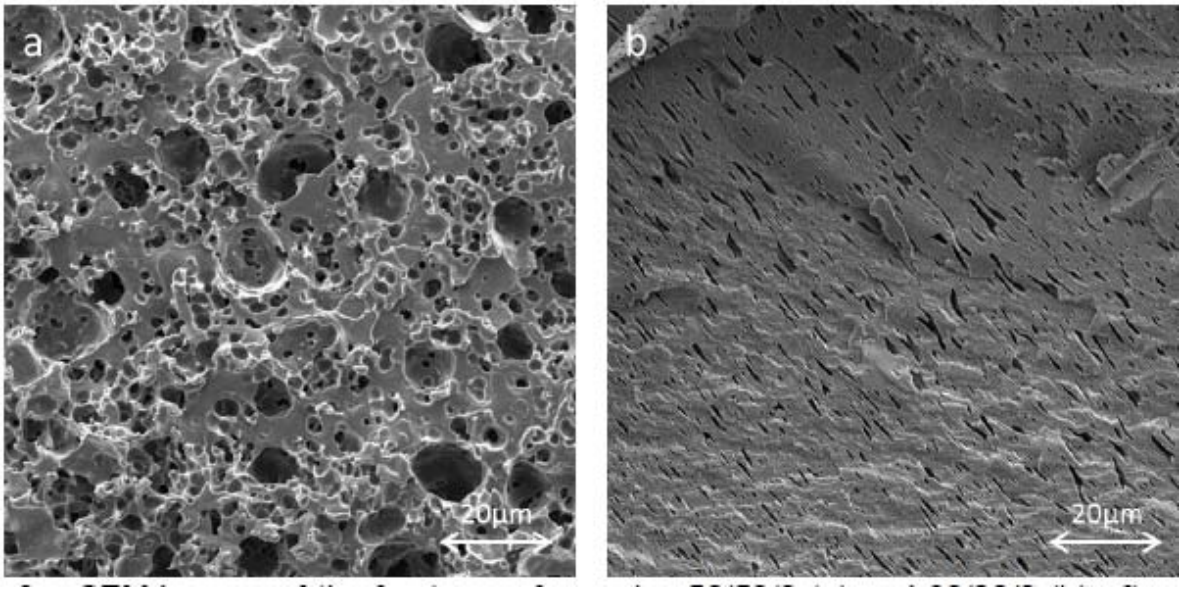

Figure 4 – SEM images of the fractures of samples 50/50/0 (a); 50/50/5 (b); 80/20/0 (c) and 80/20/5 (d). Magnification 2000x.

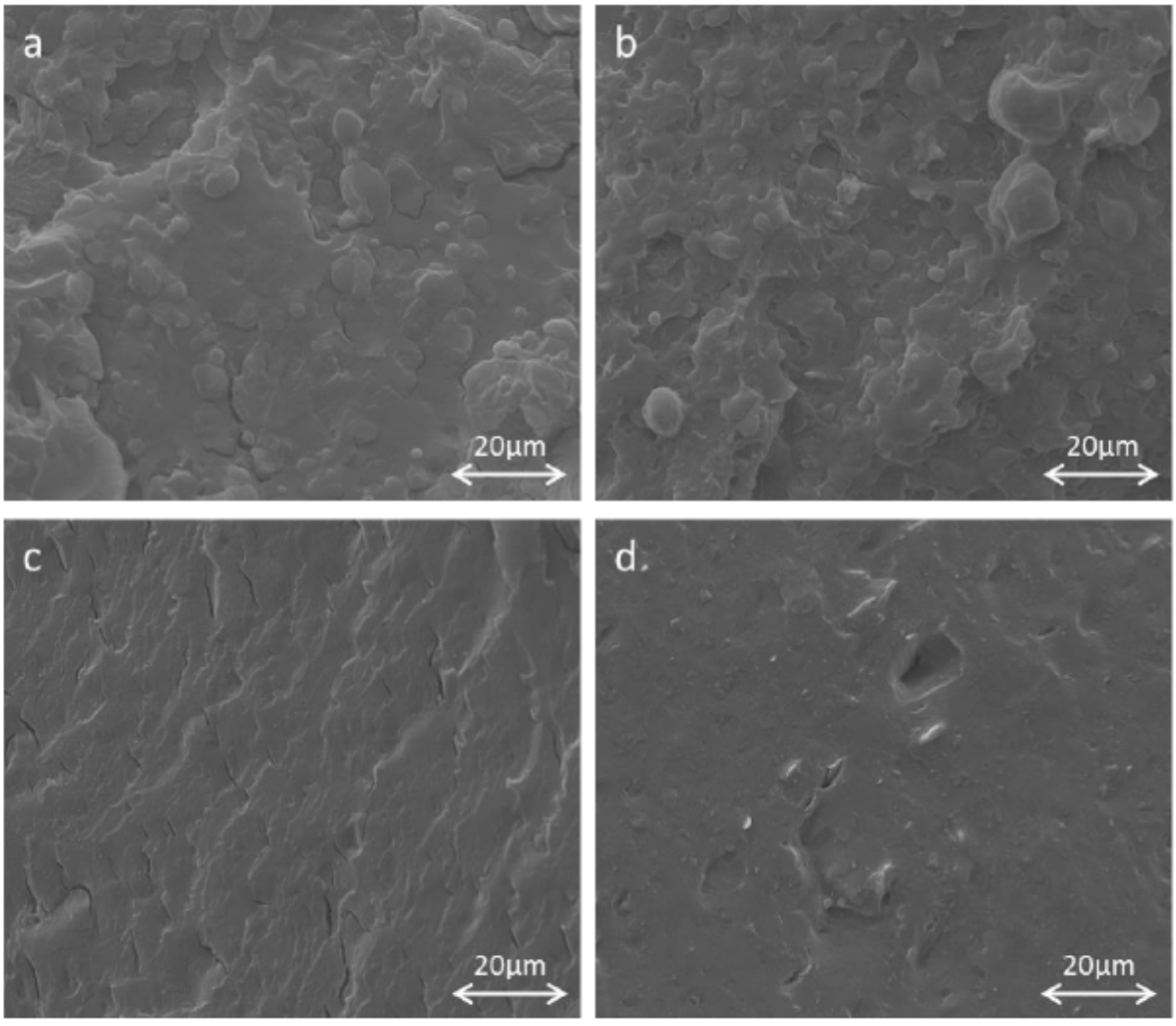

Based on this, samples produced with equal proportions of TPS and PBAT (50/50/0), contrary to expected, showed a dispersive blend, with TPS round domains, which suggests that, for this material, probably the co-continuity will occur with greater proportions of TPS. Besides the influence of process conditions, as previously cited, the critical role of water in the morphology of TPS/polyester blends was analysed by Walia et al (2000), which proved that the onset of co-continuity could shifts to higher concentrations of the disperse phase, depending of the moisture content.

For 80/20/0 samples, a dispersed phase of PBAT is observed. Comparing the mechanical properties of this material with those of the 50/50/0 sample, lower tensile strength and % elongation were observed. This fact is resulting of the morphology of the immiscible blends. In this case, the dispersed phase, formed by PBAT, was surrounded by TPS matrix. So, the mechanical properties will be determined by TPS, once this phase was responsible for absorb all the stress when the material is under load (SCHWACH; AVEROUS, 2004).

The inclusion of sepiolite nanofillers did not influenced the morphology of the TPS/PBAT blends, as showed at Figure 4. In this image, it is possible to observe the round disperse phase composed by TPS and the continous phase composed by PBAT in the 50/50/5 sample. On the other side, for the 80/20/5 samples, the structure seems to be more homogeneous due the higher proportion of TPS. The white spots represents the sepiolite clays, which are more evident at the 80/20/5 nano-biocomposites (Figure 5).

Figure 5 – SEM image of the fracture of sample 80/20/5 showing the sepiolite dispersion in the matrix. Magnification 4000x.

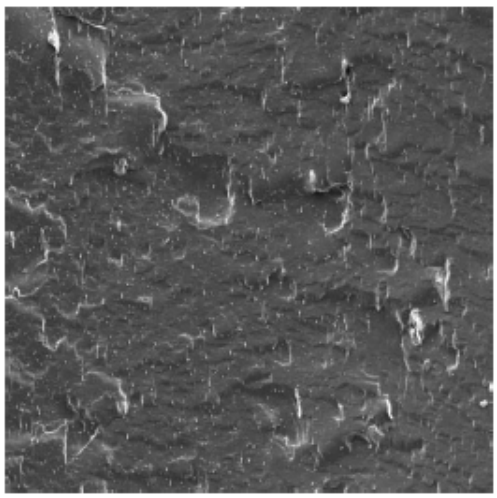

A detailed image of the 80/20/5 (Figure 5) shows a good dispersion of sepiolite clays, with low occurrence of small aggregates in polymeric matrix. This fact supports the mechanical and thermal results, once a good dispersion of the nanoclay is essential to improve the properties of the polymer. Bilotti et al. (2009) found similar SEM images for polyamide 6/sepiolite, reporting a good dispersion. Fukushima et al. (2012) also showed SEM images for single sepiolite needles and some bundles in PLA matrix.

3.4 WIDE ANGLE X-RAY DIFFRACTION (WAXD)

Figure 6 displays the WAXD curves recorded for the blends with both proportions between the polymeric phases and the nano-biocomposites 50/50/1, 50/50/3 and 50/50/5. Nano-biocomposites with proportion 80:20 TPS/PBAT had the same behaviour, noting only a small intensity for the peaks referents to the PBAT structure, once this phase was reduced in these materials.

The peak in 29 = 7.3° is referent to the inclusion of sepiolite (110) and assume higher intensity in increased proportions of the nanofiller, with no alteration in the 29 values, data in accordance to those related by Tartaglione et al. (2008). This shows that the channels present in the sepiolite clay could not be affected by the melt-blending process. For this reason, the WAXD is useful to discuss possible alterations in the polymer structure, and not generate data referent to the dispersion of the filler, as commonly used to layered nanoclays.

Five peaks are observed for all the nano-biocomposites, corresponding to 29 = 13.2°, 17.8°, 20.2°, 23.6° and 25.4°. This is an evidence of no significant alteration in the crystal structure of PBAT and starch induced by the nanofillers. The starch processing induces crystallisation (type VH), which was represented by peaks in 29 = 13.2° and 20.2° (OLIVATO et al., 2013; VAN SOEST, et al., 1996). For the PBAT crystal structure were observed in 29 = 17.8°, 23.6° and 25.4°. Chivrac et al. (2006) studied the influence of montmorillonite in PBAT matrix and also observed no influence of the nanofillers in the crystallinity.

Figure 6 – WAXD patterns of the nano-biocomposites.

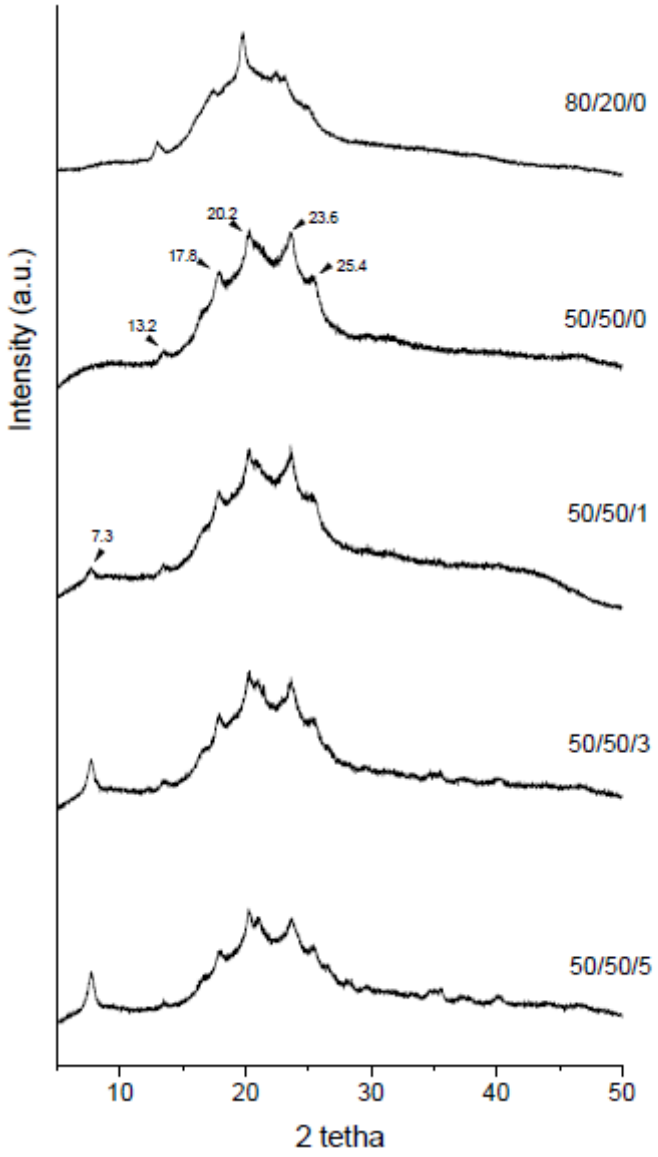

3.5 MELT VISCOSITY ANALYSIS

The torque *vs* residence time curves were registered during the processing of TPS/PBAT blends and are shown in Figure 7. All the nano-biocomposites registered an increase of torque in the beginning of the process, which refers to melting of PBAT and TPS.

The inclusion of sepiolite changed the viscosity of the samples, showing higher torque values with greater nanoclay proportions. As sepiolite clay has a needle-like morphology, they behave differently of the clay platelets that tend to assume some orientation and result in a decrease of the matrix viscosity. According to Chen et al. (2007), the sepiolite acts as a "crosslinking agent" and retards the

motion of polymeric chains. This fact could explain their contribution to increase the torque of the nano-biocomposites, as observed in the melt viscosity analysis.

Figure 7 – Torque curves registered during the elaboration of the nano-biocomposites.

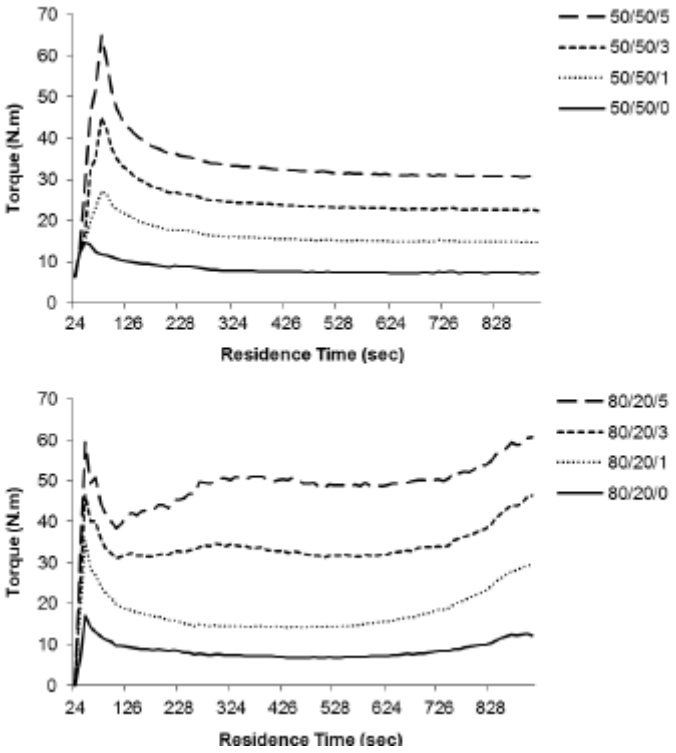

After 400 seconds, occurred a stabilisation of the torque for the 50:50 blends. On the other hand, for the 80:20 blends, the torque still increases until the end of processing and the increment was dependent of the nanofiller concentration.

Chang et al. (2012) observed that sodium rectorite clay treated with cationic guar gum increased the viscosity of TPS matrix, once they were capable to perform strong interactions with starch chains. Considering the silanol groups at sepiolite surface, the interactions can also explain the increase of registered torque, for 80:20 blends, during processing.

4 Conclusion

This study reports the incorporation of sepiolite clay in thermoplastic starch/PBAT blends, testing two different proportions between the polymeric phases, 80:20 and 50:50 TPS/PBAT, respectively. Scanning electron microscopy (SEM)

images showed no influence of sepiolite in the morphology of the TPS/PBAT blends. Furthermore, samples produced with equal proportions of TPS and PBAT showed a dispersive blend, with TPS round domains and for 80:20 TPS/PBAT samples, a dispersed phase of PBAT was observed.

For all the nano-biocomposites, wide-angle X-ray diffraction (WAXD) presented no significant alteration in the crystal structure of PBAT and thermoplastic starch induced by sepiolite inclusion. In addition, sepiolite acted as a "crosslinking agent" and retarded the motion of polymeric chains, resulting in higher torque values with greater nanoclay proportions.

The increase of degradation temperatures for the nano-biocomposites with the inclusion of 5 %wt of sepiolite was more evident in 80:20 TPS/PBAT blends, because of the better compatibility and dispersion of sepiolite in TPS matrix. Sepiolite contributed to increase the matrix stiffness for all the nano-biocomposites. A reinforcement effect was also recorded 80:20 TPS/PBAT nano-biocomposites, with an increment in the tensile strength, which was dependent of the concentration of sepiolite. Sepiolite clay has a potential to enhance the properties of TPS/PBAT blends and materials with better performance could represent an interesting way to substitute the non-biodegradable plastic materials for some applications.

5 References

ALTSKAR, A; ANDERSSON, R; BOLDIZAR, A; KOCH, K; STADING, M; RIGDAHL, M; THUNWALL, M. Some effects of processing on the molecular structure and morphology of thermoplastic starch. **Carbohydrate Polymers,** v. 71, p. 591-597, 2008.

ARVANITOYANNIS, I; NAKAYAMA, A; AIBA, S. Edible films made from hydroxypropyl starch and gelatin and plasticized by polyols and water. **Carbohydrate Polymers,** v. 36, p. 105-1199, 1998.

AMERICAN SOCIETY FOR TESTING AND MATERIAL (ASTM). **Standard test method for tensile properties of plastics.** D638-03. Philadelphia: ASTM, 2003.

BILOTTI, E; ZHANG, R; DENG, H; QUERO, F; FISCHER, H. R; PEIJS, T. Sepiolite needle-like clay for PA6 nanocomposites: An alternative to layered silicates? **Composites Science and Technology,** v. 69, p. 2587-2595, 2009.

CHEN, H; ZHENG, M; SUN, H; JIA, Q. Characterization and properties of sepiolite/polyurethane nanocomposites. **Materials Science and Engineering A,** v. 445-446, p. 725-730, 2007.

CHANG, P. R; WU, D; ANDERSON, D. P; MA, X. Nanocomposites based on plasticized starch and rectorite clay: Structure and properties. **Carbohydrate Polymers,** v. 89, p. 687-693, 2012.

CHIVRAC, F; POLLET, E; SCHMUTZ, M; AVEROUS, L. Starch nano-biocomposites based on needle-like sepiolite clays. **Carbohydrate Polymers,** v. 80, p. 145-153, 2010.

CHIVRAC, F; KADLECOVA, Z; POLLET, E; AVEROUS, L. Aromatic copolyester-based nano-biocomposites: Elaboration, structural characterization and properties. **Journal of Polymers and Environment,** v. 14, p. 393-401, 2006.

DARDER, M; LOPEZ-BLANCO, M; ARANDA, P; AZNAR, A. J; BRAVO, J; RUIZ-HITZKY, E. Microfibrous chitosan-sepiolite nanocomposites. **Chemical Material,** v. 18, p. 1602-1610, 2006.

DEAN, K; YU, L; WU, D. Y. Preparation and characterization of melt-extruded thermoplastic starch/clay nanocomposites. **Composites Science and Technology,** v. 67, p. 413-421, 2007.

DUQUESNE, E; MOINS, S; ALEXANDRE, M; DUBOIS, P. How can nanohybrids enhance polyester/sepiolite nanocomposite properties? **Macromolecular Chemistry and Physics,** v. 208, p. 2542-2550, 2007.

FUKUSHIMA, K; WU, M; BOCCHINI, S; RASYDA, A; YANG, M. PBAT based nanocomposites for medical and industrial applications. **Materials Science and Engineering C,** v. 32, p. 1331-1351, 2012.

FUKUSHIMA, K; FINA, A; GEOBALDO, F; VENTURELLO, A; CAMINO, G. Properties of poly(lactic acid) nanocomposites based on montmorillonite, sepiolite and zirconium phosphonate. **EXPRESS Polymer Letters,** v. 6, p. 914-926, 2012.

GARCIA-LOPEZ, D; FERNANDEZ, J. F; MERINO, J. C; SANTAREN, J; PASTOR, J. M. Effect of organic modification of sepiolite for PA 6 polymer/organoclay nanocomposites. **Composites Science and Technology,** v. 70, p. 1429-1436, 2010.

MOHANTY, S; NAYAK, S. K. Biodegradable nanocomposites of poly(butylene adipate-co-terephthalate) (PBAT) and organically modified layered silicates. **Journal of Polymer and Environment,** v. 20, p. 195-207, 2012.

NAYAK, S. K. Biodegradable PBAT/Starch nanocomposites. **Polymer - Plastics Technology and Engineering,** v. 49, p. 1406-1418, 2010.

OLIVATO, J. B; NOBREGA, M. M; MULLER, C. M. O; SHIRAI, M. A; YAMASHITA, F; GROSSMANN, M. V. E. Mixture design applied for the study of the tartaric acid effect on starch/polyester films. **Carbohydrate Polymers,** v. 93, p. 1705-1710, 2013.

PARK, H. M; LI, X; JIN, C. Z; PARK, C. Y; CHO, W. J ; HA, C. S. Preparation and properties of biodegradable thermoplastic starch/clay hybrids. **Macromolecular Materials and Engineering,** v. 287, p. 553-558, 2002.

RAY, S. S; OKAMOTO, M. Polymer/layered silicate nanocomposites: a review from preparation to processing. **Progress in Polymer Science,** v. 28, p. 1539-1641, 2003.

SCHWACH, E; AVEROUS, L. Starch-based biodegradable blends: morphology and interface properties. Polymer International, v. 53 (2004) 2115-2124.

TARTAGLIONE, G; TABUANI, D; CAMINO, G; MOISIO, M. PP and PBT composites filled with sepiolite: Morphology and thermal behavior. **Composites Science and Technology,** v. 68, p. 451-460, 2008.

VAN SOEST, J. J. G; HULLEMAN, S. H. D; DE WIT, D; VLIEGENTHART, J. F. G. Crystallinity in starch bioplastics. **Industrial Crops and Products,** v. 5, p. 11-22. 1996.

WALIA, P. S; LAWTON, J. W; SHOGREN, R. L; FELKER, F. C. Effect of moisture level on the morphology and melt flow behavior of thermoplastic starch/poly (hydroxy ester ether) blends. **Polymer,** v 41, p. 8083-8093, 2000.

WILHELM, H. M; SIERAKOWSKI, M. R; SOUZA, G. P; WYPYCH, F. Starch films reinforced with mineral clay. **Carbohydrate Polymers,** v. 52, p. 101-110, 2003.

WILLEMSE, R. C; DE BOER, A. P ; VAN DAM, J ; GOTSIS, A. D. Co-continuous morphologies in polymer blends: the influence of the interfacial tension. **Polymer,** v. 40, p. 827-834, 1999.

CAPÍTULO 7 – STARCH/POLYESTER NANO-BIOCOMPOSITES BASED ON SEPIOLITE CLAYS: THERMO-MECHANICAL AND WATER SORPTION PROPERTIES

ABSTRACT: This study evaluated the sepiolite effects in thermal-mechanical, barrier and optical properties of TPS/PBAT nano-biocomposites, considering two different proportions between the polymeric phases. Incorporation of sepiolite clay did not influence the Tg and Tm of the nano-biocomposites, but affected their crystallisation by acting as nucleating sites. Considering 50:50 TPS/PBAT samples, was observed an increase of 25°C at Tg of starch phase with addition of 5 %wt of sepiolite and no alteration at Tg of PBAT phase, remaining around -26°C, which support the proposition that sepiolite was preferentially localised at TPS phase. In general, the inclusion of sepiolite decreased the water adsorption rate and the water adsorption capacity of the materials, but did not change their equilibrium moisture content. Moreover, higher proportions of sepiolite in the samples tend to increase their opacity and influenced their colouration. These results highlighted the potential use of natural sepiolite clays in starch/PBAT materials.

Keywords: Nano-biocomposites. Sepiolite. Thermoplastic starch (TPS). Poly (butylene adipate co-terephthalate) (PBAT). Thermal-mechanical properties.

1 Introduction

Recently, academic researches has been focused in the development of "environmentally-friendly" materials, i. e., produced from alternative resources, with lower energy consumption, biodegradable and non-toxic to the environment (BORDES; POLLET; AVEROUS, 2009).

The polymers obtained from agro-resources, such starch, are recognised as a cheap, biodegradable and renewable material with potential as substitute of non-biodegradable synthetic polymers, for some applications (AVEROUS, 2004; GARCIA; MARTINO; ZARITZKI, 2000). It has been established that starch is a heterogeneous material containing two microstructures: linear (amylose) and branched (amylopectin), which when submitted to shear and high temperatures, in the presence of a plasticiser, results in an essentially amorphous material called thermoplastic starch (TPS) (LIU et al., 2009; ZULLO; IANNACE, 2009).

However, biodegradable materials obtained only by TPS are fragile and sensible to environment conditions. Based on this, as alternatives to overcome

TPS deficiencies, the production of blends or composites has been fully considered (CHIVRAC et al., 2008; MALIGER et al., 2006; OKAMOTO, 2005). Nanosized filler incorporated into a biodegradable matrix, producing nano-biocomposite materials, are capable to improve their mechanical, thermal and barrier properties, due the large surface area, which provides an extensive nanofiller-polymer interaction, when a good particle dispersion is achieved (CHIVRAC; POLLET; AVEROUS, 2009; RAY; OKAMOTO, 2003). In this way, the nanoclays have attracted considerable attraction, especially montmorillonite, a low cost and highly availability layered silicate (FUKUSHIMA et al., 2012; MULLER; LAURINDO; YAMASHITA, 2012; MAJDZADEH-ARDAKANI; NAVARCHIAN; SADEGHI, 2010).

Sepiolite particles are layered hydrated magnesium silicates characterised by a needle-like morphology. Interesting results concerning sepiolite application in TPS (CHIVRAC et al., 2010a), and PBAT matrix (FUKUSHIMA et al., 2012; FUKUSHIMA; TABUANI; CAMINO, 2009) were reported in literature, but there is no reports concerning the study of sepiolite clay in biodegradable blends.

In addition, blending thermoplastic starch with a good performance polyester represents a singular alternative to improve the properties of TPS, also reducing the elevated costs of a synthetic biodegradable polyester, as poly (butylene adipate co-terephthalate) (PBAT) (SCHWACH; AVÉROUS, 2004). PBAT, an aromatic-aliphatic biodegradable copolyester with good mechanical performance, presents superior elongation at break that polylactic acid (PLA), for example, which become important when the objective is to overcome the TPS deficiencies (FUKUSHIMA et al., 2012; MOHANTY; NAYAK, 2012).

Based on this, the study of the effects of sepiolite clay in thermal-mechanical, barrier and optical properties of TPS/PBAT nano-biocomposites was the focus of this work. For this purpose, two different proportions between the polymeric phases were tested, with sepiolite clays added at 1, 3 and 5 %wt in both materials.

2 Experimental

2.1 MATERIALS

Native cassava starch, obtained from Indemil (Paranavaí, Brazil), PBAT (poly(butylene adipate co-terephthalate)), supplied by BASF (Ludwigshafen, Germany), and sodium sepiolite, supplied by Tolsa (Madrid, Spain) under the commercial name of Pangel® S9, with a cationic exchange capacity (CEC) of 150 uequiv g^{-1}, were used to produce the nano-biocomposites. Glycerol (Novance (Paris, France) was used as plasticiser.

2.2 NANO-BIOCOMPOSITES PRODUCTION

2.2.1 Thermoplastic Starch (TPS) Preparation

Native cassava starch was dried overnight at 70°C in a ventilated oven and then introduced in a turbo-mixer with the slowly addition of glycerol, under stirring at 1700 rpm, until a homogenous mixture was achieved. Then, the mixture was dried at 170°C in a ventilated oven for 40 minutes to obtain the dry-blend of starch and glycerol. After this process, water was added into the dry-blend and processed in a counter-rotating internal batch mixer (Rheomix OS (Haake, USA)) at 70°C for 20 minutes with a rotor speed of 150 rpm, to obtain thermoplastic starch (TPS), based in a formulation containing 54 %wt of cassava starch, 23 %wt of glycerol and 23 %wt of water.

2.2.2 Sepiolite Masterbatch Preparation

A masterbatch containing 10 %wt sepiolite was produced, with the same processing conditions previously described for TPS, by the mixture of dry-blend (starch+glycerol), water and sepiolite clay, processed in a counter-rotating internal batch mixer (Rheomix OS (Haake, USA)).The masterbatch was used to obtain the nano-biocomposites with PBAT, according to the proposed formulations (Table 1).

2.2.3 Blends and Nano-biocomposites Production

The blends and nano-biocomposites were produced by mixing PBAT and TPS directly, also using the TPS+sepiolite masterbatch, in a counter-rotating internal batch mixer Rheomix OS (Haake, USA), at 130°C for 20 minutes and 150 rpm. The melt-blended mixtures were then compression moulded at 130°C for 12 minutes with a pressure of 20 MPa in a Scientific hot press (Labtech Engineering Company, Muang, Thailand). Two proportions between the polymeric phases were tested, 50:50 and 80:20 TPS/PBAT, containing 0, 1, 3 and 5 %wt of sepiolite clay. Along the text, these samples were designated as XX/YY/Z, where X is the proportion of TPS, Y the proportion of PBAT at the blend and Z is the %wt of sepiolite clay. For better understand the results, virgin PBAT and TPS samples were prepared by the same processing conditions. All the samples were conditioned at 53 ± 2% relative humidity and 25 ± 2°C for 20 days before the analysis.

2.3 NANO-BIOCOMPOSITES AND POLYMER CHARACTERISATION

2.3.1 Differential Scanning Calorimetry (DSC)

A DSC Q200 (TA Instruments, New castle, USA) was used to perform the differential scanning calorimetric analysis for all the samples, which were subjected to a first heating from 30°C to 240°C, with a further cooling to -80°C and a new heating cycle to 240°C, keeping rate of 10°C/min for all the steps, under nitrogen flow (50 ml/min). The melting (Tm), crystallisation (Tc) and glass transition (Tg) temperatures of pristine TPS, PBAT and nano-biocomposites were determined.

2.3.2 Dynamical Mechanical Thermal Analysis (DMTA)

A Dynamical Mechanical Analyser (DMA-Q800, TA Instruments, USA), using tension film clamp, was used to determine the storage modulus (MPa) and damping factor (tan 5) of the materials. The samples were scanned from -80°C to 100°C with a heating rate of 3°C/min, fixed frequency of 1 Hz and 15um of amplitude. Glass transition temperatures (Tg) were expressed as the temperature of the tan 5 peaks.

2.3.3 Moisture Adsorption Kinetics

Samples with about 500 mg were previously dried for 20 days (CaCl2, RH=0%) and then placed at 25 ± 2°C in separated desiccators containing saturated salt solutions, under desired relative humidity conditions (32, 53, 75 and 90% RH) (MALI et al., 2005). Weights of samples were taken as a function of time and their moisture content was determined by oven drying at 105 °C. Moisture adsorption data were fitted to a mathematical model suggested by Peleg (1988) (Eq. 1).

$$M(t) = M0 + (t / (k1+k2.t)) \qquad \textit{Eq. 1}$$

where *M(t)* is the moisture after time, *M0* is the initial moisture content, *k1* is the Peleg rate constant and *k2* is the Peleg capacity constant. All tests were conducted in triplicate.

2.3.4 Moisture Sorption Isotherms

Samples with about 500 mg were previously dried for 20 days (CaCl2, RH«0%) and then placed at 25 ± 2°C in separated desiccators containing saturated salt solutions, under desired relative humidity conditions (11, 32, 53, 75 and 90% of relative humidity) (MALI et al., 2005). Each sample was weighted until equilibrium conditions (assumed when no difference in the sample mass was recorded in two successive weighting) and the equilibrium moisture content was calculated by the increase of the mass of the sample in relation to their dried mass. Guggenheim-Anderson-de Boer (GAB) model (Eq. 2) was used to fit the data.

$$M = m_0.C.K.a_w / (1-K.a_w)(1-K.a_w+C.Ka_w) \qquad \textit{Eq. 2}$$

where *M* is the equilibrium moisture content, *aw* is the water activity, *mo* is the monolayer value (g water/ 100 g solids) and *C, K* are the GAB constants. The GAB model parameters were determined by non-linear regression, using the Origin Software 8.0 (OriginLab, USA).

2.3.5 Opacity and Colour Analysis

Opacity and colour measurements were determined by means of a colorimeter (BYK Gardner-USA) at a 10° angle and using illuminant D65 (day light) according to the Hunterlab methods (Hunter Associates Laboratory, 1997). The colour was obtained of the samples placed under a white pattern and expressed as CIELAB *L* a* b** values. The measurements were taken from three different places in each sample and the average of a* and b* parameters were reported. Sample opacity (Y) was calculated as the ratio between the opacity of the sample placed under a black pattern (Yb) and the opacity of the sample placed under a white pattern (Yw) (Eq. 3).

$$Y = (Yb/Yw) \times 100 \qquad Eq.3$$

The opacity results (Y) were divided by the sample thickness and expressed in an arbitrary scale (0-1%.µm-1). The measurements were performed in triplicate.

2.3.6 Statistical Analysis

The data were analysed using STATISTICA 7.0 software (Statsoft, Oklahoma), with analysis of variance (ANOVA) and Tukey's test at a 5% significance level.

3 Results and Discussion

3.1 Differential Scanning Calorimetry (DSC)

DSC analysis was performed in the compressed moulded samples of pure TPS and PBAT (Figure 1) and for all nano-biocomposites (Figure 2 and 3). The figures represent the second heating curves. The characteristic melting, crystallisation and glass transition temperatures are presented at Table 1.

It is well-know the difficulty in obtaining reproducible and significant data from DSC of starch and TPS because the heat capacity is quite low at the glass transition (CARVALHO et al., 2005; AVEROUS; BOQUILLON, 2004). As can be observed at Figure 1, pure TPS sample did not showed endothermal or exothermal transitions, whereas virgin PBAT sample showed a glass transition (Tg) in -28.9°C and melting temperature (Tm) in 126.5°C (Table 1). These data are according to Raquez et al (2008), which found a melting peak at 122°C and Tg in -32.4°C for pristine PBAT.

Figure 1 – DSC curves for TPS and PBAT matrices.

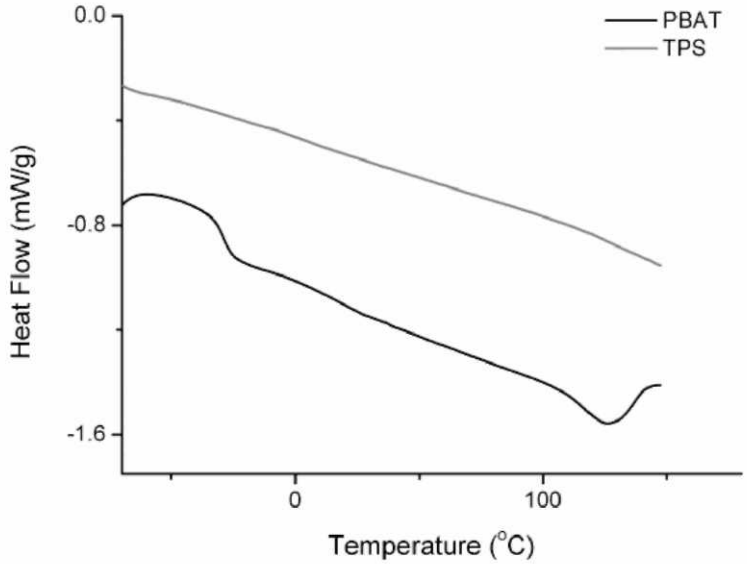

The glass transition temperatures slightly decreased when blending PBAT with starch, with Tg of -32.3°C for 50/50/0 and -32.5°C for 80/20/0 samples (Figures 2 and 3, Table 1), which indicates almost no interaction between the PBAT with TPS matrix, as a consequence of their immiscibility.

Table 1 – DSC data for TPS, PBAT and nano-biocomposites obtained by cooling and second heating scans.

Samples*	Tg (°C)	Tm (°C)	ΔHm ($J.g^{-1}$)	Tc_{onset} (°C)	Tc_{final} (°C)	Tc (°C)	ΔHc ($J.g^{-1}$)
TPS	--	--	--	--	--	--	--
PBAT	-28.9	126.5	3.7	69.4	117.6	95.5	9.4
50/50/0	-32.3	124.3	6.4	63.9	101.4	78.6	17.8
50/50/1	-30.2	125.4	5.2	60.4	107.0	81.4	17.4
50/50/3	-30.8	126.5	4.6	64.6	107.1	84.4	15.8
50/50/5	-31.4	126.2	2.3	67.2	107.4	86.3	16.4
80/20/0	-32.5	123.6	5.4	42.0	83.8	63.1	7.5
80/20/1	-32.4	125.4	2.1	58.3	84.8	70.0	7.5
80/20/3	-32.9	126.1	1.9	66.6	102.1	85.1	7.0
80/20/5	-32.5	125.2	2.0	68.6	103.7	85.6	6.5

* Samples were designated as XX/YY/Z, where X is the proportion of TPS, Y the proportion of PBAT at the blend and Z is the %wt of sepiolite clay

Incorporation of sepiolite clay, even in greater proportions, did not influence the glass transition and melting temperatures of the nano-biocomposites, recorded by DSC, registering Tm around 126°C and Tg near to -30°C for all the samples. Considering that sepiolite has a polar character, due the silanol groups at their surface, we can suppose that the clays will be localised at TPS phase, once they are more compatible with this matrix. Based on this and in the fact that no transitions were observed for TPS in DSC analysis, it is expected that the influence of sepiolite in thermal properties could be better explained by DMTA analysis.

Figure 2 – DSC curves of 50:50 TPS/PBAT blends with different sepiolite contents.

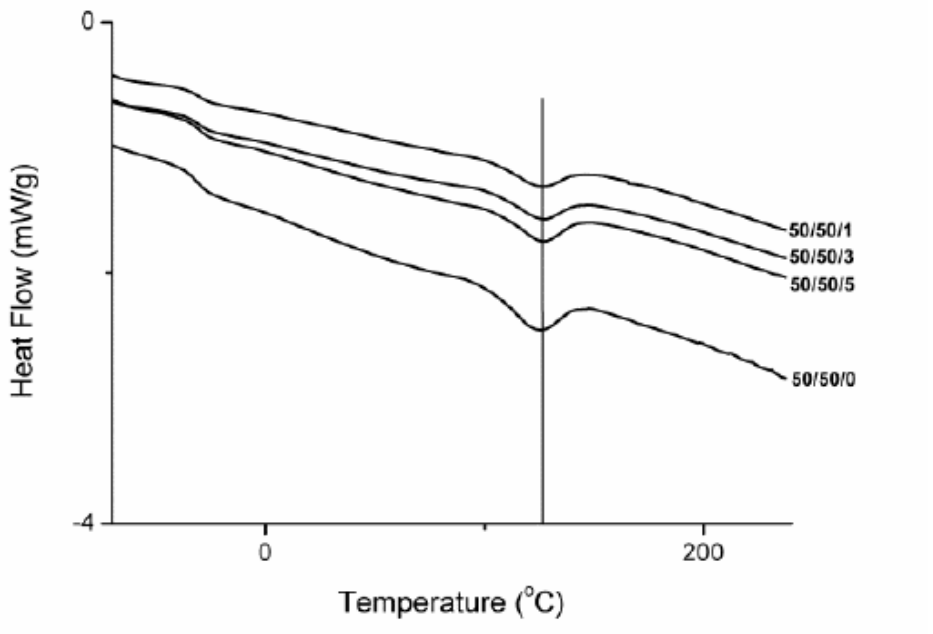

McGlashan and Halley (2003) also observed that the inclusion of montmorillonite in starch/polyester matrix did not induce significant changes in the melting temperature of the blends, but affected their crystallisation temperature.

The samples without sepiolite exhibited a crystallisation peak around 78.6°C (50/50/0) and 63.1°C (80/20/0), which increased with the incorporation of the nanoclays (Table 1). This fact pointed to the influence of sepiolite in the crystallisation of nano-biocomposites, acting as nucleating sites in the polymeric matrix (McGLASHAN; HALLEY, 2003; NAYAK, 2010; MOHANTY; NAYAK, 2012). However, no difference in the melting temperature of PBAT was observed, even with 5%wt of sepiolite, which suggests that the crystal organisation formed in nano-biocomposites tends to be similar to those of virgin PBAT.

Figure 3 – DSC curves of 80:20 TPS/PBAT blends with different sepiolite contents.

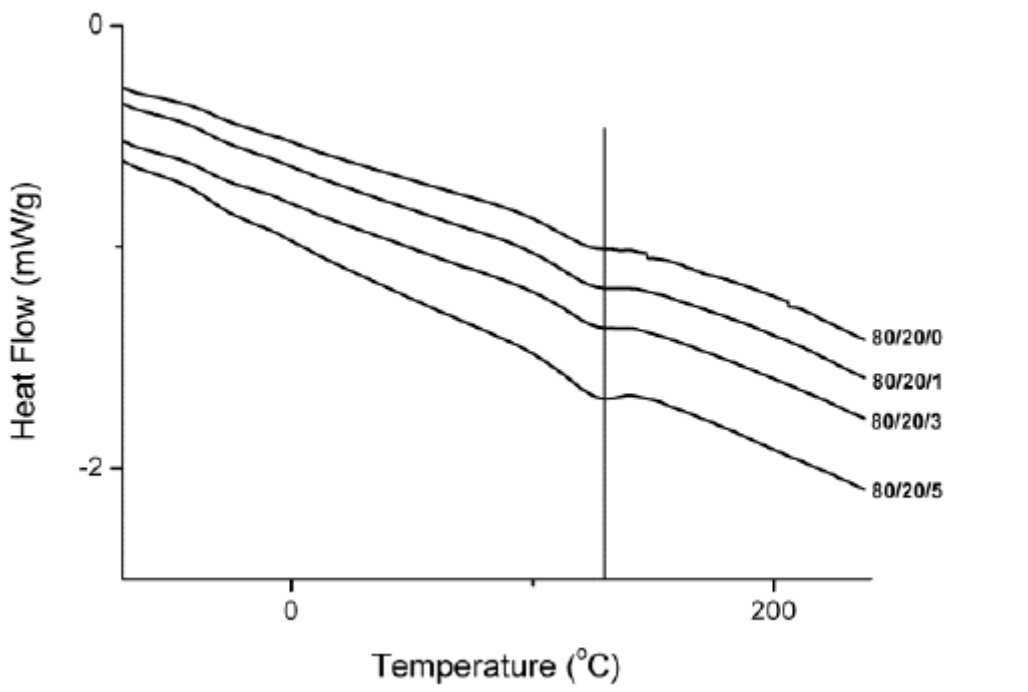

Nayak (2010) observed similar results for PBAT/starch nanocomposites incorporated with modified montmorillonite. Fukushima (2012) observed that sepiolite, in particular at higher clay contents (10 %wt), influenced the formation of crystalline zones in PBAT matrix, probably due the annealing effect of the oriented sepiolite fibers, resulting in regions more ordered which melts at higher temperatures. This phenomenon was not observed at DSC analysis performed in the

present work, considering that relatively lower concentrations (maximum 5 %wt) were tested.

3.2 DYNAMICAL MECHANICAL THERMAL ANALYSIS (DMTA)

The storage modulus and damping factor (Tan 5) versus temperature of the TPS and PBAT virgin matrices are represented at Figure 4. For both polymeric phases was evident that the storage modulus (E') decreases with the increase in temperature, showing a drastic fall beyond -20°C for PBAT. For TPS, two falls were registered, the first around -60°C and the second in 30°C.

Figure 4 – Storage modulus (MPa) and Tan δ *vs* temperature for TPS and PBAT.

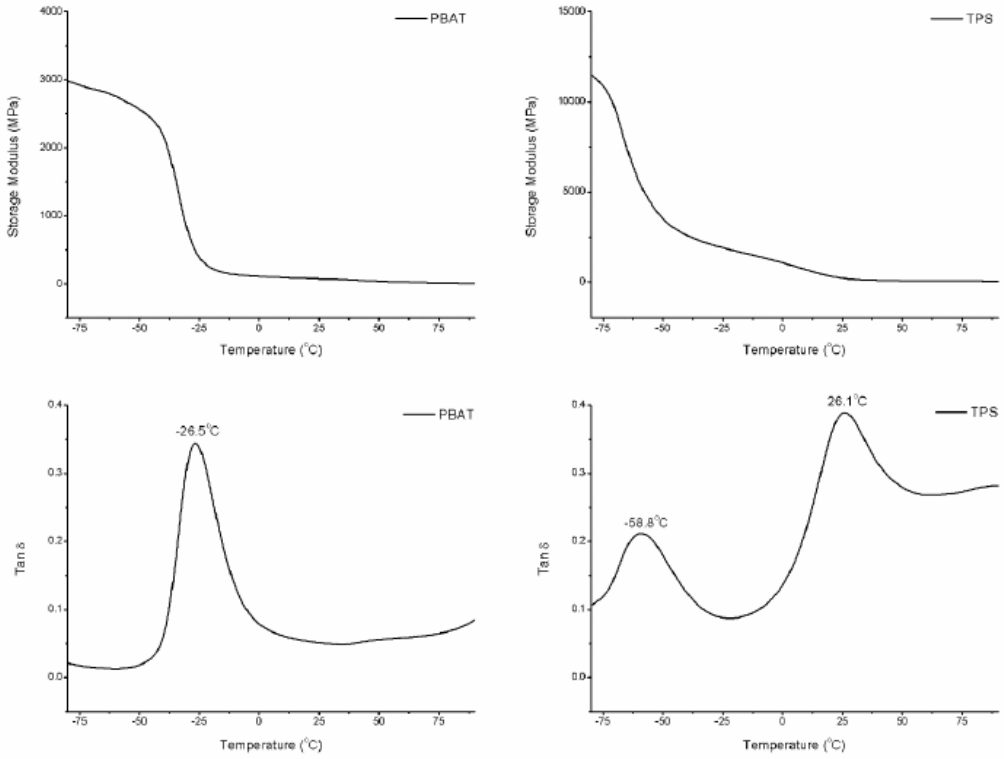

A single peak in -26.5°C was recorded for PBAT, corresponding to a arelaxation and attributed to their glass transition (Tg), which is similar to those observed in DSC curves. Damping factor (Tan 5) of TPS showed two relaxation peaks (a and (3), with the larger peak localised at 26.1°C and referent to the starch glass transition and the (3 relaxation in -58.8°C, consistent with glycerol glass transition. Averous and Boquillon (2004) related similar behaviour for plasticised

wheat starch, with Tg of starch around 31°C and Tg of glycerol between -50 and -70°C.

Storage modulus is an important parameter for rigid materials (WANG; YU; MA, 2007). TPS matrix shows greater values of E' when compared to PBAT, since physical crosslinks and chemical interactions (mostly hydrogen bonds), between polymeric chains in TPS, are responsible to increase their stiffness (Figure 4).

According to our previous work, sepiolite was preferentially localised at TPS phase, once the silanol groups at clay surface may interact with hydroxyls of starch chain. This fact resulted in an enhancement of the mechanical properties for 80:20 TPS/PBAT nano-biocomposites, producing materials with greater tensile strength and elastic modulus, without a loss in elongation at break, when compared with 50:50 TPS/PBAT materials.

Figure 5 – Variations of storage modulus (MPa) *vs* temperature for 50:50 TPS/PBAT blends with different sepiolite contents.

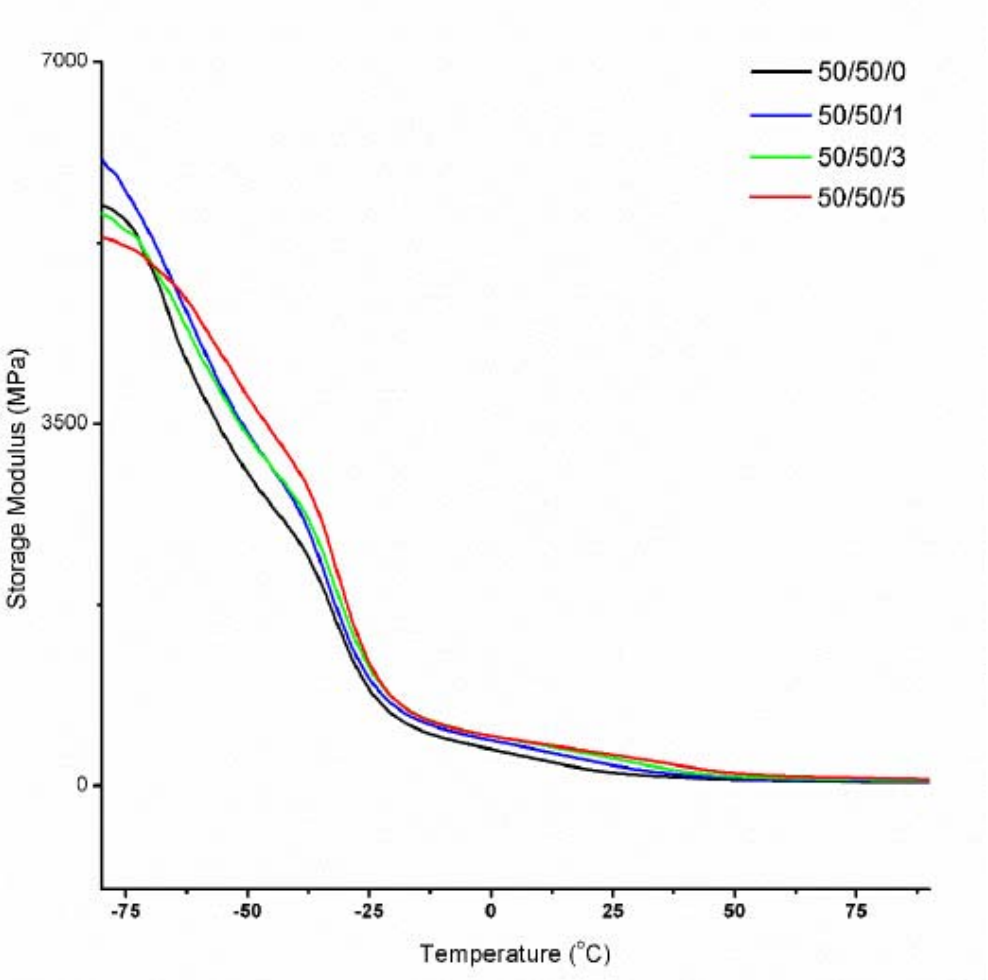

The storage modulus of all samples increased with the incorporation of sepiolite (Figures 5 and 6), whose results are more visible at 80:20 nano-biocomposites, revealing the action of this clay to reinforcing the materials. This enhancement was more noticeable below starch Tg (around 26°C) (FUKUSHIMA; TABUANI; CAMINO, 2012).

Greater values of E' were also recorded by Park, Kim and Ha (2007) for TPS/polyesters incorporated with organomodified montmorillonite. In addition, Fukushima, Tabuani and Camino (2012) showed that sepiolite resulted in noticeable increase of E' at polylactic acid (PLA) matrix, in concentrations of 5 %wt and 7 %wt, without needing an organic modification due their compatibility with the PLA matrix, which could also be applied to the present work, once sepiolite is quite compatible with TPS matrix.

Figure 6 – Variations of storage modulus (MPa) *vs* temperature for 80:20 TPS/PBAT blends with different sepiolite contents.

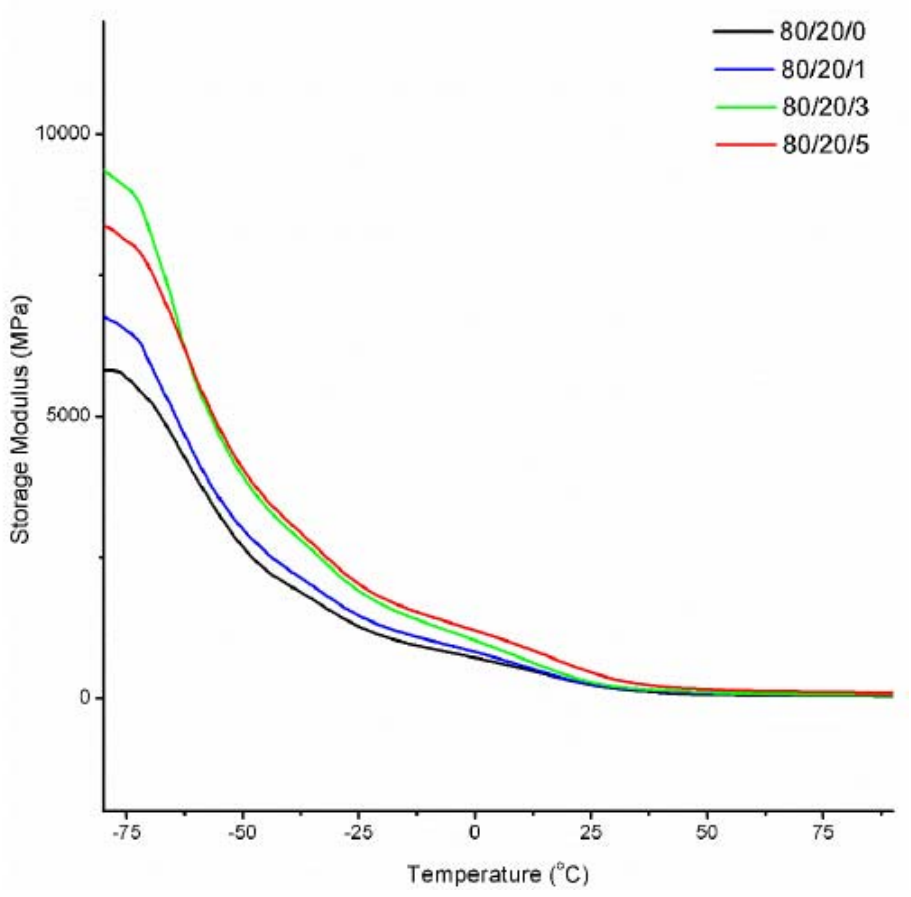

Figures 7 and 8 show the damping factor (Tan 5) graphs for all the nano -biocomposites. Three transition peaks were identified and correspond to a combination of the glass transitions registered for PBAT and TPS matrix, as showed at Figure 4. This fact pointed to almost no interaction between TPS and PBAT matrix, once their Tg peaks remain essentially unchanged when blended.

Figure 7 – Variations of Tan δ *vs* temperature for 50:50 TPS/PBAT blends with different sepiolite contents.

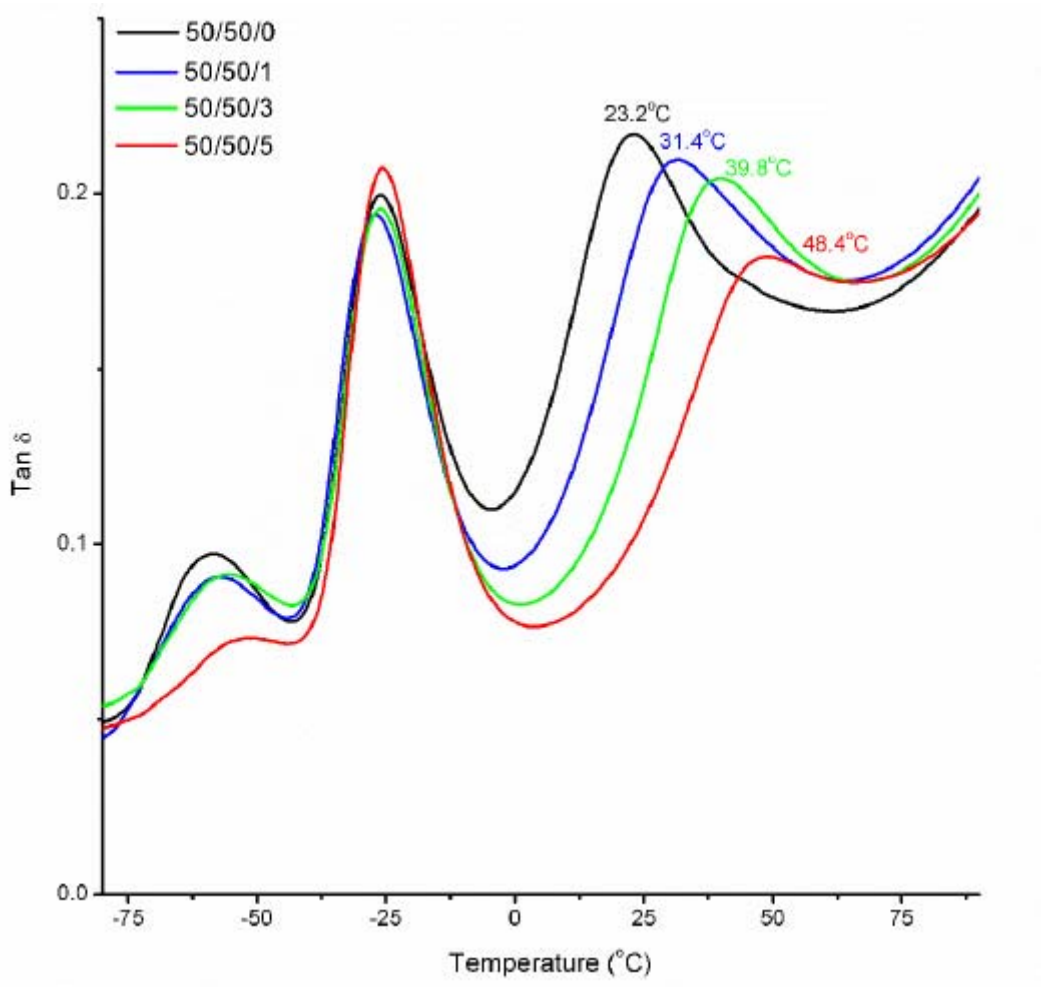

Considering 50:50 TPS/PBAT nano-biocomposites, the addition of sepiolite clays shifted the Tg of starch phase, initially at 23.2°C, to comparatively higher temperatures, reaching 31.4°C with 1 %wt of sepiolite, 39.8°C with 3 %wt of sepiolite and 48.4°C with 5 %wt of sepiolite, which is attributed to a segmental immobilisation of the matrix with the incorporation of clay. Fukushima, Tabuani and Carmino (2009) registered an increase of 14°C in Tg of PLA matrix with the incorporation of 9 %wt of sepiolite. The results showed in the present work reported

an increase of 25°C in the Tg of TPS phase with the inclusion of 5 %wt of sepiolite, which represents an important increase in thermo-mechanical properties with the inclusion of nanoclays without an organic modification, highlighting the potential use of natural sepiolite clays in starch/PBAT materials.

The glass transition of PBAT phase did not change with the inclusion of sepiolite clay, remaining around -26°C, which support the proposition that sepiolite, being more compatible with starch, was preferentially localised at TPS phase, causing also a slightly increment of Tg of glycerol rich phase, shifted from -58.8°C (50/50/0) to -51°C (50/50/5).

Figure 8 – Variations of Tan δ *vs* temperature for 80:20 TPS/PBAT blends with different sepiolite contents.

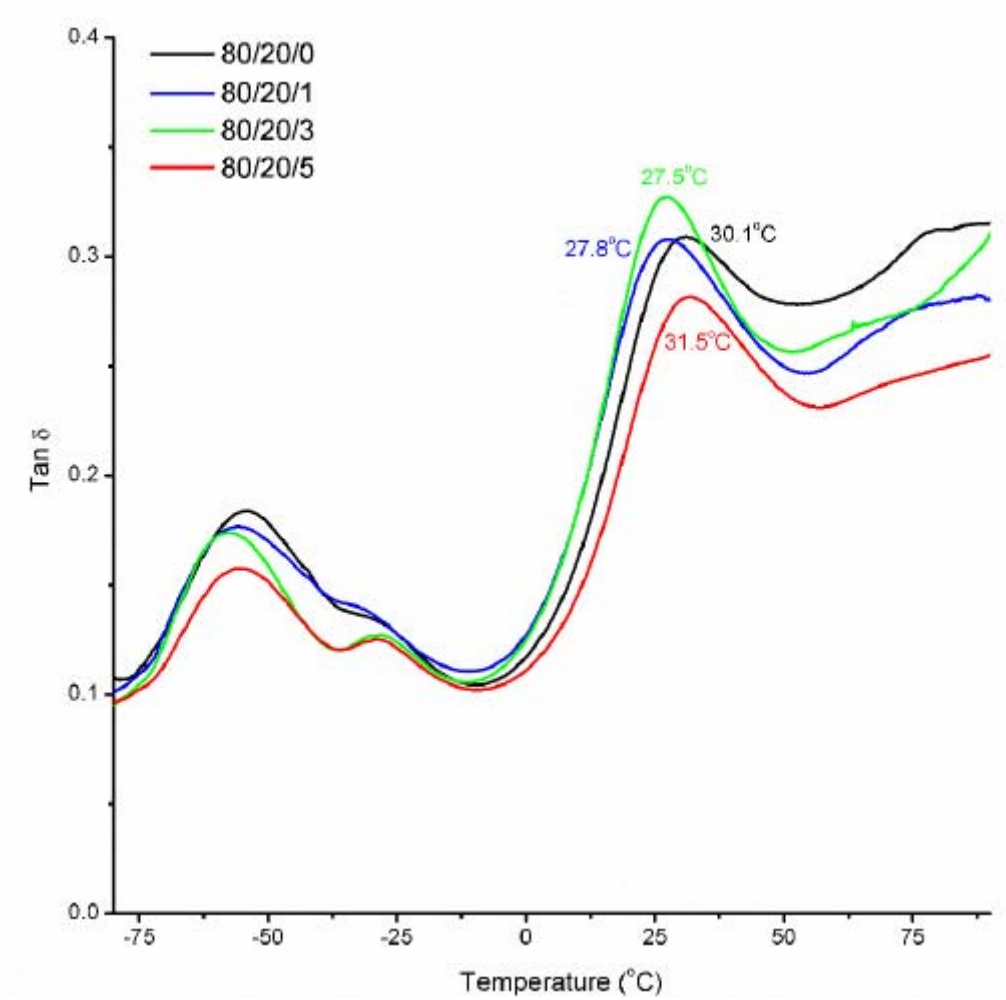

Figure 8 shows Tan δ peaks for 80:20 TPS/PBAT nano-biocomposites. Contrary to the results observed for 50:50 TPS/PBAT samples, the inclusion of sepiolite clays marginally influenced the glass transition of starch phase

in 80:20 TPS/PBAT materials. Greater proportions of TPS in these samples provide a dilution of clay particles, which despite contribute to increase the mechanical properties, were not sufficient to change significantly the thermal-mechanical properties of the materials.

At the same way, glass transition of PBAT phase for nano-biocomposites in the proportion 80:20 TPS/PBAT was not modified with the inclusion of sepiolite, which supports the results observed for 50:50 nano-biocomposites concerning the sepiolite localisation.

3.3 Moisture Adsorption Kinetics of Nano-biocomposites

To investigate the moisture adsorption kinetics of nano-biocomposites, the data of moisture content, registered against the time, were fitted to Peleg model (1988). The results of k1 and k2 parameters, which refers to the mass transfer (k1) and maximum water adsorption capacity (k2), are related at Table 2. The lower k1 value, the higher the initial water adsorption rate and the lower k2 value, the higher the water adsorption capacity. The relative humidity (RH) influenced the k1 and k2 values, with lower results of both parameters observed at 90 %RH, which means that the nano-biocomposites tends to adsorbs faster and higher quantities of water in elevated RH. Mali et al. (2005) observed similar behaviour in relation to RH for cassava starch films.

Considering the different proportions between TPS and PBAT phases, is possible to observe that 80:20 TPS/PBAT samples presented lower k2 values. As expected, 80:20 samples adsorbed more water than 50:50 TPS/PBAT samples due the hydrophilic character of starch, present in elevated proportion at these materials.

At 32% RH, 80:20 TPS/PBAT samples showed higher k1 values when compared to the 50:50 TPS/PBAT, with opposite effect at other relative humidity (53%, 75% and 90%). This means that at 32% RH, materials with 50:50 TPS/PBAT tends to adsorb water at greater initial rate than 80:20 TPS/PBAT nano-biocomposites, changing this comportment in higher RH.

In general, the inclusion of sepiolite clays decreased the water adsorption rate (higher k1 values) even as the water adsorption capacity (increased k2 values) of nano-biocomposites, pointing that even with the silanol groups in

sepiolite structure, which have a good affinity with water molecules, the clays probably strong interacted with starch hydroxyls and did not contributed to increase the water affinity of the samples. An exception to this could be observed at 90% RH for 80:20 nano-biocomposites, where lower parameters k1 and k2 were observed with the inclusion of sepiolite, i. e., resulting in greater water adsorption rate and also water adsorption capacity for these samples at higher relative humidity.

Table 2 – Values of k1 and k2 parameters, for water sorption data fitted to Peleg model, of the nano-biocomposites at different RH conditions.

Sample	32% RH		53% RH		75% RH		90% RH	
	k1	*k2*	*k1*	*k2*	*k1*	*k2*	*k1*	*k2*
50/50/0	507.94	133.45	801.98	47.98	485.90	21.48	389.50	8.02
50/50/1	638.76	131.77	840.36	52.96	538.44	18.03	395.38	8.67
50/50/3	567.93	150.23	789.76	52.00	605.92	23.51	426.04	9.83
50/50/5	633.87	135.29	765.03	46.48	668.28	21.15	370.29	8.08
80/20/0	662.67	76.36	595.20	23.07	349.55	10.07	208.94	4.40
80/20/1	904.43	89.39	603.22	21.29	394.08	10.97	186.45	3.68
80/20/3	951.31	86.20	613.25	19.35	357.53	10.09	186.02	3.61
80/20/5	902.87	79.91	662.12	20.53	380.48	9.92	185.89	3.30

k1 = h/(g water/g solids and *k2* = g solids/g water

In some cases, a tendency of samples containing 5 %wt of sepiolite (50/50/5 and 80/20/5) to register results similar to those without nanoclays (50/50/0 and 80/20/0) was observed, mostly due the higher proportion of sepiolite in these samples, that even considering the strong interaction of TPS, also contributed to increase the water affinity of the materials.

3.4 Moisture Sorption Isotherms of Nano-biocomposites

The moisture sorption isotherms at 25°C of nano-biocomposites are displayed at Figure 9 and GAB model adjusted parameters are shown at Table 3. All the curves presented a sigmoidal shape, as observed for most of starch-based materials (MALI et al., 2005; SHIRAI et al., 2013).

According to Figure 9, the addition of sepiolite did not change the equilibrium moisture content of the materials. Samples with greater proportion of TPS (80:20 TPS/PBAT) tends to absorb more water than those with 50:50 TPS/PBAT, proving that the moisture affinity of the nano-biocomposites was dependent

exclusively of the proportion of thermoplastic starch at samples, which was related to the hydrophilic character of starch molecules.

Figure 9 – Moisture sorption isotherm curves for nano-biocomposites. Symbols represents the experimental data and lines represents the curves adjusted to GAB model.

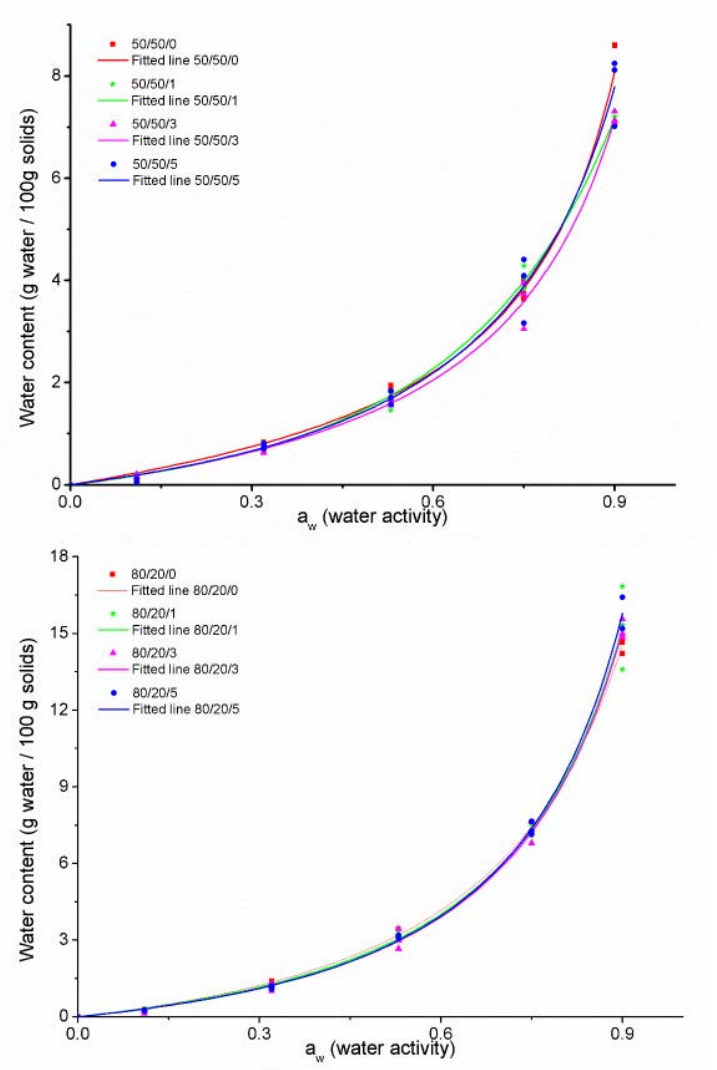

Table 3 shows that GAB model was efficient to describe the moisture sorption isotherms of the nano-biocomposites (R^2 > 0.98). Nano-biocomposites with greater proportion of TPS resulted in higher monolayer values (mo = 5.37 ± 2.04 g water / 100 g solids for 80/20/0 sample) as expected. Also for this samples, the inclusion of sepiolite marginally decrease the value for mo, independent of the clay concentration. The opposite effect was registered for 50:50 TPS/PBAT samples that

showed an increase for monolayer values with sepiolite incorporation at matrix, with lowest value of this parameter for 50/50/0 sample (1.55 ± 0.53 g water / 100 g solids).

Table 3 – GAB model parameters for water sorption isotherms of nano-biocomposites.

Sample	C	K	m_o	R^2
50/50/0	1.39 ± 0.99	0.93 ± 0.04	1.55 ± 0.53	0.984
50/50/1	1.12 ± 0.34	0.88 ± 0.05	1.72 ± 0.58	0.989
50/50/3	0.96 ± 0.50	0.89 ± 0.04	1.84 ± 0.63	0.994
50/50/5	0.80 ± 0.08	0.87 ± 0.09	2.21 ± 1.67	0.982
80/20/0	0.61 ± 0.27	0.84 ± 0.04	5.37 ± 2.04	0.999
80/20/1	0.65 ± 0.07	0.88 ± 0.09	4.51 ± 3.90	0.985
80/20/3	0.60 ± 0.35	0.88 ± 0.05	4.66 ± 2.24	0.997
80/20/5	0.61 ± 0.34	0.89 ± 0.04	4.54 ± 1.97	0.997

* m**o** is the monolayer value (g water/100 g solids), C and K are the constants (GABparameters).

Tang et al. (2008) reported that nanocomposite structure depends on the compatibility and interactions between the polymer, plasticisers and silicate layers and a competition mechanism between the strong polar-polar interactions between starch, glycerol and clay surface takes place, resulting in a balance of these interactions, which interferes on the water affinity of the materials. Chivrac et al. (2010b) observed no significant effect of montmorillonite inclusion on the curves of water sorption isotherm of starch based materials.

The C parameter is related to the sorption heat of the first layer. Nano-biocomposites showed values of C in general lower than those registered by other authors for TPS/PBAT materials (BRANDELERO; YAMASHITA; GROSSMANN, 2011), probably as a result of the different processing technique and related also to the proportions between the polymers in the blends. Moreover, no difference was observed with the inclusion of nanoclays in 80:20 TPS/PBAT samples and a slightly decrease was recorded for 50:50 TPS/PBAT nano-biocomposites.

No difference was observed at K parameter (related to the sorption heat of the multilayer) for all the samples, even with the addition of nanoclays. As previously reported (MALI et al., 2005; MULLER et al., 2008; SHIRAI et al., 2013), the K parameter is not influenced by the formulation of the samples.

3.5 OPACITY AND COLOUR ANALYSIS

A challenge to incorporate nanoclays in biodegradable materials destined to food packaging is related to the alteration of colour and lack of transparency that they can cause. Based on this, the alteration in a* and b* parameters, according to CIELAB methods, and also the opacity of the nano-biocomposites were analysed.

The films transparency provides information on the particle size of dispersed particle in starch matrix. Larger particle sizes would obstruct the light, leading to more opaque films (KAMPEERAPAPPUN et al., 2007). The opacity of the nano-biocomposites is presented at Table 4. The data shows that higher proportions of sepiolite at samples tend to elevate their opacity. Considering this, it is possible to affirm that 50/50/0 and 80/20/0 samples presented lower opacity due the absence of particles, which causes the light blockage. In 50/50/5 sample, however, as expected, the greater concentration of sepiolite clays reduces the light transmission, consequently resulting in more opaque material.

Table 4 – Nano-biocomposites opacity.

Sample	Opacity (%.μm^{-1})
50/50/0	0.099 ± 0.003^{b}
50/50/1	0.096 ± 0.002^{b}
50/50/3	0.101 ± 0.004^{b}
50/50/5	0.125 ± 0.003^{a}
80/20/0	0.076 ± 0.001^{A}
80/20/1	0.078 ± 0.003^{A}
80/20/3	0.103 ± 0.001^{B}
80/20/5	0.096 ± 0.003^{B}

^{a,b,A,B} Means in the same column, considering the same proportion between the polymeric phases, with different letters differ significantly (Tukey's Test; $p < 0.05$).

Chen et al. (2008) found a similar behaviour for poly(vinyl alcohol) (PVA)/starch films, producing more opaque materials when greater proportions of pea starch nanocrystals were incorporated in the matrix.

Sepiolite clays significantly altered the films colour (Figure 10), which becomes redder (increase of a* positive) and yellower (increase of b* positive) with

the increase of nanoclays proportion in the samples until 3 %wt concentration (Figure 10). Further increase to 5 %wt promotes only a small change in sample colour

Figure 10 – Nano-biocomposites colour parameters (a* and b*) according CIEL*a*b* colour scale for the nano-biocomposites with proportion 80:20 TPS/PBAT (above) and 50:50 TPS/PBAT (below).

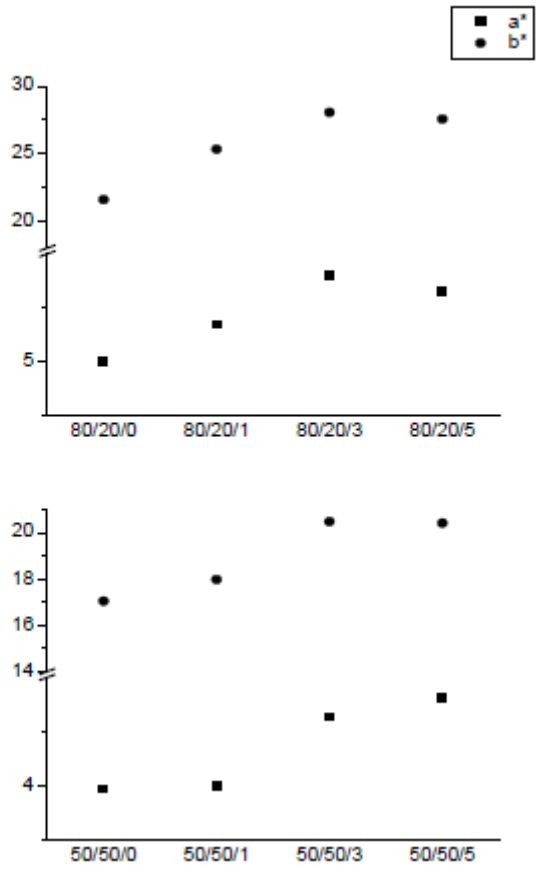

These results are consistent considering that sepiolite presents as a white powder with a yellowish or reddish tint and taking into consideration that no influence of the samples thickness could be considered, once all the samples were compression moulded with 0.5 mm.

4 Conclusion

Nano-biocomposites based on sepiolite clays produced using two different proportions between thermoplastic starch and PBAT phases showed different responses concerning the sepiolite effects. The crystallisation temperature (Tc) recorded by DSC analysis increased with the incorporation of sepiolite, which

point to the influence of the clay in the crystallisation of nano-biocomposites, acting as nucleating sites in the polymeric matrix, but no difference in melting temperatures were registered, suggesting that the crystal organisation in nano-biocomposites tends to be similar to those of virgin matrix.

The results of DMTA analysis showed an increase of until 25°C in the glass transition of TPS with the inclusion of 5 %wt of sepiolite. In addition, for both polymeric phase proportions, no significant changes were observed in Tg of PBAT, reinforcing the supposed preferential localisation of sepiolite at TPS phase, due their compatibility.

In general, the inclusion of sepiolite clays decreased the water adsorption rate and the water adsorption capacity of nano-biocomposites, pointing that even with the silanol groups in sepiolite structure, which have a good affinity with water molecules, the clays probably strong interacted with starch hydroxyls and did not contributed to increase the water affinity of the samples. In addition, samples with greater proportion of TPS (80:20 TPS/PBAT) tends to absorb more water than those with 50:50 TPS/PBAT, proving that the moisture affinity of the nano-biocomposites was dependent of the proportion of thermoplastic starch in the samples. Lastly, higher proportions of sepiolite at samples tend to elevate their opacity, since the particles caused the light blockage, and also changed the materials colour.

Considering this, the results of this work highlights the potential use of natural sepiolite clay in starch/PBAT materials, improving their thermo-mechanical properties and producing an interesting material as substitute to non-biodegradable plastics.

5 References

AVÉROUS, L. Biodegradable multiphase systems based on plasticized starch: A review. **Journal of Macromolecular Science,** v. C44, p. 231-274, 2004.

AVEROUS, L; BOQUILLON, N. Biocomposites based on plasticized starch: thermal and mechanical behaviours. **Carbohydrate Polymers,** v. 56, p. 111-122, 2004.

BORDES, P; POLLET, E; AVEROUS, L. Nano-biocomposites: Biodegradable polyester/nanoclay systems. **Progress in Polymer Science,** v. 34, p. 125-155, 2009.

BRANDELERO, R. P. H; GROSSMANN, M. V. E; YAMASHITA, F. Effect of the method of production of the blends on mechanical and structural properties of

biodegradable starch films produced by blown extrusion. **Carbohydrate Polymers,** v. 86, p. 1344-1350, 2011.

CARVALHO, A. J. F; ZAMBOM, M. D; CURVELO, A. A. S; GANDINI, A. Thermoplastic starch modification during melt processing: Hydrolysis catalyzed by carboxylic acids. **Carbohydrate Polymers,** v. 62, p. 387-390, 2005.

CHEN, Y; CAO, X; CHANG ; P. R ; HUNEAULT, M. A. Comparative study on the films of poly(vinyl alcohol)/pea starch nanocrystals and poly(vinyl alcohol)/native pea starch. **Carbohydrate Polymers,** 73, p. 8-17, 2008.

CHIVRAC, F; POLLET, E; SCHMUTZ, M; AVEROUS, L. Starch nano-biocomposites based on needle-like sepiolite clays. **Carbohydrate Polymers,** v. 80, p. 145-153, 2010a.

CHIVRAC, F; COUSSY, H.A; GUILLARD, V; POLLET, E; AVEROUS, L. How does water diffuse in starch/montmorillonite nano-biocomposite materials? **Carbohydrate Polymers,** v. 82, p. 128-135, 2010b.

CHIVRAC, F; POLLET, E; AVEROUS, L. Progress in nano-biocomposites based on polysaccharides and nanoclays. **Materials Science and Engineering R,** v. 67, p. 1-17, 2009.

CHIVRAC, F; POLLET, E; SCHMUTZ, M; AVEROUS, L. New approach to elaborate exfoliated starch-based nanobiocomposites. **Biomacromolecules,** v. 9, p. 896-900, 2008.

FUKUSHIMA, K; WU, M. H; BOCCHINI, S; RASYIDA, A; YANG, M. C. PBAT based nanocomposites for medical and industrial applications. **Materials Science and Engineering C,** v. 32, p. 1331-1351, 2012.

FUKUSHIMA, K; TABUANI, D; CAMINO, G. Poly(lactic acid)/clay nanocomposites: effect of nature and content of clay on morphology, thermal and thermo-mechanical properties. **Materials Science and Engineering C,** v. 32, p. 1790-1795, 2012.

FUKUSHIMA, K; TABUANI, D; CAMINO, G. Nanocomposites of PLA and PCL based on montmorillonite and sepiolite. **Materials Science and Engineering C,** v. 29, p. 1433-1441, 2009.

GALDEANO, M. C; MALI, S; GROSSMANN, M. V. E; YAMASHITA, F; GARCIA, M. A. Effects of plasticizers on the properties of oat starch films. **Materials Science and Engineering C,** v. 29, p. 532-538, 2009.

GARCIA, M. A; MARTINO, M. N; ZARITZKI, N. E. Microstructural characterization of plasticized starch-based films. **Starch/Stärke,** v. 52, p. 118-124, 2000.

KAMPEERAPAPPUN, P; AHT-ONG, D; PENTRAKOON, D; SRIKULKIT, K. Preparation of cassava starch/montmorillonite composite film. **Carbohydrate Polymers,** v. 67, p. 155-163, 2007.

LIU, H; XIE, F; YU, L; CHEN, L; LI, L. Thermal processing of starch-based polymers. **Progress in Polymer Science,** v. 34, p. 1348-1368, 2009.

McGLASHAN, S.A; HALLEY, P. J. Preparation and characterization of biodegradable starch-based nanocomposite materials. **Polymer International,** v. 52, p. 1767-1773, 2003.

MAJDZADEH-ARDAKANI, K; NAVARCHIAN, A. H; SADEGHI, F. Optimization of mechanical properties of thermoplastic starch/clay nanocomposites. **Carbohydrate Polymers,** v. 79, p. 547-554, 2010.

MALI, S; SAKANAKA, L, S; YAMASHITA, F; GROSSMANN, M. V. E. Water sorption and mechanical properties of cassava starch films and their relation to plasticizing effect. **Carbohydrate Polymers,** v. 60, p. 283-289, 2005.

MALIGER, R. B; McGLASHAN, S.A; HALLEY, P. J; MATTHEW, L. G. Compatibilization of starch-polyester blends using reactive extrusion. **Polymer Engineering and Science,** v. 46, p. 248-263, 2006.

MOHANTY, S; NAYAK, S. K. Biodegradable nanocomposites of poly(butylene adipate-co-terephthalate) (PBAT) and organically modified layered silicates. **Journal of Polymers and Environment,** v. 20, p. 195-207, 2012.

MULLER, C. M. O; LAURINDO, J. B; YAMASHITA, F. Composites of thermoplastic starch and nanoclays produced by extrusion and thermopressing. **Carbohydrate Polymers,** v. 89, p. 504-510, 2012.

MULLER, C. M. O; LAURINDO, J. B; YAMASHITA, F. Effect of nanoclay incorporation method on mechanical and water vapor barrier properties of starch-based films. **Industrial Crops and Products,** v. 33, p. 605-610, 2011.

MÜLLER, C. M. O; YAMASHITA, F; LAURINDO, J. B. Evaluation of the effects of glycerol and sorbitol concentration and water activity on the water barrier properties of cassava starch films through a solubility approach. **Carbohydrate Polymers,** v. 72, p. 82-87, 2008.

NAYAK, S. K. Biodegradable PBAT/starch nanocomposites. **Polymer - Plastics Technology and Engineering,** v. 49, p. 1406-1418, 2010.

OKAMOTO, M. Biodegradable polymer/layered silicate nanocomposites: A review. **Handbook of Biodegradable Polymeric Materials and Their Applications.** v. 1, p. 1-45, 2005.

PARK, H. M; KIM, G. H; HA, C. S. Preparation and characterization of biodegradable aliphatic polyester/thermoplastic starch/organoclay ternary hybrid nanocomposites. **Composites Interfaces,** v. 14, p. 427-438, 2007.

PELEG, M. An empirical model for the description of moisture sorption curves. **Journal of Food Science,** v. 53, p. 1216-1217, 1988.

RAQUEZ, J. M; NABAR, Y; NARAYAN, R; DUBOIS, P. In situ compatibilization of maleated thermoplastic starch/polyester melt-blends by reactive extrusion. **Polymer Engineering and Science,** v. 48, p. 1747-1754, 2008.

RAY, S. S; OKAMOTO, M. Polymer/layered silicate nanocomposites: a review from preparation to processing. **Progress in Polymer Science,** v. 28, p. 1539-1641, 2003.

SCHWACH, E; AVEROUS, L. Starch-based biodegradable blends: morphology and interface properties. **Polymer International,** v. 53, p. 2115-2124, 2004.

SHIRAI, M. A; OLIVATO, J. B; GARCIA, P. S; MULLER, C. M. O; GROSSMANN, M. V. E; YAMASHITA, F. Thermoplastic starch/polyester films: Effects of extrusion process and poly (lactic acid) addition. **Materials Science and Engineering C,** v. 33, p. 4112-4117, 2013.

TANG, X; ALAVI, S; HERALD, T. J. Effects of plasticizers on the structure and properties of starch-clay nanocomposite films. Carbohydrate Polymers, v. 74, p. 552-558, 2008.

WANG, N; YU, J; MA, X. Preparation and characterization of thermoplastic starch/PLA blends by one-step reactive extrusion. **Polymer International,** v. 56, 1440-1447, 2007.

ZULLO, R; IANNACE, S. The effects of different starch sources and plasticizers on film blowing of thermoplastic starch: Correlation among process, elongational properties and macromolecular structure. **Carbohydrate Polymers,** v. 77, p. 376383, 2009.

CONCLUSÕES GERAIS

Este estudo mostrou a potencialidade da utilização de ácidos orgânicos como compatibilizantes em blendas de amido/PBAT, sobretudo para o ácido tartárico, cuja ação na realização de reações de esterificação / transesterificação foi observada palas análises de FT-IR e 13C CPMAS NMR. A redução da tensão interfacial com a inclusão do ácido tartárico levou à obtenção de filmes mais homogêneos, para os quais, de acordo com a técnica da Desejabilidade, as formulações contendo proporções intermediárias deste componente apresentaram os melhores resultados de resistência á tração, elongação, módulo de Young e força de perfuração. Dessa forma, sacolas plásticas biodegradáveis produzidas a partir da formulação mais desejada foram analisadas conforme norma NBR 14937:2010 (2010) e atenderam aos requisitos constantes nesta, representando assim a viabilidade comercial, para esse fim, de plásticos biodegradáveis a base de amido e PBAT, compatibilizados com ácido tartárico.

Duas proporções entre amido termoplástico e PBAT foram adicionadas de sepiolita. A ação reforçadora da nanoargila foi observada principalmente nas blendas contendo 80:20 TPS/PBAT, nas quais aumentos do módulo de Young, da elongação na ruptura e da resistência à tração foram observados, sendo os resultados dependentes da concentração de sepiolita presente na amostra. Esse fato se deve à localização preferencial da sepiolita na fase de amido, devido à presença de grupos silanol em sua superfície, que conferem caráter hidrofílico ao nanosilicato e, assim, o tornam mais compatível com o amido. A temperatura de degradação térmica dos nano-biocompósitos foi marginalmente aumentada com a inclusão da nanoargila, entretanto, um acréscimo de 25°C na temperatura de transição vítrea da fase de amido foi observada nas amostras 50:50 TPS/PBAT com 5 % m/m do nanosilicato.

As análises de calorimetria diferencial de varredura (DSC) mostraram que a sepiolita aumentou a temperatura de cristalização dos nano-biocompósitos, entretanto nenhuma alteração na temperatura de fusão, referente ao PBAT, foi observada. Por fim, foi observada uma boa dispersão das nanopartículas na matriz polimérica, o que não causou alterações na morfologia dos materiais, fato este que foi essencial na melhoria das propriedades mecânicas com a inclusão da sepiolita. Dessa forma, a utilização de sepiolita como agente de reforço em materiais

biodegradáveis à base de amido mostrou-se promissora, especialmente naqueles contendo maiores proporções de amido termoplástico.

Por fim, a inclusão de compatibilizantes, como os ácidos orgânicos, e agentes de reforço, como a sepiolita, foram eficazes na melhoria das propriedades das blendas de amido/PBAT e constituem opções interessantes na produção de materiais biodegradáveis com melhor performance e que representem uma possível aplicação comercial.

APÊNDICES

CAPITULO 3 – Imagens dos filmes obtidos no com base no planejamento de misturas, mostrando o efeito no ácido tartárico nas amostras.

Figura 1 – Filmes soprados de amido e PBAT referentes às formulações C (sem TA -esquerda) e T1 (1.1 g.100g^{-1} de TA - direita)

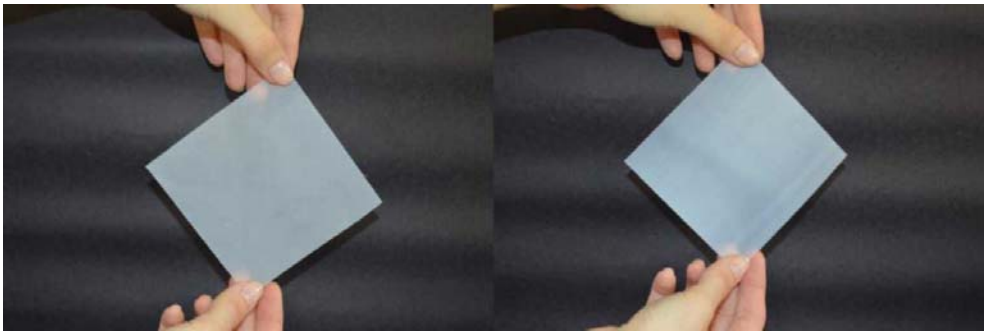

CAPÍTULO 5 – Imagens dos ensaios realizados no CETEA/ITAL para as sacolas biodegradáveis de acordo com a norma NBR 14937:2010 (2010)

Figura 2 – Foto do ensaio de resistência à carga dinâmica.

Figura 3 – Foto do ensaio de resistência à carga estática.

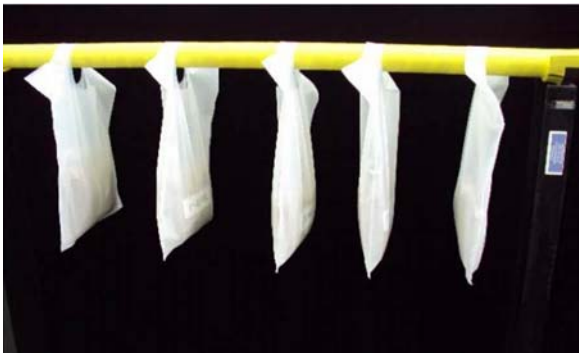

Figura 4 – Foto do ensaio de resistência ao impacto por queda de dardo.

CAPÍTULO 6 – Imagens dos nano-biocompósitos contendo 50:50 TPS/PBAT e 50:50 TPS/PBAT adicionados de sepiolite

Figura 5 – Nano-biocompósitos referentes à proporção 50:50 TPS/PBAT.

Figura 6 – Nano-biocompósitos referentes à proporção 80:20 TPS/PBAT.